# EOR by Seawater and “Smart Water” Flooding in High Temperature Sandstone Reservoirs

by

Zahra Aghaeifar

Thesis submitted in fulfillment of
the requirements for degree of
DOCTOR OF PHILOSOPHY
(Ph.D.)


Faculty of Science and Technology
Department of Energy Resources
2019

University of Stavanger
N-4036 Stavanger
NORWAY
www.uis.no



ISBN: 978-82-7644-915-0
ISSN: 1890-1387
PhD Thesis UiS no. 508

بسم الله الرحمن الرحيم

Dedicated to:

Who will come and reveal
All the treasures of science in the earth and the sky,
Who will bring peace and justice to the whole world,
A hero to stop this thousand-year-old pain of injustice;

and to all who actively waiting for him…
and the loving memory of my father…

يا ايها العزيز، مسنا و اهلنا الضر، و جئنا ببضاعة مزجاة، فاوف لنا الكيل و تصدق علينا، ان الله يجزى المتصدقين...(يوسف 88)

# Abstract

In the last decades, when the first treated injection water has resulted in incremental oil recovery, the activity to explore this technique has increased. And today, Smart Water flooding or low salinity flooding in sandstone reservoirs has been considered among the most promising choices to be implemented in some oil reservoirs, such as the western part of Norwegian Continental Shelf. The method has been widely thought-out considering both economic and environmental issues.

Offshore sandstone reservoirs are typically flooded with the most available surrounding water, which is seawater. So as main objective of this PhD it is questioned if seawater can act as a Smart Water? And if it is the case, what is the potential of low salinity EOR in tertiary mode. Due to the potential of scale precipitation and formation damage during seawater flooding, since fifty years ago removal of sulphate from seawater was considered by oil companies, and today from a Smart Water EOR perspective, it is also questioned if modified seawater could behave as Smart Water in the reservoir with incremental oil recovery as a result? And lastly, what injection strategy could be offered for high temperature offshore sandstone oil reservoirs?

To answer the oil companies' concerns above, four North Sea sandstone reservoirs, including the total number of 17 preserved core plugs with corresponding reservoir formation brine and stabilized reservoir crude oil, have been studied at each specific reservoir temperature. Reservoirs have a temperature above 100 °C and are investigated for different Smart Water EOR potentials. The reservoirs have different formation water salinity ranging from 23000 ppm up to 195000 ppm, and for each set of cores, specific injection brine salinities and compositions were tested and compared.

The optimum injection strategy has been proven to be secondary LS injection; injection from day one of the reservoir production life. Moreover, on the contrary, seawater and modified seawater for the individual study cases did not show any EOR effects and could not change the wettability of the cores. The potential of tertiary LS EOR after standard seawater flooding at high reservoir temperature was negligible. However, the tertiary low salinity EOR effect after modified seawater flooding gave an average of 11.8 %OOIP extra oil for the studied reservoir.

A secondary objective of this PhD-work was more theoretical. The chemical understanding of the low salinity EOR-mechanism in sandstones has improved significantly during the last ten years by Smart Water EOR group at the University of Stavanger. It is believed the incremental oil recovery by Smart Water in sandstones is due to wettability alteration of clay minerals which involves two main steps: firstly substitution of $Ca^{2+}$ and $Mg^{2+}$ with $H^{+}$ which results in an alkaline environment close to the clay surface and secondly is the desorption of polar organic components from clay by an ordinary acid-base reaction which is favoured at high pH. Since both initial wetting and wettability alteration processes towards more water wet conditions have the highest impact on the prediction of Smart Water EOR potential at high temperature, thus parametric studies on each specific element are important to complete our understanding.

This Ph.D. thesis is aimed at investigating the wetting controlling factors more in detail. To do that, some parametric studies under static and dynamic conditions have been performed. The dynamic tests performed using synthetic sand packs with different mineralogy to study the affinity of active cations towards different minerals at 20 and 130 ◦C. Furthermore, the crucial role of polar organic components in crude oil was investigated by static tests in the presence of different clay minerals, temperature, and different pHs using quinoline as a basic model.

The fundamental studies carried out showed a negligible reactivity of quartz surface towards both active cation and quinoline. Both cations and quinoline showed more tendency to adsorb on the negatively charged clay active surface. Among active cations, $Ca^{2+}$ showed higher affinity towards both illite and kaolinite clays, which is reflected in the higher retention time during the desorption process. In addition, the batch static test proved that adsorption of quinoline is strongly pH depended and the amount of quinoline adsorption is reducing as the temperature increases. The amount of adsorption was higher on the illite surface compare to the kaolinite, while the quinoline adsorption towards illite was not fully reversible, in contrary to fully reversible adsorption on the kaolinite. Furthermore, the last and most interesting is that the amount of adsorption is highest when a low salinity brine surrounds the clay, compared to the high salinity brine. This is evidence against the expansion of double layer mechanism, which is considered by many researchers, and modelling programs.

# List of papers

I. "**Smart Water injection strategies for optimized EOR in a high temperature offshore oil reservoir**", Z. Aghaeifar, S. Strand, T. Puntervold, T. Austad. Journal of Petroleum Science and Engineering, June 2018, 165, pp 743-751. https://doi.org/10.1016/j.petrol.2018.02.021

II. "**Significance of Capillary Forces during Low-Rate Waterflooding**", Z. Aghaeifar, S. Strand, T. Austad, T. Puntervold. Energy Fuels, 2019, 33 (5), pp 4747–4754. https://doi.org/10.1021/acs.energyfuels.9b00023

III. "**Seawater as a Smart Water in Sandstone reservoirs?**", Iván D. Piñerez Torrijos, Zahra Aghaeifar, Tina Puntervold and Skule Strand. Manuscript submitted to SPE Reservoir Evaluation & Engineering journal, 2019.

IV. "**Low Salinity EOR Effects After Seawater Flooding In A High Temperature And High Salinity Offshore Sandstone Reservoir**", Z. Aghaeifar, T. Puntervold, S. Strand, T. Austad, B. Maghsoudi and J. C. Ferreira, SPE-191334-MS, SPE Norwegian One Day Seminar, Bergen, Norway, 2018. https://doi.org/10.2118/191334-MS

V. "**Influence of Formation Water Salinity/Composition on the Low- Salinity Enhanced Oil Recovery Effect in High-Temperature Sandstone Reservoirs**", Z. Aghaeifar, S. Strand, T. Austad, T. Puntervold, H. Aksulu, K. Navratil, S. Storås, and D. Håmsø. Energy Fuels, 2015, 29 (8), pp 4747–4754. https://doi.org/10.1021/acs.energyfuels.5b01621

VI. "**The role of kaolinite clay minerals in EOR by low salinity water injection**", T. Puntervold; A. Mamonov, Z. Aghaeifar, G. O. Frafjord, G. M. Moldestad, S. Strand, T. Austad. Energy Fuels, 2018, 32 (7), pp 7374–7382. https://doi.org/10.1021/acs.energyfuels.8b00790

VII. "**Adsorption/desorption of $Ca^{2+}$ and $Mg^{2+}$ to/from Kaolinite Clay in Relation to the Low Salinity EOR Effect**", Z. Aghaeifar, S. Strand, T. Puntervold, T. Austad, S. Aarnes and Ch. Aarnes. 18th European Symposium on Improved Oil Recovery, At Dresden, Germany, April 2015. https://doi.org/10.3997/2214-4609.201412132

## Additional presentations:

I. "Evaluation of sea water (SW) as smart water in North sea sandstone reservoirs". 40th annual iea EOR, At September 16-20, 2019 – Cartagena, Colombia, 2019.

II. "Influence of formation water salinity on the low salinity EOR-effect in sandstone at high temperature", 77th EAGE Conference & Exhibition, Madrid, Spain, May 2015.

III. "Smart Water EOR in Sandstones: Wettability alteration controlled by desorption of divalent ions from Clays", First annual IOR Conference by the National IOR Centre of Norway 28-29, Stavanger, Norway, April 2015.

# Acknowledgments

This dissertation was greatly assisted by the kind efforts of individuals that I would acknowledge them. Thanks to the Norway ministry of science and technology for providing me the financial resources and University of Stavanger for all the technical support to pursue and complete my doctoral degree.

Firstly, I would like to express my sincere and highest measure gratitude to my supervisors Dr. Skule Strand ad Dr. Tina Puntervold for the continuous support of my PhD study and research, for their motivation, enthusiasm, patience, and immense knowledge. Skule's exceptional support in the lab and having answer to all the technical problems and Tina's constructive discussion and comments on the writing of reports and papers proved monumental towards the success of this study and thus I feel very much honoured to be a PhD student under their supervision. I also acknowledge and appreciate Professor Tor Austad, the first and former head of Smart Water EOR group at UiS. I was very fortunate to benefit from his mentorship and sit behind a desk in his last PVT course lectures at UiS. I would like to recognize the invaluable assistance that he provided during the writing of my first paper.

Besides my supervisors, I would like to thank my thesis assessment committee members, both my examiners: Dr. Patrick V. Brady (Sandia National Laboratories, USA), and Dr. John W. Couves (BP, UK) for their encouragement and insightful comments, and also Dr. Dora Luz Marin Restrepo for administrating the assessment.

I wish to express my special gratitude to the lab assistant Jose D. C. Ferreira for enlightening me the first glance of my research, for all the restless evenings and holidays that we were working together in the laboratory. I thank my fellows in Smart water EOR group at UiS: PhD students Iván D. Piñerez Torrijos, and Paul A. Hopkin, and the research assistants: Hossein A. Akhlaghi Amiri, Aleksandr Mamonov and Alireza Rostaei for all the scientific discussions, and for all the fun we have had in the laboratory. I gratefully acknowledge Ivan for his encouraging attribute not only in the successes, but also in the failures. I am also indebted to Gadiah Albraji who helped me during last months of my pregnancy.

I also appreciate the help of all the technical staff at petroleum engineering department particularly Reidar I. Korsnes, Kim Andre N. Vorland, Jorunn H.

Vrålstad and Inger Johanne M. K Olsen for their technical support in the laboratories. Thanks to the administrative staff of the faculty of science and technology and department of petroleum engineering, particularly Kathrine Molde, Norbert Puttkamer and Nina Ingrid Horve Stava, who are truly the unsung heroes of every doctoral student's career, and especially mine. They made navigating the endless paperwork.

It is a pleasure to also mention the name of students who had contribution to my experimental work during my PhD research. I convey my gratitude to Farasdaq Muchibbus Sajjad, Abdi H. Wakwaya, Behrouz Maghsoudi, Gadiah Albraji, Gunvor Oline Frafjord, Gyrid Marie Moldestad, Aarnes brothers (Steinar Aarnes and Christian Aarnes), Petter Schøien, Gunnleiv Dahl, and Christer Halvorsen. I must also thank the former lab assistant Hakan Aksulu, and former students Kine Navratil, Silje Storås, and Dagny Håmsø for their extensive work. Unfortunately, Abdi, one of my best co-workers during my PhD, recently has passed away. My God bless his soul.

My pursuit of a doctoral degree in petroleum engineering would not have occurred had I not benefited from the mentorship of Dr. Mohammad Chahardowli and Dr. S. Alireza Tabatabaeinezhad during my undergraduate years at the Sahand University of Technology (SUT).

Alongside the university, I am eternally indebted to all my family whose love, understanding, and unconditional support served as the anchors that kept me grounded. I owe my sincere and earnest thankfulness to my parents for their prayers and for motivating me to pursue my education. I would like to show my gratitude also to my sister, Fatemeh, my brother, Ali, and my parents in-law, brothers in-law and sisters in-law for all their support and encouragements. The last year of my career at UiS were blessed by the arrival of my lovely son, AmirHossein, whose presence has already enriched my life beyond calculation. He serves as both my paramount motivation and the most welcome distraction. Finally, my best friend and better half, my compassionate Husband, Milad Golzar, is to whom I owe the deepest and most enduring gratitude. His boundless love, selflessness, support, encouragement, and patience are the sole reason I was able to survive this doctoral program and complete this work. Thank you, Milad.

Lastly and foremost, praises and thanks to the God, the Almighty, for His showers of blessings throughout my life and specially my PhD research work.

*Zahra Aghaeifar*

# Table of contents

# List of figures

# List of tables

# Nomenclature

**List of abbreviations:**

| | |
|---|---|
| AN | Acid Number, mg KOH/g |
| BET | Brunauer-Emmett-Teller/Specific surface area, $m^2/g$ |
| BN | Base Number, mg KOH/g |
| CEC | Cation-Exchange Capacity, meq/100g |
| CoBR | Crude oil-Brine-Rock |
| DI | Deionized water |
| EOR | Enhanced Oil Recovery |
| FI | Forced Imbibition |
| FW | Formation Water |
| HS | High Salinity |
| HTHP | High-Temperature High-Pressure |
| IFT | Interfacial Tension, mN/m |
| IS | Ionic Strength, M |
| LFR | Limited Fines Release |
| LS | Low Salinity |
| MIE | Multi-ion exchange |
| NCS | Norwegian continental shelf |
| NPD | Norwegian Petroleum Directorate |
| OOIP | Original Oil In Place |
| PEEK | Polyether Ether Ketone |
| POC | Polar Organic Compounds |
| ppm | parts per million |
| PV | Pore Volume |
| PV/D | Pore Volumes per Day |

| | |
|---|---|
| PW | Produced Water |
| RF | Recovery Factor |
| scm | standard cubic metres |
| SEM | Scanning Electron Microscope |
| SI | Spontaneous Imbibition |
| SW | SeaWater |
| TDS | Total Dissolved Solids, mg/l |
| UV | Ultraviolet |
| WAG | Water Alternative Gas |
| XRD | X-Ray powder Diffraction |

## List of symbols

| | |
|---|---|
| B | Base brine in Ads./Des. study of cations, Pure NaCl brine. |
| E | Displacement efficiency |
| $E_D$ | Microscopic displacement efficiency |
| $E_V$ | Macroscopic (volumetric sweep) displacement efficiency |
| $FW_i$ | Formation water from reservoir **i** |
| g | Acceleration due to gravity, 9.8 $m/s^2$ |
| $g_c$ | Conversion factor |
| h | Height of the liquid column, m |
| *k* | Permeability, mD |
| $k_{ro}$ | Relative permeability of oil, mD |
| $k_{rw}$ | Relative permeability of water, mD |
| L | Capillary tube length, m |
| $LS_i$ | Low salinity brine used for oil recovry of core from reservoir i |
| mSW | Pretreated seawater |
| $N_b$ | Bond number |

| | |
|---|---|
| $N_c$ | Capillary number |
| $P_c$ | Capillary pressure, Pa |
| pH | A logarithmic scale used to specify the acidity or alkalinity of an aqueous solution |
| $P_o$ | Oil-Phase pressure, Pa |
| $P_w$ | Water-phase pressure, Pa |
| r | Radius of cylindrical pore channel |
| $S_{wi}$ | Initial water saturation, % PV |
| T | Temperature, °C |
| V | Velocity of the displacing phase, m/s |
| $W_d$ | Dry weight of the core |
| $W_s$ | Weight of the 100% saturated core with diluted $FW_i$ |
| $W_T$ | Target weight of the core at desired $S_{wi}$ |
| wt% | Weight percent |
| $\Delta P$ | Differential pressure, bar |
| $\Delta P$ | Pressure difference across the capillary tube, Pa |
| $\Delta P_g$ | Pressure difference between oil and water due to gravity, Pa |
| $\Delta\rho$ | Density difference between oil and water, $Kg/m^3$ |
| $\mu$ | Viscosity of flowing fluid, $N.s/m^2$ |
| $\alpha$ | Acceleration associated with the body force, almost always gravity, |
| $\theta$ | Contact angle measured through the wetting phase, degree (°) |
| $\nu$ | Average velocity in a capillary tube, m/s |
| $\sigma$ | Interfacial Tension, N/m |
| $\sigma_{os}$ | Interfacial tension between oil and solid, N/m |
| $\sigma_{ow}$ | Interfacial tension between oil and water, N/m |
| $\sigma_{ws}$ | Interfacial tension between water and solid, N/m |
| $\phi$ | Porosity, % |

# 1 Introduction and objectives

## 1.1 Oil recovery in sandstone

Siliciclastic reservoirs known as sandstone reservoirs are the major reservoirs, approximately 74% (Ehrenberg et al., 2009), and about 60% of the world discovered oil reservoirs are believed to be sandstone. The recovery factor of these reservoirs varies from 20–30% original oil in place (OOIP) up to 40–60% OOIP (Bjørlykke and Jahren, 2010). The oil recovery mechanisms from oil reservoirs have commonly been classified as primary, secondary and tertiary recovery, which are chronologically named (Green and Willhite, 1998).

### 1.1.1 Primary oil recovery

The primary recovery is the first mechanism, which refers to the production by reservoir natural energy, which is the high pressure sourced by solution gas, gas cap, water drive, fluid and rock expansion, gravity drive, or combination of some of them. Recovery factor after pressure depletion is normally up to 5 %OOIP for heavy oil and up to 25 %OOIP for light oil (Thomas, 2008).

### 1.1.2 Secondary oil recovery

As the natural drive is reducing by time, when it is insufficient to produce more oil, the secondary stage could be introduced by gas or water injection either to increase the reservoir pressure or to displace the oil to

the producer. As water is the more available source and more efficient, especially in the offshore reservoirs, the secondary stage is entitled "Water flooding"(Green and Willhite, 1998).

### *1.1.3 Tertiary oil recovery*

Tertiary oil recovery, traditionally known as enhanced oil recovery (EOR), which is the stage of recovering the residual oil remained after primary and secondary stages (Taber et al., 1997). A miscible or immiscible injection that could be obtained by gas, water, steam, polymer, surfactant, nano particles, etc. injection or combination of two of them can be targeted as a tertiary method to recover more oil. The mechanism at this stage could be mobility modification, chemical reactions or thermal processes (Ahmed and McKinney, 2005; Green and Willhite, 1998). Some EOR methods could be applied in the earlier stages despite the traditional meaning of EOR as a tertiary method, such as steam injection, which is suggested to be implemented in the earlier stages, secondary or even at the same time of primary stage (Fuaadi et al., 1991; Hanzlik and Mims, 2003).

Babadagli (2019) recently provided a new definition for EOR which covers any fluid injection with the purpose of increasing the recovery factor. He stated that EOR is: "injecting a fluid, with or without additives, to the reservoir to displace oil while changing the oil and/or interfacial properties and providing extra pressure at the secondary, tertiary, or even primary stage". Figure 1 shows the importance of investment to study and think about EOR methods in the Norwegian

continental shelf (NCS). It presents the amount of produced oil, remaining oil reserves and residual oil after planned production cessation for the 27 largest oil fields in NCS at 31 August 2019 (NPD, 2019).

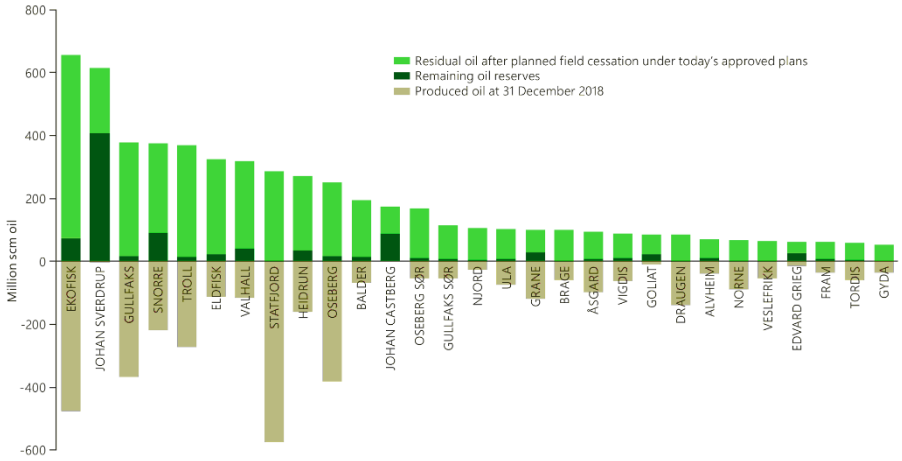


Figure 1. The amount of produced oil, remaining oil reserves and residual oil after planned production cessation for the 27 largest oil fields in NCS at 31 August 2019. (Redrawn data from NPD (2019) )

The results from figure 1, reported by Norwegian Petroleum Directorate (NPD) show an overall technical EOR potential of 320-860 million standard cubic metres (scm) at the beginning of 2019, which of course, has a significant amount of economic benefit for the companies. The report of 2016 (NPD) for the same fields predicted an average recovery factor of 47%, which can be increased by EOR methods to 52% (figure 2).

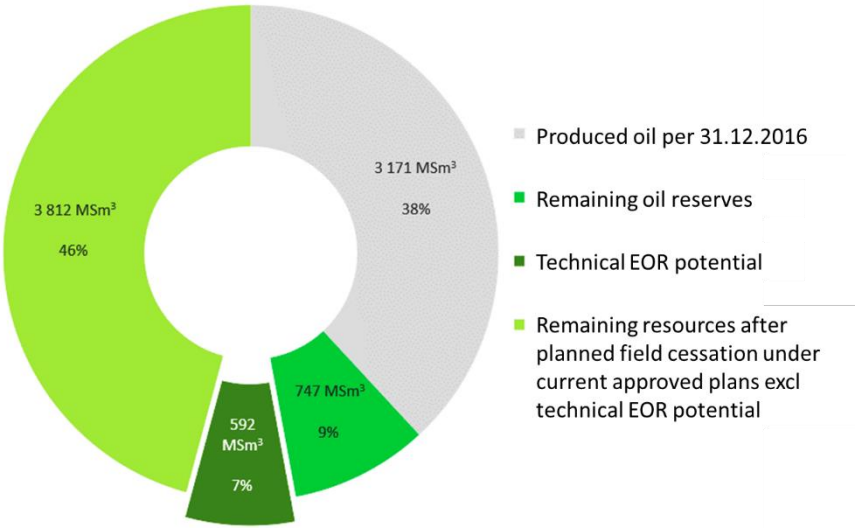


Figure 2. Technical EOR potential for the 27 largest fields in the NCS. (Redrawn data from NPD (2017) )

## 1.2 Oil recovery forces in sandstone

Different EOR methods are evaluated by their displacement efficiency, which is a factor of microscopic displacement efficiency in the pore scale and also macroscopic displacement efficiency in the areal and vertical direction towards production wells (Green and Willhite, 1998), equation 1.

$$E = E_D \times E_V \quad (1)$$

Where,

E is displacement efficiency,
$E_D$ is microscopic displacement efficiency
And, $E_V$ is macroscopic (volumetric sweep) displacement efficiency.

Green and Willhite (1998) subjected three main forces that determine the microscopic displacement in porous media. These forces are:

One of the essential aspects of the EOR process is the effectiveness of process fluids in removing oil from the rock pores at the microscopic scale. Green and Willhite (2008) describe three microscopic displacement forces for determining the fluid flow in porous media, which are: capillary forces, viscous forces, and gravitational forces.

Before explaining these three forces, two important terms, interfacial tension (IFT) and wettability, have to be briefly introduced.

### *1.2.1 Interfacial tension, IFT*

Interfacial tension arises when two immiscible fluids get in contact in a porous medium. It referes to the difference in the cohesive force in the molecular pressure across the boundary. Interfacial tension is presented by symbol σ, and it is measured by force per unit length (Ahmed and McKinney, 2005).

### *1.2.2 Wettability*

When studying the distribution of oil, water, and gas in hydrocarbon reservoirs, not only the fluid-fluid interface forces, but also the fluid-solid interface forces also must be considered. The tendency of one fluid to spread or adhere on a solid surface, in presence of another immiscible fluid is called wettability (Green and Willhite, 1998). The fluid which has spread more, is called wetting phase. A common way to stablish the

wettability of a specific crude oil-brine-rock (CoBR) system, is to measure the tangent of oil-water surface in the triple point solid-water-oil, which is called contact angle, θ. The variation of θ from zero to 180° ranges a CoBR system from strongly oil-wet to strongly water-wet, figure 3. Neutral wettability refers to a system when θ= 90°, and it means the rock surface does not have preference for any of oil and water.

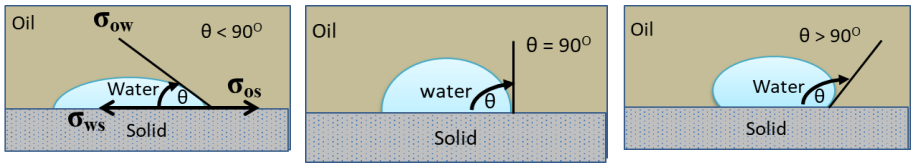


(a) Water wet (b) Neutral wet (c) Oil wet

Figure 3. Different kind of wettability in a static system. (a) Water wet, (b) Neutral wet and (c) Oil wet.

## *1.2.3 Capillary Forces*

Capillary pressure arises from pressure difference on the interface of two immiscible fluids due to surface and interfacial tensions in a porous medium. The Laplace equation shows the relationship between the curvature of the meniscus in a cylindrical capillary, which may be considered as a representation of single pore and the capillary pressure, equation 2 (Green and Willhite, 1998):

$$P_c = P_o - P_w = \frac{2\sigma_{ow}.\cos\theta}{r} \qquad (2)$$

Where:

$P_c$ : Capillary pressure

$P_o$ : Oil-Phase pressure at a point just above the oil-water interface
$P_w$ : Water-phase pressure just below the interface
$r$ : Radius of cylindrical pore channel
$\sigma_{ow}$ : Interfacial tension between oil and water
$\theta$ : Contact angle measured through the wetting phase (water)

Thus, the capillary pressure is a function of IFT and wettability, which shows itself in the contact angle. Positive values of the capillary pressure give an indication that the water phase has less pressure, and that is the wetting phase.

### *1.2.4 Viscous Forces*

Viscous forces in the porous media arise by pressure drop when flowing the fluids into the porous media. This force is dominated by viscosity and velocity of the fluid and can be calculated by equation 3.

$$\Delta P = -\frac{8\mu L\bar{v}}{r^2\, g_c} \tag{3}$$

Where:

$\Delta P$ : Pressure across the capillary tube
μ : Viscosity of flowing fluid
$L$ : Capillary tube length
$\bar{v}$ : Average velocity in a capillary tube
$r$ : Capillary tube radius
$g_c$ : Conversion factor

Viscose force is the basis of Darcy's law in porous media. In order to have fluid flow, viscose forces must overcome the capillary forces (Green and Willhite, 1998).

### *1.2.5 Gravitational Forces*

As a result of multi-phase flow in the reservoir and density difference between the fluids, phases segregation could be happened due to gravitational force which is defined by equation 4:

$$\Delta P_g = \Delta\rho . g . h \qquad (4)$$

Where:

$\Delta P_g$ : Pressure difference between oil and water due to gravity
$\Delta\rho$ : Density difference between oil and water
g : Acceleration due to gravity
h : Height of the liquid column

These forces are mostly active in immiscible floods and can cause to override of the injecting fluid when injecting fluid is light, such as immiscible $CO_2$ injection (Abdelgawad and Mahmoud, 2015)) or it can lead to gravity under-ride when the situation is opposite such as water flooding. Gravitational effects could be negligible when performing the oil recovery test in the core samples, which are small in size, i.e. 4 cm diameter and 7 cm height.

### *1.2.6 Flow Regime Characterization*

Water based EOR processes at reservoir porous media are influenced by capillary, viscous, and gravitational forces. The interplay of these three could be represented by two dimensionless numbers of Bond Number, and Capillary number (Green and Willhite 1998).

### 1.2.6.1 **Bond Number**

Bond number denoted as $N_b$, characterizes the ratio of gravitational forces to capillary forces, which has importance in vertical displacements:

$$N_b = \frac{Gravity\ force}{Capillary\ force} = \frac{\rho\ a\ L^2}{\sigma} \quad (5)$$

Where:

$N_b$ : Bond number (dimensionless),
$\rho$ : Density, or the density difference between fluids ($\Delta\rho$),
$a$ : Acceleration associated with the body force, almost always gravity,
L : "characteristic length scale", e.g. radius of a drop or the radius of a capillary tube,
and $\sigma$ : is the surface tension of the interface.

### 1.2.6.2 **Capillary number**

The dimensionless magnitude of the ratio between viscose and capillary force is denoted as Capillary number. There are many expressions for Capillary number (Taber, 1981), one of the most commonly used form is defined by Moore and Slobod (1955) as:

$$N_c = \frac{Viscose\ force}{Capillary\ force} = \frac{V\ \mu_w}{\sigma_{ow} \cos\theta} \quad (6)$$

Where

$N_c$ : Capillary number (dimensionless),

$\sigma$ : Interfacial tension between the two immiscible fluids (N $m^{-1}$),
V : Velocity of the displacing phase (m $s^{-1}$),
$\mu$ : Displacing fluid viscosity (N s $m^{-2}$),
$\theta$ : Contact angle (degrees, °),
and subscripts w and o denote displacing and displaced phase, respectively water and oil in water based EOR.

Laboratory experiments resulted in that the oil recovery in immiscible EOR methods increased when viscose forces are increased and overcome the capillary forces which are responsible for oil entrapments. Moore and Slobod (1955) and also Abram (1975) attempted to correlate the residual oil saturation as a function of capillary number, figure 4. They concluded that to increase the oil recovery, i.e. reduction in residual oil saturation, the capillary number must be increased. This can happen by increasing the velocity of injection fluid or its viscosity, which means the creation of a favourable mobility ratio, or by reducing the interfacial tension and of course, by optimizing of contact angle (Lake, 1989).

Considering the limitations of injection facilities in compare to the enormous volume of reservoir, the big variation in velocity is not achievable. Favourable mobility and IFT can be achieved respectively by polymer injection and adding surfactants to the injection water. Both methods are extremely expensive so that can not be even examined in a single reservoir. Following restrictions emphasizes the importance of fourth parameter, which is change in contact angle, i.e wettability alteration (Abrams, 1975; Green and Willhite, 1998; Johannesen and Graue, 2007; Lake, 1989).

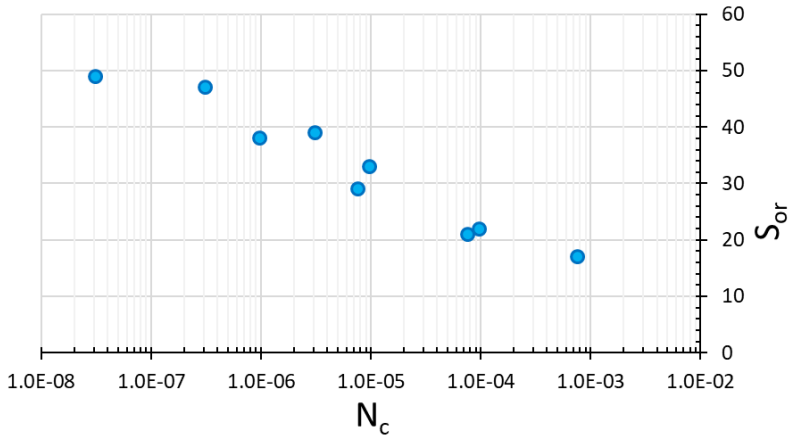


Figure 4. Illustrating the relationship between $N_c$, the capillary number, given in Equation 6 and the residual oil saturation, $S_{or}$ (Redrawn with data from Moore and Slobod (1955))

Note: The values of $N_c$ in this chart are multiplied by100 due to the use of pois as unit of μ instead of cp, which is the unite Morre, and Slobod plotted their chart based on it.

## *1.3 LS Smart Water flooding as a low cost environmentally friendly EOR method*

Over the past decade, low salinity (LS) water flooding has been considered as one of the high ranked options to be applied in many sandstone oil reservoirs. NPD using an extensive screening of different EOR methods on each of the oil fields placed in NCS, proved that LS EOR is among high potential methods, which can significantly reduce the residual oil saturation, figure 5 (NPD, 2019). In addition to pure low salinity method, a hybrid method such as LS brine injection combined with polymer injection also proved to have a high potential specially in

the Utsira High and the surrounding area located in the North Sea (Smalley et al., 2018).

The LS EOR method has two main advantages in addition to successful field trials and laboratory reports, which cause it to be promising for future plans of the oil reservoirs. The main advantages are relatively low cost of the implementation for both offshore and onshore fields and the second benefit that must be considered is environmental issues, and it has been qualitatively reported that LS EOR is among the most environmentally friendly methods.

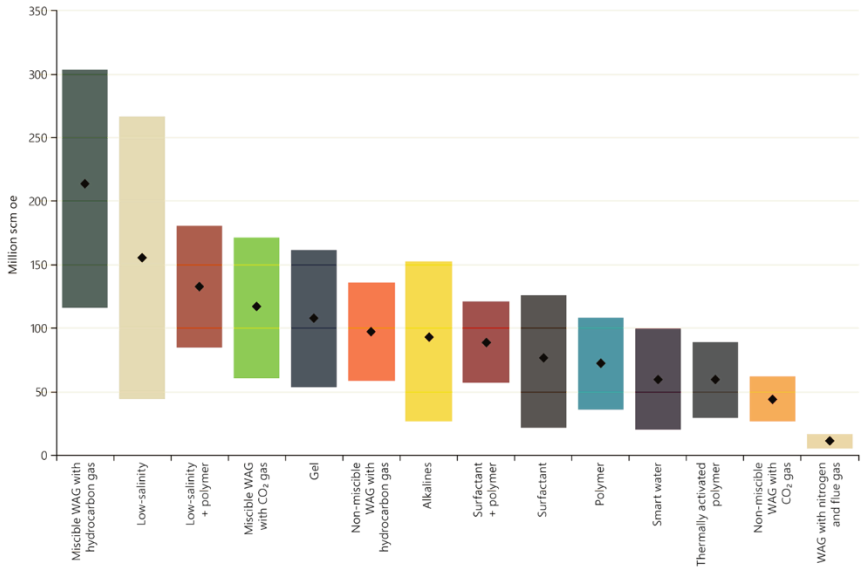


Figure 5. EOR potential considering the technical potential multiplied by operational and economic factors, based on the investigations performed on 27 largest NCS oil fields at the end of 2018. (Redrawn data from NPD (2019)).

### *1.3.1 Costs of implementing LS EOR*

One of the critical factors that influence the implementation of any EOR project is economic issues. Considering the expected amount of extra oil recovered, building water desalination plants, and oil price, the LS EOR method has been considered as one of the beneficial EOR methods especially for the reservoirs, which are nearby an appropriate aquifer (Althani, 2014; Reddick et al., 2012).

Forasmuch as all the factors, BP reported that they are expecting to recover over 40 million additional barrels of oil using LS EOR method at the Clair Ridge Field, UK, by a development cost of only 3 $/bbl (Mair, 2010; Robbana et al., 2012). Layti (2017) also simulated economic potential of LS EOR at the Clair Ridge Field, and she concluded that by the implementation of LS EOR method in Clair Ridge field, the net present value will be about 697$ million, where 6% increase in recovery will be achieved by only 2% increase in investments. In addition, she emphasized the importance of secondary LS EOR by reckoning of 37 million barrels extra oil compared to the tertiary LS EOR. Abdulla et.al (2011) also economically investigated the LS EOR project in the Burgan Wara field in Kuwait with considering all the uncertainties and they confirmed that this method could be economically efficient for a reduction of 1% of the $S_{or}$ even at low oil price condition.

### *1.3.2 Environmental Issues*

There is a lack of documented discussion about the different aspects of environmental issues linked to LS EOR. Donaldson et al. (1989) subjected eight issues that could be concerned in different types of EOR methods which are: atmospheric emissions, water use, water quality impacts, waste water effluents, solid wastes, occupational safety and health, physical disturbances and noise. Researchers agree that the LS EOR method is among the most environmentally friendly methods. The main worry is about sludges, salts, and high harnesses, which are expelled from the input of the desalination plant either by nanofiltration or reverse osmosis method. In addition, reduction of sulphate ion, which is the case in most of the common LS brines, will reduce the risk of souring and scaling problems in the pipelines and also the reservoir by itself (Hardy et al., 1992).

## *1.4 LS Smart Water EOR mechanism by wettability alteration*

In order to be able to make a strategy for optimal water flooding of oil reservoirs, detailed knowledge about initial properties and relevant parameters, which have influence on the wetting conditions, are needed. Improved chemical understanding about the rock fluid interaction during the last years has made it possible to take benefit on wettability modification to improve oil recovery during water flooding. The wetting properties have great impact on important physical parameters like

capillary pressure, $P_c$, and relative permeability of oil and water, $k_{ro}$ and $k_{rw}$. In the following some important issues are commented.

***Formation water salinity:*** Morrow and co-workers performed parametric studies on oil recovery using the same brine as both FW and flooding fluid, and they observed an increase in oil recovery when using a LS brine compared to a HS brine (Morrow et al., 1998; Tang and Morrow, 1997). In those cases, no wettability alteration took place during the flooding because the injected water, FW, was already in equilibrium with the system. The authors explained the results by increased capillary trapping of oil using the HS brine, which means that the rock became more water wet at high salinities compared to low salinities.

***Wetting condition for optimum oil displacement*** It is well documented by laboratory work that the optimum in oil recovery by water flooding was obtained at neutral to slightly water wet conditions (Jadhunandan and Morrow, 1995; Tang and Morrow, 1999).

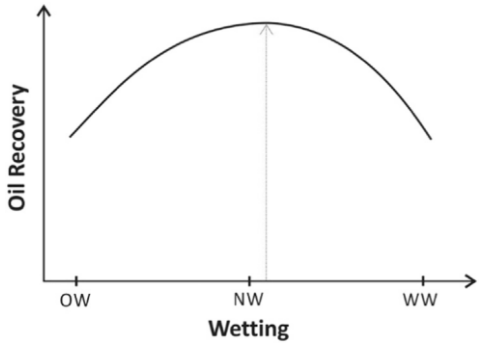

Figure 6. Maximum waterflood oil recovery at neutral to slightly water-wet conditions. OW=oil-wet, NW=neutral-wet and WW=water-wet. (Redrawn after Jadhunandan and Morrow (1995)).

***Wettability alteration by induced pH gradient:*** Buckley and Morrow tested adhesion properties of 22 crude oils onto silica surfaces as a function of brine composition and, pH and, noticed remarkable similarities in the results. In the adhesion map, they observed characteristic pH values in the range of 6-7, above which, adhesion did not occur at different salinities, and they concluded that the pH was the dominant factor (Buckley and Morrow, 1990). Similar results were recently confirmed by Didier et al.(2015) in adhesion studies of crude oil using two different sands. At given pH, it was also observed that the adhesion of oil increased by lowering the salinity, i. e. in direct contradiction to the ionic double layer model and the DLVO theory, which has been used by many researchers to explain the LS EOR mechanism (Ligthelm et al., 2009).

The mechanism for wettability modification by LS or "*Smart Water"* was proposed by Austad et al. and can be illustrated chemically by the following equations (Austad, 2013; Austad et al., 2010; Rezaeidoust et al., 2010):

$$\text{Clay-}Ca^{2+} + H_2O = \text{Clay-}H^{+} + Ca^{2+} + OH^{-} + \textbf{heat} \quad (7)$$

Slow reaction

$$\text{Clay-}R_3NH^{+} + OH^{-} = \text{Clay} + R_3N: + H_2O \quad (8)$$

Fast reaction

$$\text{Clay-RCOOH} + OH^{-} = \text{Clay} + RCOO^{-} + H_2O \quad (9)$$

Fast reaction

A schematic of the reaction involved in Smart water EOR by a LS brine is illustrated in figure 7.

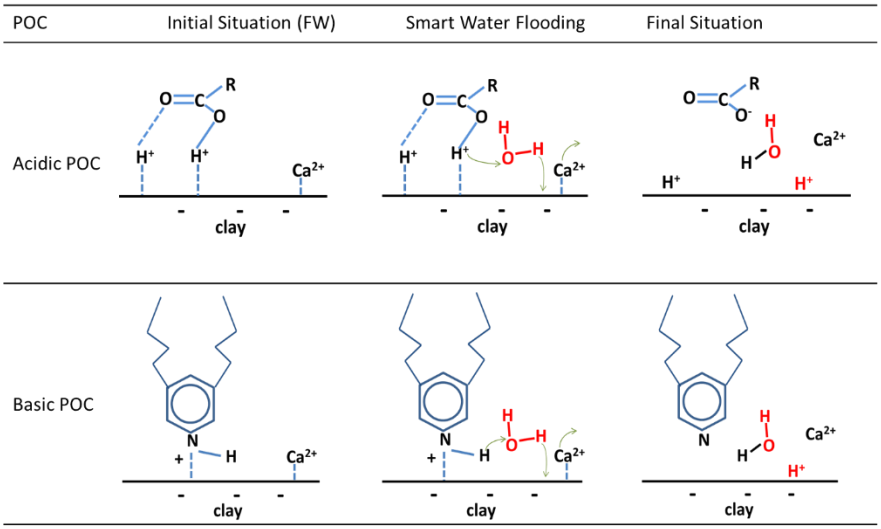


Figure 7. Illustration of chemical reactions involved in wettability alteration by a LS brine (Redrawn from Austad et al.,(2010).

Analysis and calculations have shown, that it is only a very small fraction of the desorbed $Ca^{2+}$ ions from the clay surface that are exchanged by $H^+$. It should also be noticed that the desorption of active cations from the clay minerals, equation 7, is an exothermic process, meaning that the imposed pH gradient when switching from HS to LS brine will be smaller. It is therefore difficult to observe LS EOR effects at high temperatures, $T_{res}$>100 $^oC$ (Aksulu et al., 2012).

Static adsorption studies on clay minerals using both model compound and crude oil are supporting the suggested mechanism by confirming maximum adsorption of organic material close to pH≈5 and that the

adsorption decreased as pH increased, figure 7 (Fogden, 2012; Fogden and Lebedeva, 2011; RezaeiDoust et al., 2011).

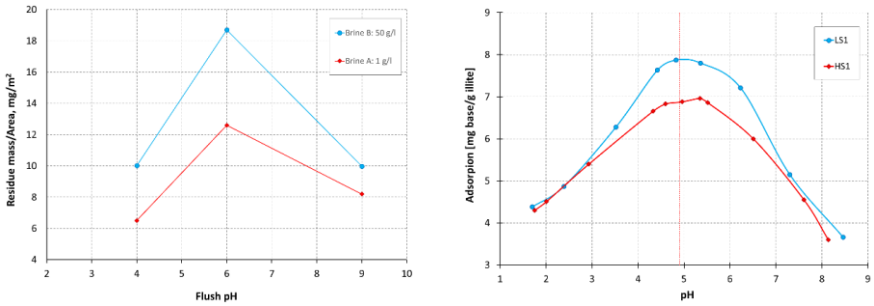


(a) (b)

Figure 8. (a) Adsorption of crude oil sample onto kaolinite in contact with brines of varying concentration and pH. (Redrawn with data from Fogden (2012)), (b) adsorption of Quinoline onto illite as a function of pH in presence of high and low salinity brine (Redrawn with data from Aksulu et al. (2012)).

In the LS two-well pilot test in the Endicott field in Alaska, BP made several chemical observations of the produced water from the production well, which are in complete agreement with the proposed mechanism (Lager et al., 2011; RezaeiDoust et al., 2011).

The induced pH gradient is the key parameter to promote wettability modification in sandstone oil reservoirs. Normally, the LS EOR effect is related to mixed wet conditions or close to optimum wetting conditions for water flooding. The “Smart Water” or LS brine improves the water wetness to achieve a better microscopic sweep efficiency due to increased capillary forces. The imposed pH gradient as the HS formation brine is exchanged with the Smart Water depleted in divalent cations, like $Ca^{2+}$, will cause a redistribution of the residual oil in the porous network as the rock becomes more water wet.

# 2 Objective

Offshore sandstone oil reservoirs are usually flooded with seawater for two reasons: to give pressure support and to displace the oil towards the producing wells. At low temperatures, if the salinity difference between the formation water initially in place and the injected seawater is significant, excluding other parameters, the concentration difference of active cations could make a potential to recover more oil by wettability alteration (Austad et al., 2010), and seawater act as a "Smart Water" EOR-fluid and get an incremental oil recovery factor. But how it will be if the reservoir temperature is high? This is an actual topic for the North Sea sandstone oil reservoirs, which is one of the main objective of this PhD thesis; "*If seawater can act as a smart water at high temperature*"?! and if that is the case, is there still a further potential for improved oil recovery by subsequently injecting an "even smarter" fluid, LS, in a tertiary waterflood? What are the requirements for obtaining low salinity EOR-effects in a tertiary flooding process?

To investigate these issues, about 40 surface reactivity and oil recovery tests have been performed using 15 preserved reservoir cores which were obtained from four different high temperature North Sea oil reservoirs. The material and methodology are explained in section 3 and the main results are presented and discussed in section 4.3.

Alongside the oil recovery test, to improve our chemical understanding of the low salinity EOR-mechanism in sandstones, it was planned to

perform some parametric studies on the key factors dictating both the initial wetting condition and wettability alteration process. Numerous static three phase (Crude oil-Brine-Rock, CoBR) studies and dynamic two phase Rock-Brine studies were performed to obtain a conclusion based on the promising reproducible results presented in section 4.1 and 4.2.

# 3 Experimental methodology

This study consists of two main series of experiments, firstly some fundamental parametric study and secondly oil recovery experiments included both forced and spontaneous oil recovery. In the following section of chapter 3, the materials used and also the methods applied on each set of experiments are explained, and in the end, the performed analyses are briefly listed and described. It must be noticed that nomenclatures of materials and tests may vary for the ones mentioned in the papers.

## *3.1 Materials*

### *3.1.1 Minerals*

Pure quartz, kaolinite clay, and illite clays are used in this study. The detailed information is presented in the following sections.

#### 3.1.1.1 **Quartz**

Quartz is one of the most common minerals found in clastic rock. The crystal structure is built up of $SiO_2$ unit-cell and can be noticed by their unique shape. To make a sand pack and mimic physical properties of real sandstone rock material (porosity and permeability) and to keep small clay particles immobile, a mixture of fine (>8.4 μm) and coarse (>8.4 μm) milled quartz provided by Sibelco company, previously known as North Cape, was used. Target particle size was achieved using

cylindrical containers, filled with a slurry of milled quartz and distilled water, and applying Stoke`s law (Rhodes 2008) on the settling time of particles with two main assumptions: (1) Particles are spherical and (2) Settling happens at Reynolds number less than two. Figure 9 shows that particle sizes are from 8 μm up to ~500 μm

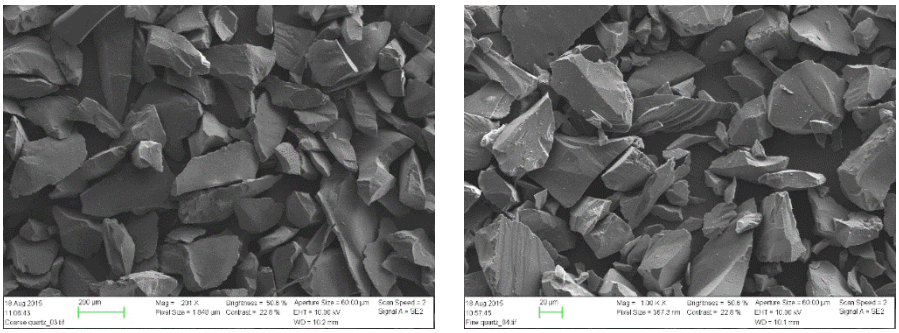

(a) (b)

Figure 9. SEM image of fine quartz clay provided by PROLABO: (a) Coarse particles with a magnification of 201 and (b) fine particles with a magnification of 1000.

### 3.1.1.2 **Kaolinite**

Kaolinite clay was provided by PROLABO in the form of very fine particles. SEM picture of the kaolinite clay prior to use in packing shows that the particle sizes are in the range of few micrometers, μm (figure 10). The surface area of the cleaned kaolinite particle measured by BET analysis was 13 $m^2/g$.

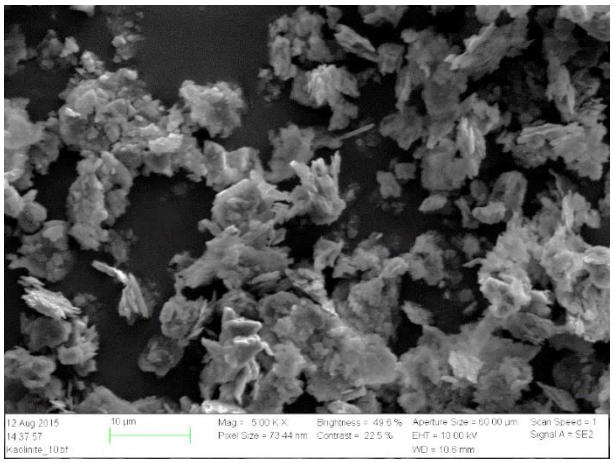


Figure 10. SEM image of kaolinite clay provided by PROLABO with a magnification of 5000

### 3.1.1.3 **Illite**

Illite clay was provided by Ward´s Natural Science Establishment. It is sampled in the form of green shale containing about 85 % illite from Rochester formation in New York. It was crushed and milled into powder with a particle size of a few μm. Then to remove any impurities, possible divalent cations on the clay surface, and precipitated salts on it, the milled illite was cleaned and protonated with 5 M hydrochloric acid at pH~3. Lastly, the Illite was washed with distilled water (until the pH adjusted about 5) and dried at 90 ºC. Figure 11 shows that particle sizes of illite clay, after cleaning procedures, are in the range of a few μm. The surface area of the cleaned illite particle measured by BET analysis was 22 $m^2/g$.

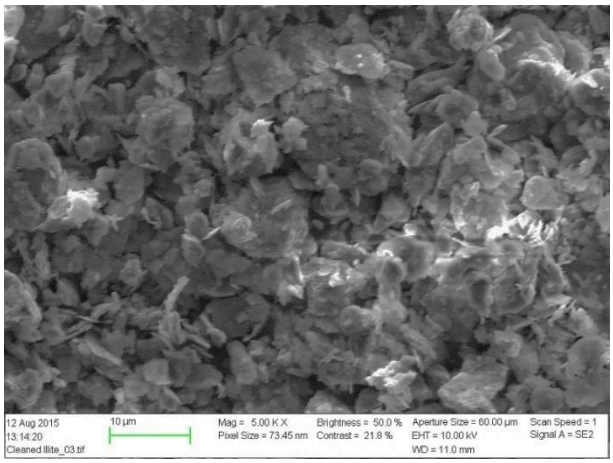


Figure 11. SEM image of cleaned Illite clay provided by Ward´s Natural Science Establishment with a magnification of 5000

### *3.1.2 Sand pack*

Sand packs were prepared to fundamentally study the effect of some important parameters involved in the LS smart water EOR mechanism such as clay presence, active cations, and temperature. The packings have done in a Polyether Ether Ketone (PEEK) cell, which was the sand pack holder during the experiments too. PEEK is a semi-crystalline thermoplastic (up to 260) with excellent mechanical and chemical resistivity (Park and Seo, 2011), which ensure the secure condition during the experiments at low and high temperatures. To avoid trapping of air bubbles in the column and to prevent swelling of clays, wet packing was performed using a low concentration of NaCl brine. Both end caps of the sand pack cell contain a PEEK filter. The filter distributes the fluid through the sand column in each side and also prevents movements of the particle into the tube line.

To investigate the role of different minerals, three different sand packs with different mineralogy were made (Table 1). One containing only pure quartz particle (SP#1), the second sand pack (SP#2) was made by a mixture of quartz and about 8%wt kaolinite by wet packing. The porosity of 29.9% confirms very good packing, which can be a good sandstone representative. The third and fourth sand packs (SP#3 and SP#4) are made by wet packing of a mixture of illite clay and quartz, resulted in a sand pack with a porosity of ~31%.

Table 1. Sand pack properties for SP#1-4.

| SP# | Quartz [wt%] | Kaolinite [wt%] | Illite [wt%] | Pore Volume, PV [ml] | Porosity, Φ [%] | Permeability, k [mD] |
|---|---|---|---|---|---|---|
| 1 | 100 | -- | -- | 12.0 | 32.8 | 7.0 |
| 2 | 92.1 | 7.9 | -- | 10.8 | 29.9 | 3.0 |
| 3 | 91.1 | -- | 8.9 | 11.4 | 30.8 | 2.8 |
| 4 | 89.9 | -- | 10.1 | 11.2 | 31.1 | -- |

### *3.1.3 Reservoir cores*

15 different preserved reservoir cores were used in this PhD project. They are sampled from five different reservoirs: Reservoir M, reservoir P, reservoir T, reservoir Y, and reservoir L. This thesis only includes the main results from six cores originated from three Reservoirs M, P and T. Mineralogical data from a representative rock sample was obtained by either XRD analysis or QEMSCAN analysis, performed by oil companies and Rocktype Ltd, UK, respectively. Physical core properties and also mineralogical data for each set of the test are presented in table

2 and 3, respectively. Note that during core cleaning, dissolution of anhydrite, $CaSO_4$ (s), were detected in some of the water effluent samples, while anhydrite minerals were not detected in the XRD or QEMSCAN analysis.

Table 2. Physical core properties

| Core | Length, cm | Diameter, cm | Pore Volume, ml | Porosity, % | Permeability $^{*}k_{wro}$, mD | $^{**}$BET, $m^2/g$ |
|---|---|---|---|---|---|---|
| M3 | 7.03 | 3.84 | 11.82 | 14.6 | 9.0 | 0.92 |
| M5 | 7.25 | 3.84 | 11.64 | 13.9 | 8 | 0.97 |
| P41 | 6.99 | 3.78 | 14.61 | 18.6 | -- | 0.75 |
| P49 | 5.57 | 3.78 | 13.97 | 22.3 | -- | 1.00 |
| T1 | 5.53 | 3.87 | 14.3 | 21.9 | 3.4 | 3.36 |
| T2 | 5.26 | 3.78 | 14 | 23.7 | 3.4 | 4.14 |

*$k_{wro}$ : NaCl (1000 ppm) permeability at $S_{or}$ (heptane) during the first restoration

**BET: Specific surface area using TriStar II PLUS from Metromeritics®.

Table 3. Mineralogical data of the cores

| Sample# / Minerals | Reservoir M M3 & M5 | Reservoir P P41 & P49 | Reservoir T T1 & T2 |
|---|---|---|---|
| Quartz | 75.01 | 88.53 | 50.24 |
| K-Feldspar | 9.82 | 0.04 | 20.94 |
| Albite | 4.17 | 0.05 | 9.19 |
| Biotite | 0.04 | 0 | 0.15 |
| Muscovite | 3.19 | 4.41 | 1.28 |
| Illite | 0.33 | 0.24 | 1.54 |
| Chlorite | 0.38 | 0 | 0.09 |
| Kaolinite | 4.39 | 5.33 | 0.01 |
| Smectite | 0.19 | 0.29 | 0.33 |
| QuartzClayMix | 0.11 | 0.44 | 3.37 |
| OtherClays | 0.83 | 0.36 | 2.15 |
| Heulandite | 0.06 | 0.15 | 0.31 |
| Rutile_Anatase | 0.41 | 0 | 0.27 |
| Apatite | 0 | 0 | 0.12 |
| Calcite | 0 | 0.01 | 0.02 |
| Dolomite | 0 | 0 | 4.71 |
| FeDolomite | 0 | 0 | 3.88 |
| FeOxides | 0 | 0 | 0.13 |
| Pyrite | 0.31 | 0.1 | 0.48 |
| Other minerals/Phases | 0.73 | 0.02 | 0.51 |
| Unclassified | 0.03 | 0.03 | 0.28 |
| *Total* | *100* | *100* | *100* |

### *3.1.4 Quinoline*

Quinoline ($C_9H_7N$) is a heterocyclic aromatic organic compound which is delivered by Merck by the purity of >97%. Quinoline can be slightly dissolved in the cold distilled water at low concentrations and controlled pH, but it is easily dissolvable in the water at higher

temperatures (Jones, 1997). Initially, a ~0.07M quinoline stock solution is made by adding pure Quinoline to distilled water at pH 5. Mixing of a low salinity brine (LS), a high salinity brine (HS), a brine containing only $CaCl_2$ (HSCa) and a special formation water (FW) with a particular portion of stock Quinoline solution produce respectively a low salinity brine-quinoline solution (LSQ), high salinity brine-quinoline solution (HSQ), high salinity Ca brine-quinoline solution (CaQ) and formation water brine-Quinoline solution (FWQ) with desired optimum concentration of 0.01 M Quinoline. The composition of each brine listed in section 3.1.4.2.

### *3.1.5 Crude Oil*

Three stabilized reservoir crude oils from different fields were delivered by oil companies. The crude oils were centrifuged to remove any solid particles and brines. Then the oils were filtered through a 5.0 µm filter paper to remove any dispersed particles in the crude oil. The physical properties of the crude oils, such as density, viscosity, acid and base numbers were measured and are listed in table 4.

Table 4. Physical and chemical properties of stabilized crude oil

| | AN (mg KOH/g) | BN (mg KOH/g) | Asphaltenes (wt%) | Density@20 °C ($g/cm^3$) | Viscosity@20°C (cp) |
|---|---|---|---|---|---|
| Oil M | 0.16 | 0.76 | 1.1 | 0.85 | 7.0 |
| Oil P | <0.05 | 1.35 | 0.6 | 0.85 | -- |
| Oil T | 0.04 | 0.77 | 1.2 | 0.84 | 6.6 |

### *3.1.6 Brines*

The brines synthetically made in the laboratory based on the compositions either designed by Smart Water EOR group at UiS (used in static and dynamic fundamental studies) or specifically given by companies along with different core materials. Brines are prepared by mixing deionized water (DI) and Chemicals which are delivered by Merck laboratories. The brines were stirred for about one hour and then filtrated using a 0.22 µm membrane filter using a vacuum pump to prevent the presence of any gas dissolved and unsolved particles.

The detailed brine compositions of each set of experiments are listed in the following.

#### 3.1.6.1 **Brines used in $Ca^{2+}$/$Mg^{2+}$ Ads. /Des. study**

Synthetic brines were used to study the reactivity of active divalent cations towards quartz, kaolinite, and illite surfaces in adsorption/desorption tests. Pure NaCl brine termed B was used as the base brine for initial saturation of the sand pack, and also during the desorption studies of $Ca^{2+}$ and $Mg^{2+}$ ions. The brines containing $Ca^{2+}$ and $Mg^{2+}$ as active cations with $Li^{+}$ as a tracer were termed BCL and BML, respectively. The last brine, termed BCM, contained both $Ca^{2+}$ and $Mg^{2+}$ and was used to compare the affinity of the two cations towards the kaolinite. Brine compositions and properties are given in table 5.

Table 5. Brines composition and properties used in active cations Ads. /Des. study

| Ion \ Brine | B (mM) | BCL (mM) | BML (mM) | BCM (mM) |
|---|---|---|---|---|
| $Na^+$ | 40.2 | 40.2 | 40.2 | 40.2 |
| $Li^+$ | -- | 10.0 | 10.0 | -- |
| $Ca^{2+}$ | -- | 10.0 | -- | 10.0 |
| $Mg^{2+}$ | -- | -- | 10.0 | 10.0 |
| $Cl^-$ | 40.2 | 70.2 | 70.2 | 80.2 |
| Ionic Strength, IS (M) | 0.04 | 0.08 | 0.08 | 0.10 |
| TDS (mg/l) | 2350 | 3882 | 3725 | 4413 |

mM $=10^{-3}$ mole/l

### 3.1.6.2 **Brines used in quinoline Ads. /Des. study**

Four brines with different salinities/compositions were prepared based on the procedure described in section 3.1.3. The compositions are listed in Tables 6 and 7.

Table 6. Brine compositions and properties used in Quinoline Ads. /Des. study

| Ion \ Brine | HS (mM) | LS (mM) | HSCa (mM) | FW (mM) |
|---|---|---|---|---|
| $Na^+$ | 355.0 | 13.7 | - | 2384 |
| $Ca^{2+}$ | 45.0 | 1.7 | 270.3 | 613 |
| $Mg^{2+}$ | 45.0 | 1.7 | - | 164 |
| $Ba^{2+}$ | -- | -- | -- | 8 |
| $Sr^{2+}$ | -- | -- | -- | 9 |
| $Cl^-$ | 535.0 | 20.5 | 540.6 | 4030 |
| IS (M) | 0.624 | 0.024 | 0.811 | 4824 |
| TDS (mg/l) | 30000 | 1150 | 30000 | 230000 |

mM $=10^{-3}$ mole/l

Table 7. 0.01 M quinoline-brine solutions used in the Ads. /Des. study of quinoline onto illite(Aksulu et al., 2012), kaolinite, and quartz.

| Ion \ Brine | HSQ (mM) | LSQ (mM) | CaQ (mM) | FWQ (mM) |
|---|---|---|---|---|
| $Na^+$ | 295.9 | 11.7 | 0.0 | 2085.8 |
| $Ca^{2+}$ | 37.5 | 1.5 | 225.3 | 536.1 |
| $Mg^{2+}$ | 37.1 | 1.5 | 0.0 | 143.9 |
| $Ba^{2+}$ | -- | -- | -- | 7.0 |
| $Sr^{2+}$ | -- | -- | -- | 7.9 |
| $Cl^-$ | 445.1 | 17.6 | 450.6 | 3526.0 |
| IS (M) | 0.520 | 0.021 | 0.676 | 4.221 |
| TDS, mg/l | 24 990 | 990 | 25 000 | 201 560 |

#### 3.1.6.3 **Brines used in oil recovery tests**

For each set of oil recovery test performed on the cores from known reservoir **i**, three main brines were used. The notation of brines used are **$FW_i$** for formation water from reservoir **i**. **SW** for north seawater, **mSW** for pretreated seawater to reduce scaling problem by sulfate removal by membrane filtration. **$LS_i$** is a low salinity brine based on different receipts i.e 20 times diluted **FW** or **SW** or **mSW** received by company **i**.

Table 8 lists the ion composition and properties of the brine used in oil recovery tests.

Table 8. Brines composition and properties used in oil recovery tests

| | SW (mM) | mSW (mM) | $FW_m$ (mM) | $FW_p$ (mM) | $FW_t$ (mM) | $LS_m$ (mM) | $LS_p$ & $LS_t$ (mM) |
|---|---|---|---|---|---|---|---|
| $Na^+$ | 450 | 477.2 | 929.8 | 370.9 | 2563.2 | 23.9 | 17.0 |
| $K^+$ | 10 | 8.1 | 17.8 | 3.1 | 58.8 | 0.4 | 0.4 |
| $Ca^{2+}$ | 13 | 8.2 | 44.2 | 3.5 | 123.8 | 0.4 | 0.3 |
| $Mg^{2+}$ | 45 | 13.5 | 7.0 | 1.4 | 18.3 | 0.7 | 1.8 |
| $Ba^{2+}$ | - | - | 5.2 | 0.6 | 0.6 | - | - |
| $Sr^{2+}$ | - | - | 3.0 | 0.9 | 0.9 | - | - |
| $HCO_3^-$ | 2 | 0.3 | 7.7 | 2.7 | 3.4 | 0.02 | - |
| $Cl^-$ | 525 | 527.9 | 1058.8 | 384.0 | 2905.7 | 26.4 | 19.9 |
| $SO_4^{2-}$ | 24 | 0.4 | - | - | - | 0.02 | 0.8 |
| TDS (mg/l) | 33390 | 30725 | 63000 | 22763 | 170010 | 1536 | 1245 |
| ρ* ($g/cm^3$) | 1.024 | 1.020 | 1.042 | 1.014 | 1.133 | 0.999 | 0.999 |
| μ* (cP) | 0.99 | 0.99 | 1.07 | 0.97 | >1.3 | 0.94 | 0.99 |
| pH* | 7.6 | 7.0 | 6.8 | N/A | 6.1 | 6.4 | 6.8 |

* Measured at @ 20°C

## *3.2 Methodology*

### *3.2.1 Active cations adsorption/desorption study:*

The activity of $Ca^{2+}$ and $Mg^{2+}$ ions towards different minerals, as two main ions involved in the wetting properties of reservoirs, are studied using synthetic sand packs (properties are described in section 3.1.2).

The sand pack is vertically positioned in a heating chamber, and the brines are injected using a Gilson HPLC-pump from top to reduce/prevent mobilization of fine particles. The flow rate is adjusted to 4 PV/D, and the tests are performed at 10 bar using a backpressure valve.

Prior to each test, the sand pack was saturated and equilibrated with the base brine, brine B, which is 40.2 mM NaCl brine. Each test is consisting of a dynamic key ions adsorption process followed by dynamic key ions desorption using base brine, Brine B.

The dynamic process is performed by flooding of brines BCL or BML or BCM, and it is continued until the relative concentration of the key ions in the effluent was ~1, i. e. $[Ca^{2+}(ad)] / [Ca^{2+}(aq)]$ ~1. Then the dynamic desorption was

Then, desorption was deliberate by flooding with brine B. Due to the difference in concentration of active cation, the desorption will take place. The flooding of brine B was continued until the least amount of $Ca^{2+}/Mg^{2+}$ was detected in the effluent. The tests were performed at 23 and 130 °C.

The schematic of the active cations Ads./Des. study is shown in figure 12.

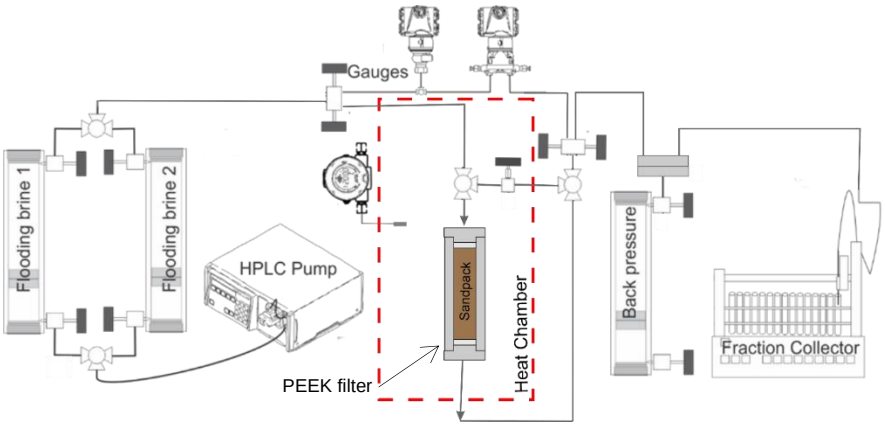


Figure 12. Illustration of active cations adsorption/desorption study set up

### *3.2.2 Quinoline adsorption/desorption study*

To investigate the oil phase interactions with rock surface, the adsorption of quinoline, as a polar basic organic component, onto different minerals exists in sandstone rock materials is investigated using different brines at T= 23 and 130 °C with distinctive pHs in parallel batch samples.

Each test consists of a batch sample which is a mixture of 10 wt% mineral powder in contact with 0.01 M brine-quinoline solution in an 18 ml gas sealed HT-sample glasses. To adjust the pH and prevent change in the total salinity and weight of each sample very small volumes (few µl) of concentrated HCl and NaOH solutions (1M) were used. Then the sample equilibrated for 24 h at either T=23 °C or T= 130 °C using a rotator (2-3 rpm). After 24 hours keeping the Quinoline-brine solution in contact with mineral, the sample was centrifuged for 20 min at 2500 rpm in a Hettich Universal 1200 centrifuge at T=23 °C. For the high

temperature experiments, it is assumed there will be no change in the amount of adsorbed Quinoline by reduction of temperature from 130 to 23°C due to immediate centrifuging of the samples and thus separation of liquid and solid phases. A mass balance between quinoline concentration in the supernatant and the original quinoline solution indicates the amount of adsorption.

## *3.2.3 Core cleaning*

Reservoir cores went through a standard mild cleaning process using Kerosene and n-Heptane, before performing the oil recovery and pH screening tests. Then the cores were flooded with 1000 ppm NaCl for four PV to remove any dissolvable salts. The presence of dissolved sulphate in effluent samples was detected manually by adding $Ba^{2+}$ to a portion of each samples and the quantity is monitored by analysing their composition using an ion chromatograph (IC). If needed. the depletion process of sulphate was continued until the $SO_4^{-2}$ concentration was less than 0.1 mM. The presence of $SO_4^{-2}$, could be explained as anhydrite ($CaSO_4$) presence initially in the core. At the end, the cores were dried at 60-90 °C and dry weight of each core was measured.

## *3.2.4 Core Restoration*

### 3.2.4.1 **Initial water saturation**

Initial FW saturation ($S_{wi}$) was established in the cleaned and dried cores using the desiccator technique (Springer et al., 2003). A dry core was

evacuated and placed on marbles inside a plastic container situated inside a desiccator. Firstly, the set up completely vacuumed to remove any gas inside the core. Then the diluted formation water was slowly poured into the plastic container until the core is fully submerged in the saturation brine. Figure 13 illustrates the setup schematic of the 100% diluted formation water saturation apparatus. The initial water saturation percentage compare to the 100% saturation tells us how much the dilution degree must be. In the end, the 100% saturated core with diluted $FW_i$ brine must be placed inside a sealed desiccator containing silica gel at the bottom, until the desired initial water saturation is achieved by evaporation of water molecules. Equation 10 shows the relation to calculate the desired weight after the evaporation process.

$$W_T = (W_s - W_d)S_{iw} + W_d \quad (10)$$

Where:

$W_T$ : Target weight of the core at desired $S_{wi}$
$W_s$ : Weight of the 100% saturated core with diluted $FW_i$
$W_d$ : Dry weight of the core
$S_{wi}$ : Initial water saturation as a fraction of the pore volume

To get an equilibrated $FW_i$ distribution, the core placed in a sealed container for three days.

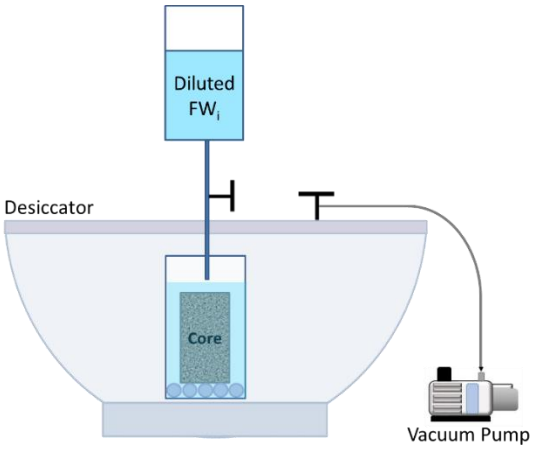


Figure 13. Schematic of 100% diluted $FW_i$ saturation

#### 3.2.4.2 **Initial crude oil saturation**

The core with a $S_{wi}$ establishment was inserted into a rubber sleeve and placed in Hassler core holder, and it the whole set up was gently vacuumed to remove all the gas from lines and inside the core. The core was then flooded with 4 PV of reservoir oil (2 PV from each side) at 50 °C.

Finally, the saturated core was aged at reservoir temperature, under the pressure, for two weeks.

### *3.2.5 Surface reactivity test-pH screening*

pH screening tests are designed to study the chemical interaction between brines and sandstone core surfaces in the absence of oil phase. For this purpose, the mildly cleaned core was 100% saturated with FW prior to the pH screening test. The core was then inserted into a rubber

sleeve and mounted into a Hassler core holder with a confining pressure of 20 bar and backpressure of 10 bar. Then different brines were successively flooded in the core at adjusted temperature with a rate of 4 PV/D. The flooding sequence for different set of cores are presented later in the result and dissection chapter. Effluent samples were collected in sealed vials using a liquid handler. The pH and density of the produced water was monitored, and different ions concentration analyzed using an IC.

### *3.2.6 Oil recovery test by spontaneous imbibition (SI)*

The restored core was vertically placed on marble balls in a steel high-temperature, high-pressure (HPHT) SI cell which has a conical top. The cell was filled with imbibing brine and the setup pressurized to 10 bar with the same brine, and the temperature was adjusted to the specific reservoir temperature. The schematic of set up shown in figure 14. The cumulative oil production as a percentage of original oil in place (%OOIP) versus time is monitored at this test. The produced oil during each brine imbibition into the core will be accumulated at the top of cell due to density difference (Gravity segregation). Before each produced oil volume reading the cell gently has to be shacked to exorcise the oil drops produced but adhered to the outer layer of the core surface. Then it is needed to open the outlet valve of the cell connected to a graduated valve and drain the oil very slowly and carefully to keep the pressure constant and prevent any forced flow due to sudden pressure drop.

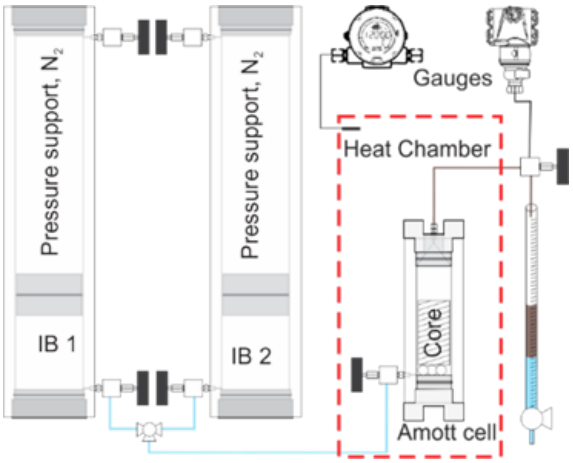


Figure 14. Schematic spontaneous imbibition (SI) setup.

### *3.2.7 Oil recovery test by forced imbibition (FI)*

To perform the forced imbibition oil recovery experiments, the aged core was inserted into a rubber sleeve and placed into the Hassler core holder under 20 bar confining pressure and 10 bar back pressure at reservoir temperature. The schematic of the core flooding setup is shown in figure 15. The core was then flooded with different brines with a flow rate of 4 PV/D and the oil recovery, flooding pressure and the effluent water pH, density and ion composition were monitored. The details of the tests are discussed in the related sections.

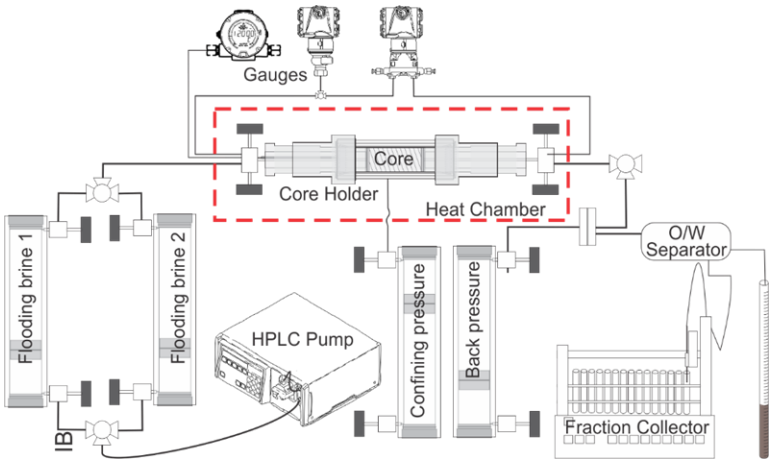


Figure 15. Core flooding setup for oil recovery tests by viscous flooding. IB = injection brine. O/W = Oil/Water

The list of all the experiments performed on the reservoir cores are presented in table 9.

Table 9. List of all the experiments performed on the reservoir core

| Core | Test name | Type of the recovery process | Recovery sequences | T (°C) |
|---|---|---|---|---|
| M3 | M3-R2 | FI | $LS_m$ | > 130 |
| | M3-R3 | FI | mSW - $LS_m$ | |
| | M3-R4 | SI | $FW_m$ - $LS_m$ | |
| | M3-R5 | SI | $LS_m$ | |
| | M3-R6 | SI | mSW - $LS_m$ | |
| M5 | M5-R1 | FI | $LS_m$ | > 130 |
| | M5-R2 | FI | mSW - $LS_m$ | |
| | M5-R4 | FI | SW | |
| | M5-R5 | FI | $FW_m$ | |
| P41 | P41-R1 | FI | $FW_p$ | 136 |
| | P41-R2 | FI | $LS_p$ | |
| | P41-R3 | SI | $FW_p$ - $LS_p$ | |
| P49 | P49-R1 | FI | $FW_p$ | 136 |
| | P49-R2 | FI | $LS_p$ | |
| T1 | T1-R1 | FI | SW - $LS_t$ | 148 |
| | T2-R2 | FI | $LS_t$ | |
| T2 | T2-R1 | FI | $LS_t$ | 148 |
| | T2-R2 | FI | SW - $LS_t$ | |

## 3.3 Analysis

The analyses are listed based on the order of the tests presented in the result and discussion chapter.

### 3.3.1 Ion Chromatography

Different ions concentration in effluent brine samples were analysed using Dionex ICS5000+ ion chromatograph (IC). Prior to analyses of the

samples, effluent samples were diluted 500-1000 times using a GX-271 Liquid Handler to reduce the concentrations into the optimum detection range of each ion. Diluted samples then filtered through a 0.2 um filter into sealed sample glasses. It has to be noticed that an external sample also must be analysed in between of main diluted samples to be able to calculate ions concentration.

### *3.3.2 pH measurements*

The pH of brines and effluent samples were measured using Seven Easy™ pH meter delivered by Mettler Toledo, with a Semi-micro pH electrode. The repeatability of measurement was ± 0.02 pH units at ambient temperature.

### *3.3.3 Quinoline concentration measurement*

The amount of quinoline adsorption is indirectly indicated using a Shimadzu UV-1700 PharmaSpec UV-VIS spectrophotometer at ambient temperature. The spectrophotometer measures absorbance (ABS) of Quinoline at wavelength of 312.5 nm by scanning in the wavelength of 190-700 nm. To accomplish an exact ABS measurement of quinoline in the solution, the sample must be 100 times diluted with DI water at pH≈3.5. The reason to perform the ABS measurement at this low pH is that the degree of protonation of quinoline increases as the pH of the solution goes below the pKa value and reaches 100% around pH∼3.5.(Burgos et al., 2002), figure 16.

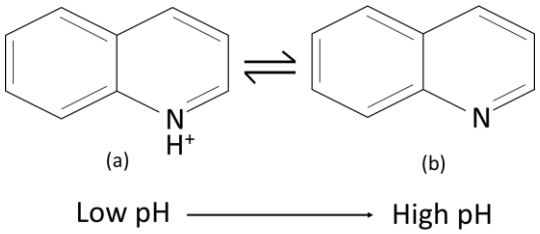


Figure 16. Protonated, (a), and neutral, (b), form of Quinoline

To convert the ABS to the amount of adsorption calibration curve is needed. Figure 17 shows the calibration curves linearly correlated using different concentration of quinoline in the solutions with different salinities. Figure 19 also confirms that the sensitivity of the instrument to detect the quinoline concentration is almost independent of the salinity of the solution.

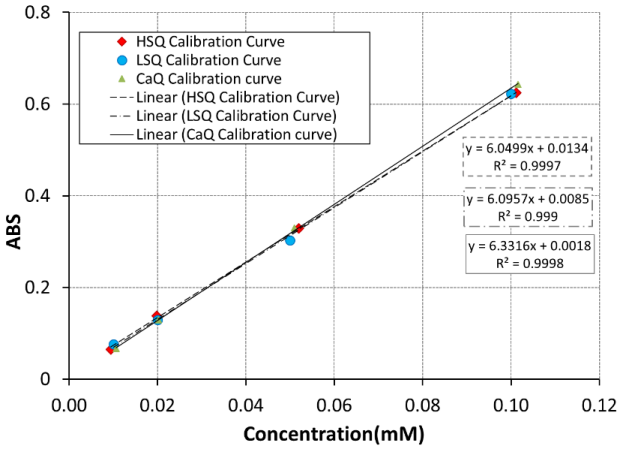


Figure 17. Calibration curves at pH≈3 and T=23 °C

### *3.3.4 BET surface area*

Specific surface area measurement of the rock materials was carried out in a TriStar II PLUS instrument from Metromeritics® based on Brunauer-Emmett-Teller theory called BET surface area. The measurement is determined at atomic level by adsorption of an unreactive gas into the rock samples taken from the same block/container as the material used in this study.

### *3.3.5 viscosity measurements*

Oil and brines viscosity measured using a Physica MCR 302 rheometer delivered by Anton Paar. Both cone and plate geometry used to perform the measurement at constant shear rates in the range of 10 to 100 $s^{-1}$, and at temperatures 23 °C.

### *3.3.6 Acid and base number measurement*

The Acid Number (AN) was determined by potentiometric titration. The used method was developed by Fan and Buckley (2006), and it is a modified version of ASTM D664. The Base Number (BN) was determined by potentiometric titration. The used method was developed by Fan and Buckley (2000) and it is a modified version of ASTM D2896.

# 4 Main results and discussions

As discussed, oil reservoirs are complex systems that consist of three main phases, Crude oil, Brine, and Rock (CoBR), as described in figure 18. Initially the pores systems in reservoirs are filled with Brine and are regarded as water wet. The Crude oil are the main wetting phase and during reservoir filling contribute with organic components that could interact with the mineral surfaces, creating a wetting toward less water wetness. Temperature controls the kinetics of chemical reactions and need also to be considered. In clastic reservoirs clays with a huge reactive surface area, are regarded as the most important wetting mineral, and the established wettability could be described as a competition between the reactive species in the brine and Crude oil

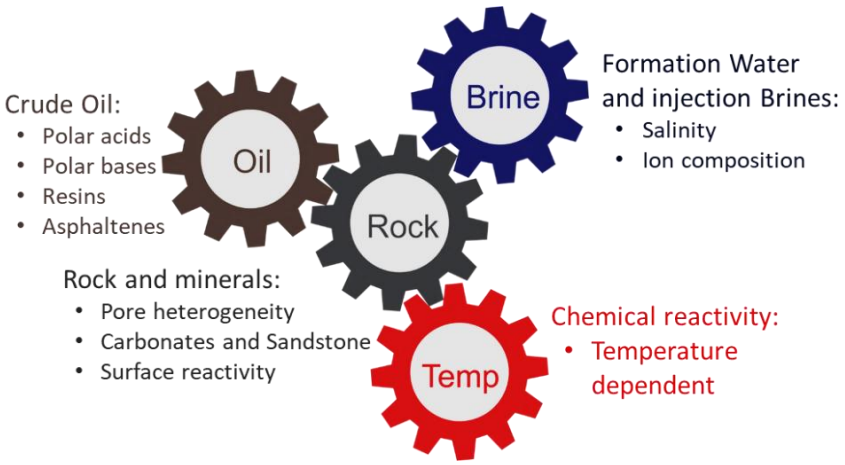


Figure 18. The key parameters to study the smart water EOR effect in the reservoirs

In this thesis, some fundamental parametric studies in two and three phases performed to get a better understanding of the key role of clays

on the initial wettability and also the wettability alteration process during the smart water EOR effect. And then using real reservoir cores, the potential of different LS brine, compare to SW and mSW and also after those brine in tertiary mode are investigated at high reservoir temperature.

## 4.1 Reactivity of divalent ions towards sandstone mineral surface

In clastic reservoirs, there are three main groups of minerals, Quartz, Feldspars, and Clays. Clays are important because they have permanently negative surface charges giving a Cation Exchange Capacity (CEC), and contribute with a large portion of the mineral surfaces. With a huge reactive surface area, clays are regarded as the most important wetting mineral, and the established wettability could be described as a competition between the reactive species in the brine and Crude oil.

Tang and Morrow (1999) were the first discussed the importance of clay present in order to see the LS brine EOR effect, by recovering no more oil in the clay free sandstones. Further studies confirmed that the adsorption/desorption of both polar organic component of crude oil and also ions from brine, both happen on the negative charge surface of clays (Austad et al., 2010). It is also argued that presence of active cations such as $Ca^{2+}$ and $Mg^{2+}$ in the FW, are important to create the optimum initial wetting condition, and also to create the alkaline environment during the

smart water LS brine injection (Austad et al., 2010; Lager et al., 2007; Ligthelm et al., 2009).

In the following section, the rate-determining reaction of chemically induced wettability alteration is fundamentally studied by investigating the affinity of two important cations presenting in the FW, i.e $Ca^{2+}$ and $Mg^{2+}$, towards three different minerals, at ambient and high temperature. And also the affinity of those two cations compared to each other towards different minerals.

### *4.1.1 Reactivity of divalent cations towards quartz*

'Even though Quartz is the most dominant mineral in sandstone reservoirs, the minerals contribute with low surface area and low reactivity towards cations and are expected to have limited effect on wetting and wettability alteration processes in Sandstone reservoirs.

A sand pack containing only quartz (SP#1) was used as a "blank" test to evaluate the reactivity active cations, i.e $Ca^{2+}$ and $Mg^{2+}$, towards the quartz mineral surfaces in a dynamic flooding process. Three different injection brines, B, BCL, and BML were used. B contains only NaCl. BCL contains $Ca^{2+}$ and $Li^{+}$ as a tracer in addition to NaCl. in BML the $Ca^{2+}$ is substituted with $Mg^{2+}$.

The sand pack was initially equilibrated with brine B (pure NaCl) prior to the test. Then the flooding continued with BCL (with $Ca^{2+}$ and $Li^{+}$) or with BML (with $Mg^{2+}$ and $Li^{+}$) for an adsorption process. Ion concentrations in effluent samples at 130°C are presented in figure 19.

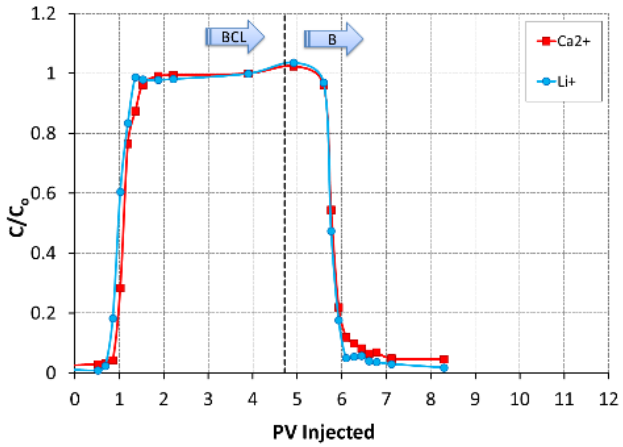


(a)

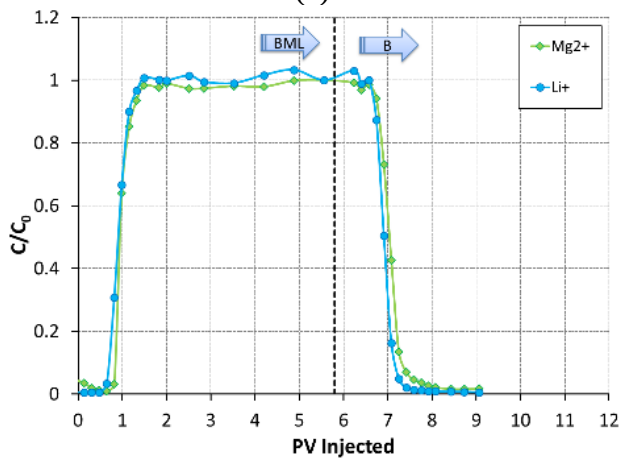


(b)

Figure 19. Cations adsorption/desorption in a sand pack (SP#1) containing 100% Quartz at T=130 °C. (a) $Ca^{2+}$ adsorption/desorption, (b) $Mg^{2+}$ adsorption/desorption.

We observe no separation between the $Li^{+}$ tracer and $Ca^{2+}/Mg^{2+}$, confirming low reactivity of divalent cations towards the quartz surfaces.

Then the flooding continued with brine B (pure NaCl brine) to observe any desorption effects of divalent ions from the surfaces. The effluent analyses confirm no separation between the tracer and $Ca^{2+}/Mg^{2+}$ eluent

curves, confirming low reactivity of divalent ions even at high temperatures when $Ca^{2+}$/$Mg^{2+}$ reactivity is at the highest due to reduced hydration.

The Smart Water EOR effect in sandstone systems has been described as a cation exchange on mineral surfaces during injection of low salinity or brines depleted in divalent cations, promoting an alkaline environment needed to remove the organic component from the mineral surfaces. The process is described by the equations 7-9.

Figure 20 shows the modified result of figure 19 by adjusting the start time of injection of brine B to zero PV injected. It is noticeable that after 1.5 PV all almost all the tracer active cations are displaced by brine B. A very nice opposite S shape of the desorption curve confirms well homogenous packing of the sand pack in absence of clay particles.

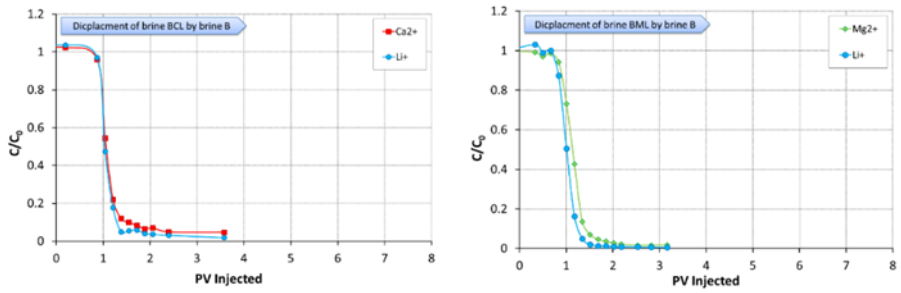


(a) (b)

Figure 20. Cations desorption from a sand pack (SP#1) containing 100% quartz at T=130 °C. (a) $Ca^{2+}$ desorption, (b) $Mg^{2+}$ desorption.

### *4.1.2 Reactivity of divalent cations towards clay surfaces*

Clay minerals are an important mineral in most clastic oil reservoirs. The two most common reservoir clays are illite and kaolinite.

To study the reactivity of clay minerals towards divalent cations, sand pack experiments containing close to 10 wt% clays in quartz has been performed. Both kaolinite and illite clays have been used, and the reactivity of $Ca^{2+}$/$Mg^{2+}$ ions has been tested at both high and ambient temperatures, using the same brine systems as for pure Quartz. When the adsorption equilibrium for both tracer and active cations was established using BCL or BML brines, the flooding fluid was switched to brine B (pure NaCl), to study the relative desorption rate of $Ca^{2+}$ and $Mg^{2+}$ to the tracer, $Li^{+}$.

#### 4.1.2.1 **$Ca^{2+}$ and $Mg^{2+}$ desorption from kaolinite at T=130 °C**

A sand pack with 8% kaolinite in quartz (SP#2) was prepared. The system was equilibrated by flooding with brine B followed by $Ca^{2+}$ adsorption with brine BCL. The desorption process of $Ca^{2+}$ ions from the kaolinite surfaces was monitored during B brine flooding at 130 °C, figure 21.

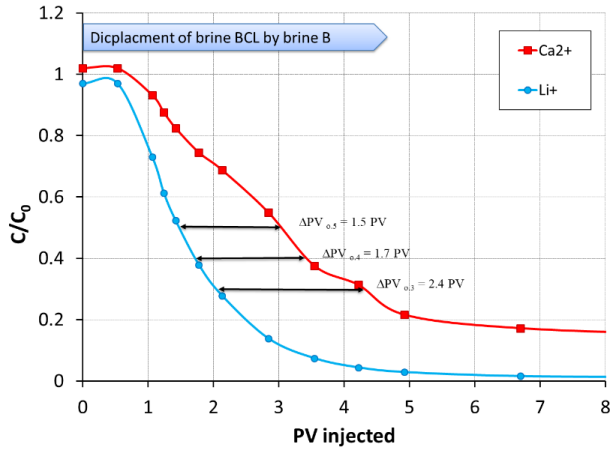


Figure 21. $Ca^{2+}$desorption from SP#2 surface (containing kaolinite) at T=130 °C.

The results confirm that $Ca^{2+}$ ions interact more towards Kaolinite compared to Quartz. A significant delayed desorption of $Ca^{2+}$ is observed in SP#2 compared to $Li^{+}$. The high affinity of $Ca^{2+}$ towards the kaolinite clay, confirms that $Ca^{2+}$ could influence the kaolinite reactivity linked to adsorption of polar organic components, wettability, and the kinetics involved during wettability alteration processes reported during Smart Water injection.

Ion exchange reaction on mineral surfaces could contribute with an alkaline environment near the rock surface (Austad et al., 2010; Lager et al., 2007; Seccombe et al., 2008). The results could also explain why no LS EOR effect was observed in the tests by Tang and Morrow(1999) performed on the clay-free sandstone core samples.

To obtain a quantitative measurement of the affinity of $Ca^{2+}$ toward the clay surface, the delay in the desorption process in terms of injected PV

was obtained by calculating the average difference in elusion time (ΔPV) between the tracer $Li^+$, and $Ca^{2+}$ at the relative ion concentrations of 0.5, 0.4, and 0.3, as shown in figure 1 and summarized in Table 3. The average retention value of $Ca^{2+}$ relative to tracer $Li^+$, was 1.9 PV in SP#2 at 130 °C.

The reactivity of $Mg^{2+}$ toward Kaolinite clays was also measured at 130 °C. SP#2 was equilibrated with brine B, before exposed to $Mg^{2+}$ ions by flooding with and flooded with BML brine. The desorption of $Mg^{2+}$ relative to $Li^+$ ions was monitored during the B brine flooding, figure 22. The desorption curves of $Li^+$ and $Mg^{2+}$ show that $Mg^{2+}$ interacts stronger to kaolinite clays compared to $Li^+$. The average elusion time was calculated to 0.65 PV which is only 34% compared to $Ca^{2+}$ at 130 °C, (Table 10).

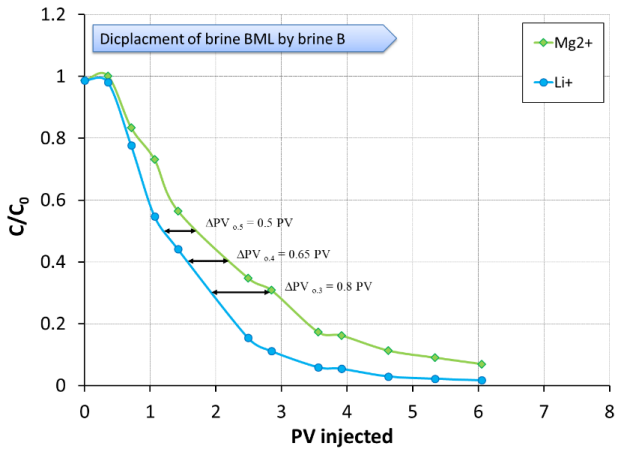


Figure 22. $Mg^{2+}$ desorption from kaolinite surfaces in SP#2 at 130 °C.

### 4.1.2.2 $Ca^{2+}$ and $Mg^{2+}$ desorption from kaolinite at 23 °C

In order to study the effect of temperature on the desorption process, experiments were also performed in SP#2 at 23 °C. The results for both $Ca^{2+}$ and $Mg^{2+}$ ions are presented in figure 23 and 24:

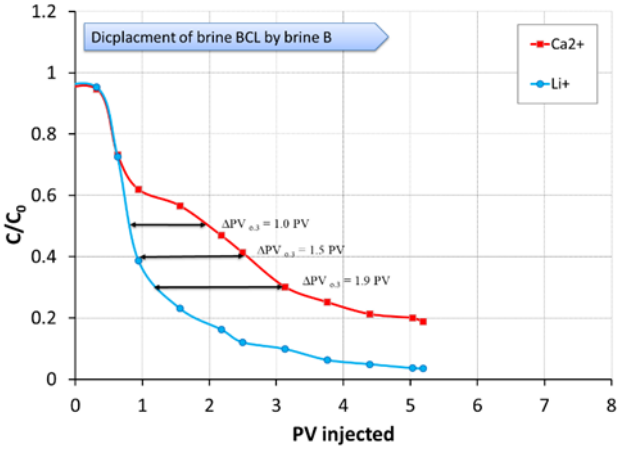


Figure 23. $Ca^{2+}$desorption from kaolinite surfaces in SP#2 at 23 °C

The average retention of $Ca^{2+}$ relative to tracer $Li^{+}$ at 23 °C, at room temperature was calculated to 1.5 PV, which is significantly less than 1.9 PV at 130 °C. This is in line with the nature of the desorption process described in Eq.1 which is an exothermic process. At high temperature $Ca^{2+}$ ions are more dehydrated (Austad et al., 2010; Zavitsas, 2005), and the affinity towards negative clay surfaces will be increased.

When the test was repeated for $Mg^{2+}$, the same behavior was observed. The average retention time of $Mg^{2+}$ is reduced from 0.65 PV to 0.4 PV, when the temperature was reduced from 130 to 23 °C. This represents a reduction of 61%.

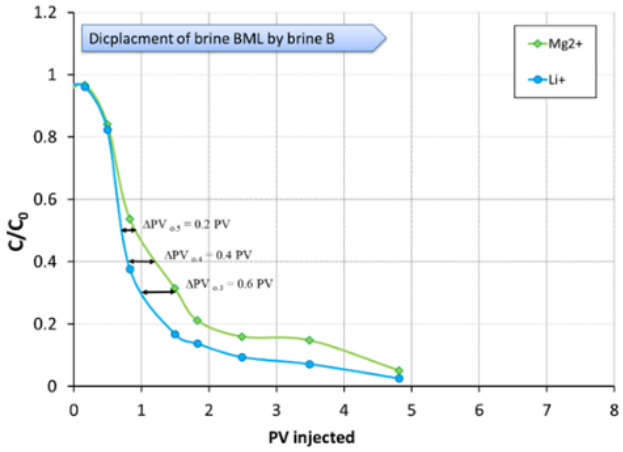


Figure 24. $Mg^{2+}$ desorption from kaolinite surfaces in SP#2 at 23 °C.

### 4.1.2.3 $Ca^{2+}$ and $Mg^{2+}$desorption from illite clays at 23 °C

Illite clays are also common in clastic reservoir systems. The reactivity of divalent cations towards illite surfaces is also important to evaluate. Cissokho et. al. (2010) have reported that illite clay could also play a key role as well as kaolinite in the LS EOR mechanism.

Sand Packs containing illite clays were prepared in the same way as for the kaolinite. SP#3 contained 8 wt% illite in quartz. Adsorption /desorption studies was performed to evaluate the $Ca^{2+}$ reactivity toward illite at 23 °C. The desorption curves are presented in figure 25.

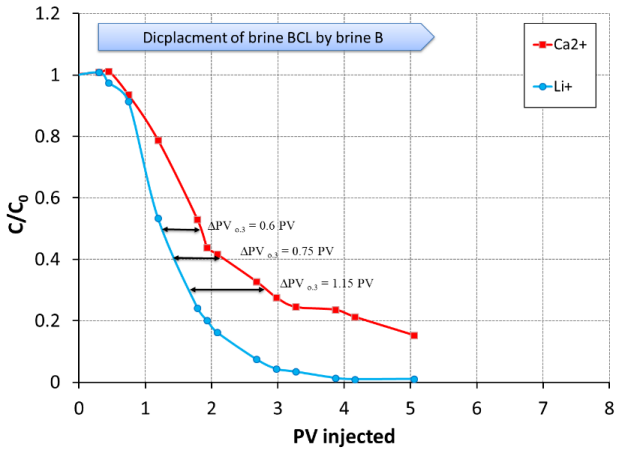


Figure 25. Desorption of $Ca^{2+}$ ions from Illite surfaces in SP#3 at 23 °C.

The $Ca^{2+}$ retention compared to tracer $Li^{+}$ was calculated to 0.83 PV. The value is significantly less than the value of 1.5 PV observed kaolinite at 23 °C, even though illite has higher CEC. A possible explanation could be the grouped structure of illites with less exposed surfaces.

Table 10. Retention of $Ca^{2+}$ and $Mg^{2+}$ relative to tracer, $Li^{+}$, in contact with kaolinite and illite clay at room temperature and 130 °C, in ΔPV.

| Sand pack | SP#2, Kaolinite | | | | SP#3, Illite |
|---|---|---|---|---|---|
| Rel. conc. (desorption) $C/C_0$ | Delayed $Ca^{2+}$ @23°C [ΔPV] | Delayed $Ca^{2+}$ @130 °C [ΔPV] | Delayed $Mg^{2+}$ @ 23°C [ΔPV] | Delayed $Mg^{2+}$ @130 °C [ΔPV] | Delayed $Ca^{2+}$ @23°C [ΔPV] |
| 0.5 | 1 | 1.5 | 0.2 | 0.5 | 0.6 |
| 0.4 | 1.5 | 1.7 | 0.4 | 0.65 | 0.75 |
| 0.3 | 1.9 | 2.4 | 0.6 | 0.8 | 1.15 |
| Avg. ΔPV | 1.5 | 1.9 | 0.4 | 0.65 | 0.83 |

The quantitative comparison of the five desorption studies performed at 23 °C and 130 both in kaolinite and illite sand packs are summarized in table 10.

## *4.1.3 Competitive reactivity of $Ca^{2+}$ and $Mg^{2+}$ onto clays*

Formation water (FW) has typically 5 times higher $Ca^{2+}$ conc. than $Mg^{2+}$, while Seawater (SW) as typical injection water has 4 times $Mg^{2+}$ compared to $Ca^{2+}$. Smart water EOR brines have modified brine compositions depending on the type of reservoir mineralogy. In sandstone reservoirs, injection brines depleted in divalent cations have been observed as very efficient Smart Water. Competitive reactivity between $Ca^{2+}$ and $Mg^{2+}$ toward clay surfaces have been performed in Sand Pack studies, to verify any symbiotic effects.

### 4.1.3.1 **Competitive desorption of $Ca^{2+}$ and $Mg^{2+}$ from Illite surface**

To compare the affinity of $Ca^{2+}$ and $Mg^{2+}$ towards illite surface, SP#4 with 10 wt% Illite in Quarz sand were used. Brine flooding sequence was B – BCM – B. The BCM brine contain equal amounts of $Ca^{2+}$ and $Mg^{2+}$, 10 mM. Experiments were performed at both 23 °C and 130 °C. The results from the desorption process is presented in figure 25 and 26.

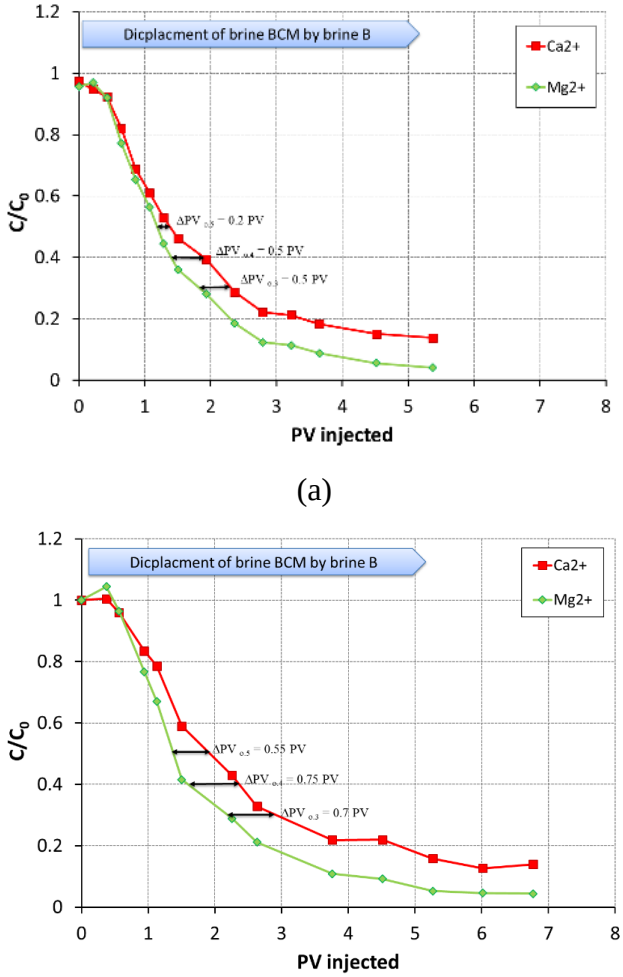


Figure 26. Competitive adsorption/desorption of $Ca^{2+}$ and $Mg^{2+}$ onto illite surface in SP#4. (a) 23°C and (b) 130°C

$Ca^{2+}$ has a higher affinity to the illite clay surface than $Mg^{2+}$, observed as delayed desorption compared to $Mg^{2+}$ at both 23 and 130 °C.

Quantitative values of the delayed desorption d $Ca^{2+}$ compared to $Mg^{2+}$ is 0.4 and 0.67 PV, respectively, and reported in table 11.

The shift of whole desorption curves to the right by an increase of temperature, confirms an increase in affinity of both divalent cations at higher temperatures due to dehydration.

The results highlight the key role of $Ca^{2+}$ in FW and temperature will have on reservoir wettability. It could also explain the delayed chemical wettability alteration processes observed during Smart Water injection in Clastic reservoir systems with kaolinite clays according to equation.7.

#### 4.1.3.2 **Competitive desorption of $Ca^{2+}$ and $Mg^{2+}$ from Kaolinite surface**

Competitive desorption of $Ca^{2+}$ and $Mg^{2+}$ was also studied in sand pack SP#2 containing kaolinite clay at 130 ºC with the same test procedure as for illite, figure 27.

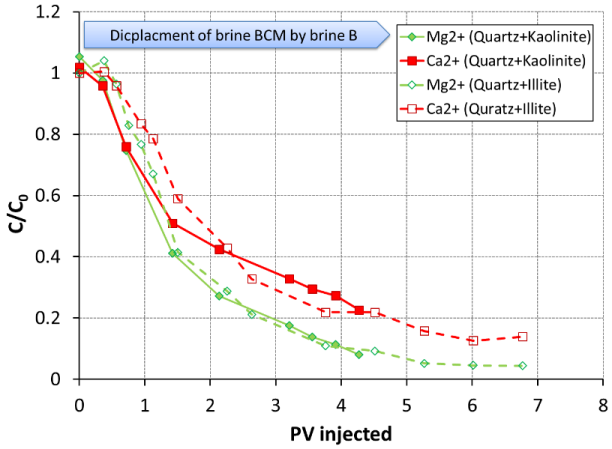


Figure 27. Desorption of $Ca^{2+}$ and $Mg^{2+}$ from Kaolinite clays in SP#2 at 130°C.

The desorption of $Ca^{2+}$ from the kaolinite surfaces are significantly delayed compared to $Mg^{2+}$, and calculated to 0.88PV, table 11. The results are in line with the observation for the kaolinite clay. Both kaolinite and illite clays behaved more selective to the $Ca^{2+}$ compare to the $Mg^{2+}$ ions. The $Ca^{2+}$ affinity towards kaolinite clay is higher with the factor of 1.3 (0.88/0.67), also in line with desorption tests for single ions.

Table 11. Comparative retention of $Ca^{2+}$ and $Mg^{2+}$, in contact with kaolinite and illite clay at room temperature and 130°C, in ΔPV.

| Sand pack type | Illite, SP#4 | | Kaolinite, SP#3 |
|---|---|---|---|
| Rel. conc. (desorption) $C/C_0$ | Delayed $Ca^{2+}$ at 23°C [ΔPV] | Delayed $Ca^{2+}$ at 130°C [ΔPV] | Delayed $Ca^{2+}$ at 130°C [ΔPV] |
| 0.5 | 0.2 | 0.55 | 0.25 |
| 0.4 | 0.5 | 0.75 | 0.9 |
| 0.3 | 0.5 | 0.7 | 1.5 |
| Avg. ΔPV | 0.40 | 0.67 | 0.88 |

The results should not be generalized for all clay systems. We should be aware of that clays present reservoir systems have gone through different diagenesis processes which could influence the surface reactivity. Autogenic clays contribute with significantly more surfaces than detrital clays.

## 4.2 Adsorption of basic POC towards mineral surfaces

The wettability of reservoir minerals is generally regarded as water wet prior to the oil invasion. Crude oils with polar organic components (POC) could interact with charged mineral surfaces or precipitate in the pore space as resin and asphaltenes, reducing the degree of water wetness. Clay minerals contribute with a large portion of mineral surfaces present in clastic reservoir systems and are regarded as an important wetting mineral, which are needed to observe Smart Water EOR effects in the sandstone systems (Austad et al., 2010; Tang and Morrow, 1999).

In the previous section, the importance of the chemical reactivity of divalent cations towards clay surfaces was investigated in rock-brine two phases study. Both $Ca^{2+}$ and $Mg^{2+}$ ions present in the formation water (FW), and could affect the chemical reactivity of negatively charged clay surfaces, linked to reservoir wettability and chemical-induced wettability alteration processes.

In this section, behavior of the third phase, the oil phase, in relation to the initial wetting and wettability alteration requirements has been fundamentally investigated. The wettability of clay surfaces is generally controlled by adsorption of POC in the Crude oil (Denekas et al., 1959; Fogden, 2012; Lager et al., 2008; Morrow, 1990; Wolcott et al., 1993). Quinoline, as a representative model for POC in crude oil is selected to be studied in contact with different minerals and brines. Previous experimental studies have confirmed that Quinoline which is a Basic POC and present in crude oil, could promisingly be used as a model component in parametric laboratory studies evaluating the affinity towards mineral surfaces. (Aksulu et al., 2012; Fogden, 2012),

### *4.2.1 Adsorption of quinoline to the quartz and Clay surfaces*

The adsorption of quinoline towards illite and kaolinite clays was compared with quartz. 10 mM quinoline in LS brine (LSQ) was equilibrated with 10 wt% mineral phases, and the adsorption of quinoline as a function of pH was measured. The results are presented in figure 28.

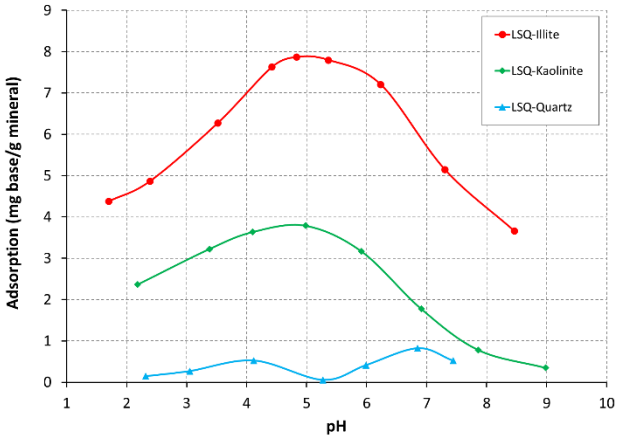


Figure 28. Adsorption of quinoline towards mineral surfaces vs. pH. 10mM Quinoline in LS brine (LSQ) was equilibrated with 10 wt% illite, kaolinite or quartz t at 23°C

As expected, quartz minerals have the least adsorption of quinoline at all pH values from 2-8. This could be explained by less specific surface area (BET=0.3$m^2$/g) and less negative charge densities (Allard et al., 1983). In Addition, the low observed adsorption is not pH depended. The results are also in line with the observation of divalent cation adsorption and desorption towards quartz in sand pack experiments.

The adsorption of quinoline towards kaolinite and illite surfaces are significantly higher and confirms a pH dependence. The amount of adsorption towards illite is twice the kaolinite adsorption at peak values close to pH 5. The BET values of kaolinite and illite are measured to 13 and 22 $m^2$/g respectively, confirming increased adsorption with increased reactive surfaces.

At high pH, the adsorption of quinoline towards kaolinite is very low compared to illite clay. A stacked clay structure with less easily

accessible illite surfaces could explain why low adsorption is not reached for illite. The results are also in line with sand pack experiments with reduced delay in desorption of divalent cation from illite surfaces.

### *4.2.2 Quinoline adsorption onto kaolinite – Effect of pH, salinity, and temperature*

Quinoline adsorption towards Kaolinite surfaces was also studied by using 3 different brines solutions, LSQ, HSQ and CaQ . 10 wt% kaolinite clay was equilibrated with the brine solutions at constant pH with values in the range of 2-10. Experiments were performed at both 23 and 130°C, and the results are presented in figure 29 and 30.

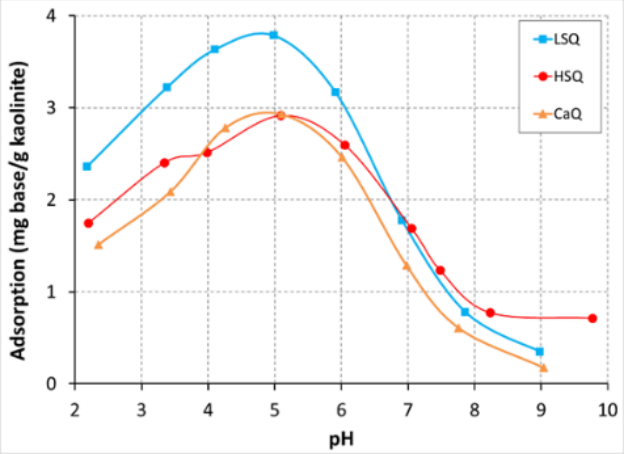


Figure 29. Adsorption of quinoline onto 10 wt% kaolinite clay in contact with LSQ, HSQ and CaQ solutions vs. pH at (a) T=23 °C

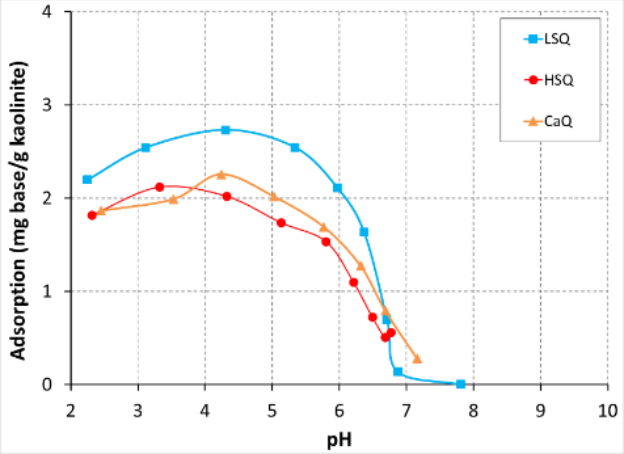


Figure 30. Adsorption of quinoline onto 10 wt% kaolinite clay in contact with LSQ, HSQ and CaQ solutions vs. pH at T= 130°C.

**Effect of pH**

The adsorption of quinoline onto kaolinite is strongly pH-dependent and varies with pH from 2 – 9, Figures 29 and 30. The maximum adsorption is observed close to pH 5 at 23°C, and at pH 4 when the temperature is increased to 130 °C. This is very close to the $pK_a$ values for Quinoline.

At 23 °C, the adsorption of quinoline to kaolinite surfaces decreases when the pH decreases below 5, because the concentration of $H^+$ increases. $H^+$ will also compete with protonated quinoline and other charged cations to adsorb to negatively charged mineral surfaces. So even though the concentration of positively charged quinoline increases at lower pH, less adsorption is observed.

At pH higher than 5, the quinoline adsorption also decreases. Increased amount of $OH^-$ will neutralize the quinoline and the adsorption decreases. As expected, very low quinoline adsorption are observed at pH above 7.

**Effect of Temperature**

As the temperature increases, the quinoline adsorption decreases at all pH values, figure 30. The reactivity of divalent cations increases with increasing temperature due to less hydration as described by the equation 7:

$$Ca^{2+} \cdots Clay \; + \; H_2O \; \rightleftarrows \; H^+ \cdots Clay + Ca^{2+} + \; OH^- + \; \text{HEAT}$$

When heat is added to the system, the equilibrium will move to the left. At high temperature the reactivity of the divalent cations, especially $Ca^{2+}$, increases. This leads to less available sites on the clay surface for quinoline adsorption.

**Effect of ion composition and salinity**

The ion composition and salinity of the brines are also important regarding quinoline adsorption. At all tested pH and temperatures, we observe significant higher quinoline adsorption using the 1000 ppm LSQ brine system compared to 25 000 ppm HSQ and CaQ brines, figure 24. The chemical reactivity of species seems to dominate the adsorption process. Reduced competition of inorganic cations towards the negative sites on the clay surfaces, promotes increased adsorption of protonated

organic quinoline. This is in contradiction to competition between attractive and repulsive forces and the double layer extension theory.

If the wettability is controlled by the adsorption of polar organic components towards mineral surfaces, low salinity brines should result in reduced water wetness, in opposite to the general excepted knowledge. A pH change towards alkaline conditions could however promote reduced adsorption of quinoline and promote more water wet conditions.

### *4.2.3 Quinoline adsorption onto Illite – effect of brine salinity*

Illite clay is also a typical clay mineral present in Clastic Sandstone reservoirs, and the effect of Brine Composition Salinity on Quinoline adsorption towards Illite clays have been characterized.

A set of experiments was performed at pH 5, which supposed to promote the highest amount of adsorption as observed for illite in figure 31. The brine systems used are LSQ (1000 ppm), HSQ and CaQ (25 000 ppm) and FWQ (200 000 ppm). The result is presented in figure (figure 31):

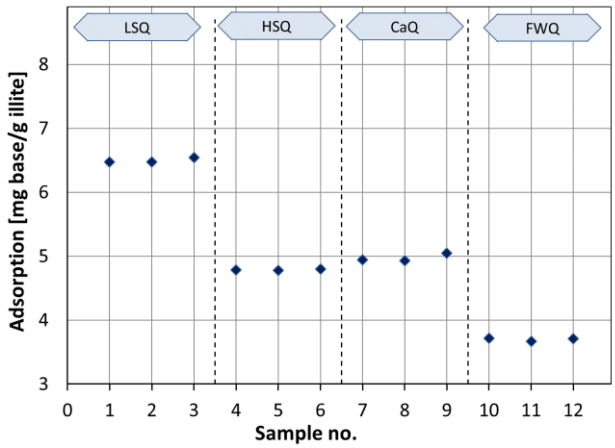


Figure 31. Effect of brine composition and salinity on the adsorption of quinoline onto illite clay at 23 °C at a constant pH of 5.

The adsorption of Quinoline significantly decreases with increased salinity. The adsorption follows the same trend as observed for Kaolinite. The lowest adsorption belongs to FWQ with a salinity of 200 000 ppm. The results indicate that reservoirs with high FW salinity could behave more water wet. When the temperature is increased, a further reduction in adsorption of basic POC could be expected.

### *4.2.4 Reversibility of Quinoline adsorption onto Illite clay*

The LS EOR mechanism suggested by Austad et al. (2010), involving cation exchanges on mineral surfaces, promoting adsorption/desorption of POC is pH depended.

The reversibility of quinoline adsorption onto kaolinite clay has previously been investigated by RezaeiDoust et al. (2011), figure 32. The same investigation has also been performed using illite clay. Three

parallel experiments were performed with 10wt% illite equilibrated with LSQ or HSQ at 23 °C at an initial pH of 5. The results are presented in figure 32.

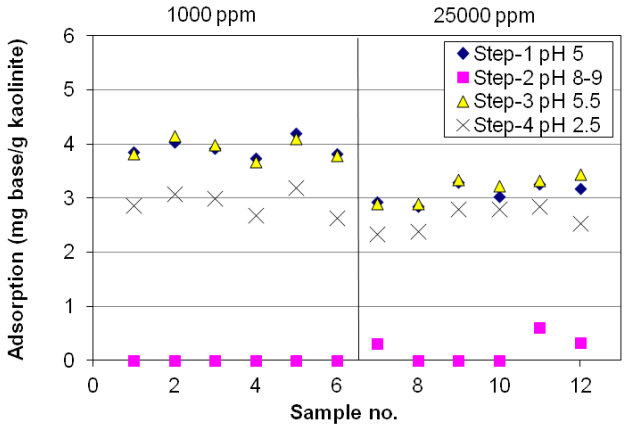


Figure 32. Reversibility test of adsorption of quinoline from kaolinite clay at T=23 °C (RezaeiDoust et al., 2011)

LSQ gives higher adsorption compare to HSQ, and the results are quantitively in line with the results for kaolinite, figure 29. When the pH was increased to 8-9, the pH increase facilitates quinoline desorption from the illite clay, from 7.7mgQ/g to 4.2mgQ/g for LSQ, and 7.0 to 4.0 for HSQ, confirming 45% desorption of Quinoline, figure 33.

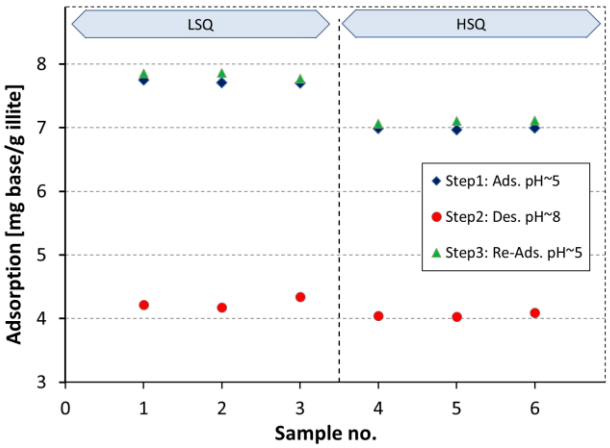


Figure 33. Adsorption/desorption of Quinoline onto Illite clay in LSQ and HSQ at 23°C. Step 1 - initial pH adjusted to 5. Step 2 - pH increased to 8. Step 3 – final pH reduced back to 5.

When the pH is reduced back to 5 by adding a few µl of HCl, all the desorbed Quinoline is resorbed again, confirming that adsorption/desorption processes are completely pH dependent, and that the adsorption is dependent on the presence of positively charged quinoline.

Comparing the results between kaolinite and illite clays, figure 33 and figure 34, it can be concluded that significant desorption are observed for both illite and kaolinite when the pH was increased. For kaolinite, a complete desorption was observed, while for illite only 45% desorption was observed. This could be explained by the difference in the layered structure of the clay minerals. The three-layered structure of illite with $K^+$ between the sheets have less accessible mineral surfaces for desorption compared to the two-layered structure of kaolinite. as presented in figure 34.

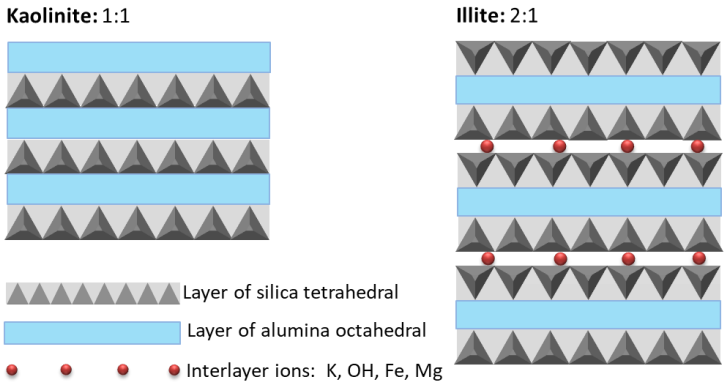


Figure 34. Schematic of kaolinite and illite layered structure

## 4.3 EOR by wettability modification of sandstone reservoirs at high temperature

In order to be able to make a strategy for optimal water flooding of oil reservoirs, detailed knowledge about initial properties and relevant parameters which have an influence on the wetting conditions are needed. Improved chemical understanding of the rock-fluid interactions discussed in the previous subchapters, add new knowledge and makes it easier to discuss wettability and wettability modifications during smart water flooding for improving oil recovery.

Previous studies using outcrop material have confirmed high EOR potentials using LS brine as Smart Water at both low and high reservoir temperatures. Based on the mechanism proposed by Austad et al.(2010),

the main controlling reactions are exothermic, which means that higher reservoir temperatures could have negative effects on the EOR potential.

In this section results from individual Smart Water EOR projects are presented. Five sets of preserved reservoir core materials from different high temperature North Sea oil reservoirs have been studied, and the EOR potential of smart water flooding has been investigated.

### *4.3.1 Secondary LS EOR at high temperature*

Preserved reservoir cores from the BRENT formation of a North Sea oil reservoir were received from the operator to study the secondary LS EOR potential. The core mineralogy was obtained by QEMSCAN analysis. The reservoir contained a light crude oil. As expected, the acid number, AN, was below the detection limit for the analysis. Due to the high reservoir temperature, $T_{res}$=130°C, decarboxylation of the carboxyl group could take place over geological time. The base number, BN, is, however, large, 1.35 mgKOH/g, which indicates enough available polar components to make the rock surface mixed wet, provided the presence of sufficient clay minerals.

The salinity and composition of the formation water, $FW_P$, was rather low, with a total salinity of 22 763 ppm, and $Ca^{2+}$ and $Mg^{2+}$ concentrations of 3.5 and 1.4 mM, respectively. Compared to SW where the concentration of $Ca^{2+}$ and $Mg^{2+}$ is 13.0 and 44.5 mM, the divalent concentrations in $FW_p$ appeared very low.

The preserved reservoir core P41 was mildly cleaned prior to core restorations as described in the experimental chapter.

2 oil recovery experiments were performed on core P41. In the first oil recovery test termed P41-R1, the restored core was flooded with $FW_p$ brine, figure 35.

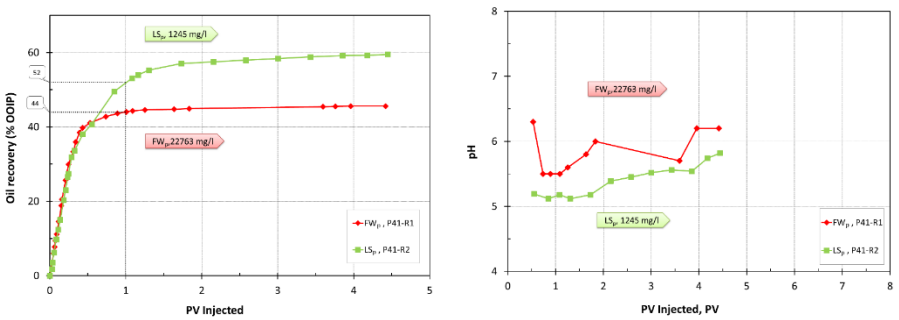


Figure 35. Oil recovery tests at 130 °C by viscous flooding with (left) $FW_p$ on core P41-R1, and (right) $LS_p$ on core P41-R2. The injection rate was 4 PV/D.

An ultimate oil recovery of 45 %OOIP was reached after less than 2 PV injected. The Produced Water PH was close to 6, confirming slightly acidic conditions favorable for adsorption of POC creating mixed wet conditions.

The core P41 was then prepared for a second oil recovery test, by mild core cleaning in front of a new core restoration. This time the core was flooded with $LS_P$ in secondary mode, P41-R2. The ultimate oil recovery plateau of 60% of OOIP was reached after 4 PV injected.

Compared to $FW_p$ injection, P41-R1, a significant reduced water production was observed during $LS_p$ injection, confirming increased displacement efficiency using a LS brine. After 1PV injected, $FW_p$

reached 44% OOIP, while $LS_p$ reached 52% OOIP. This could not be explained by mobility ratios, because the viscosity of the LS brine is slightly lower than the FW. The increased sweep efficiency during LS injection could not be an effect of viscous forces.

Improvement of microscopic sweep efficiency caused by wettability alteration can be examined in spontaneous imbibition tests. So, the core P41 was restored once again using the same restoration procedure as for the previous tests. The restored core P41-R4 was spontaneous imbibed (SI), first with $FW_p$, before changing the imbibing brine to $LS_p$. The result of SI test performed at 130 °C are shown in figure 36.

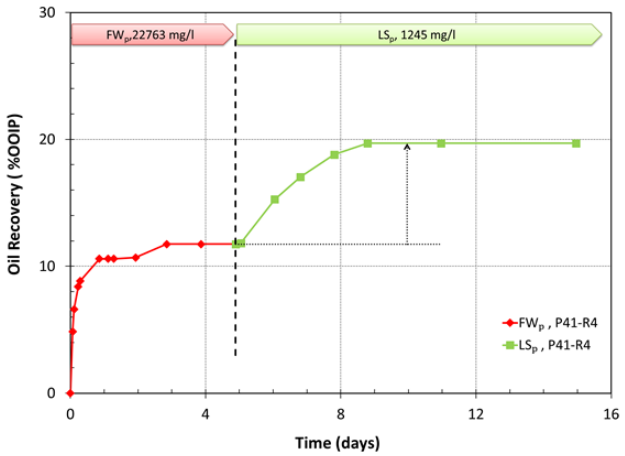


Figure 36. Oil recovery test at 130 °C by spontaneous imbibition (SI) on core P41-R4. The core was SI with $FW_p$ followed by $LS_P$.

SI with $FW_P$ will not promote any chemical induced wettability alteration, and a recovery plateau of 12 %OOIP was reached after 3 days, confirming slightly water wet initial wetting. When the imbibing brine was switched to $LS_P$ after 5 days, a gradual increase in the oil recovery was observed. A new ultimate recovery plateau of 20 %OOIP was

reached after 9 days, confirming that the $LS_P$ brine are able to change the core wettability towards more water wet conditions, and promoting increased positive capillary forces that facilitates increased oil recovery. The results confirm that capillary forces also needs to be accounted for in oil recovery processes from porous systems.

A second core, P49, from the same reservoir was also tested to verify reproducibility in between different reservoir cores, Figure 37.

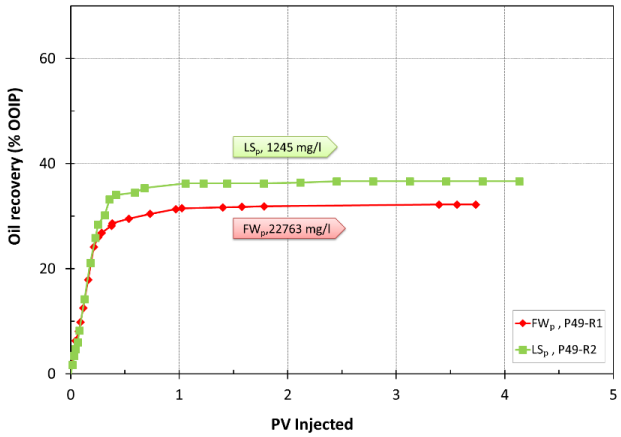


Figure 37. Oil recovery tests at $T_{res}$ of 130 °C by viscous flooding of core P49. The injection rate was 4 PV/D. In the first test, P49-R1, the injection brine was $FW_p$, while in the second test, P49-R2, the injection brine was $LS_p$ .

Also for core P49, injection of $LS_p$ are significantly more efficient than $FW_p$, confirming that wettability alteration and increase in positive capillary forces promote increased oil recovery in viscous flooding processes. Positive capillary forces are a main driving mechanism and need to be accounted for when fluid flow in porous media should be described.

### *4.3.2 Seawater (SW) as a smart water?*

For offshore oil reservoirs, SW is the natural injection water. From a scientific and an economic point of view, it is of great interest to compare the oil recovery efficiency between SW and LS brine at secondary conditions.

To investigate the smart water EOR potential of SW three different high temperature North Sea sandstone reservoirs have been studied in individual projects, and the results are summarized in the following sections.

**Case 1: High temperature reservoir with low FW salinity**

The effect of SW as an EOR fluid in secondary mode has also been tested for reservoir P. After the third restoration of core P41-R3, SW was injected in secondary mode. The results are presented in figure 38 and are compared to the oil recoveries observed during $FW_P$ and $LS_P$ injection.

After one PV with SW injection, only 38 %OOIP was recovered which is very close to the production plateau of 39% OOIP which was reached after 1.5 PV injected. This confirms a significantly lower efficiency of SW compared to $LS_p$ injection. And the recovery was even lower than obtained during $FW_p$ injection where no chemical-induced wettability alteration should take place. The results indicate that SW has the poorest oil recovery potential among the tree tested brine. SW has the highest salinity, 33390 mg/l, and a much higher concentration of $Ca^{2+}$ and $Mg^{2+}$ ions compared to $LS_p$ and $FW_p$.

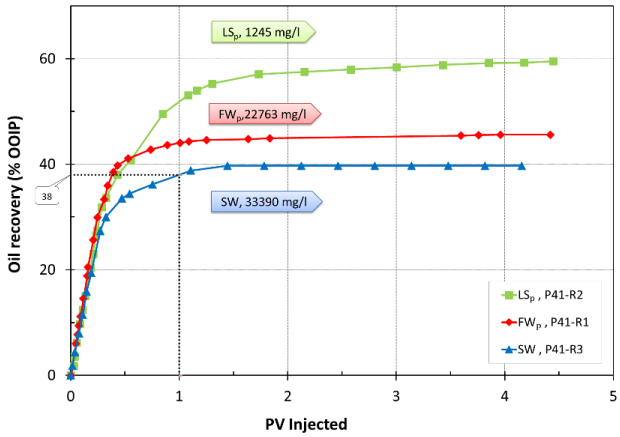


Figure 38. Secondary oil recovery tests at 130 °C by viscous flooding of core P#49 by SW with a rate of 4 PV/D after the third restoration, P#41-R3.

$Ca^{2+}$ concentration in the SW is 13 mM while $FW_p$ and $LS_p$ have a concentration of 3.5 and 0.3 mM respectively. $Mg^{2+}$ concentration in the SW is 44.5 mM while $FW_p$ and $LS_p$ have a concentration of 1.4 and 1.8 mM, respectively. Based on the chemical mechanism suggested by Austad et al., increased divalent cation ion concentrations as observed for SW will reduce the potential for wettability alteration, Eq. 7. At high reservoir temperatures, both $Ca^{2+}$ and $Mg^{2+}$ will make a complex with the $OH^-$, $(Mg^{2+} \cdots OH^-)^+$, which will reduce the pH increase needed to facilitate a wettability alteration.

### Case 2: High temperature reservoir with high FW salinity

With limited access to core material, it is needed to use each core in multiple experiments. Optimized core cleaning and core restoration procedures need to be developed to minimize the differences in the initial wetting condition in between each core experiment (Loahardjo et al., 2008).

Mild core cleaning with Kerosene and Heptane, followed by 1000 ppm NaCl injection seems to be a preferred core cleaning procedure. The desiccator technique to establish initial water saturation in the core will give reproducible initial water saturations and allow the same amount of POC during crude oil exposure which could influence the restored wettability.

Reservoir T is the second North Sea sandstone reservoir that have been evaluated for Smart Water EOR potential. The reservoir temperature is 148 °C and with a $FW_t$ salinity of 170 000 ppm.

Two preserved twin cores were used to evaluate the smart water EOR potential of the reservoir using SW and LS brine, $LS_t$. QEMSCAN analysis of core material detected significant amounts of feldspars and total clay content of t 8%. In addition, the ion analysis of the effluent samples during the mild core cleaning indicated high concentrations of $SO_4^{2-}$ ions, which is a sign of the considerable amount of dissolvable $SO_4^{2-}$ bearing minerals, most likely anhydrite.

Two oil recovery experiments were performed on each core. To exclude any effects of core restorations, the injection sequences were changed for the two cores. For core T1, SW was used as the injection brine after the first restoration, T1-R1, while $LS_t$ was used as the injection brine after the second restoration, T1-R2. For core T2, $LS_t$ was used after the first restoration, T2-R1 and SW was the injection brine after second restoration, T2-R2.

The oil recovery profiles of secondary SW and LS brine injections are compared for both cores T1 and T2 in figure 39.

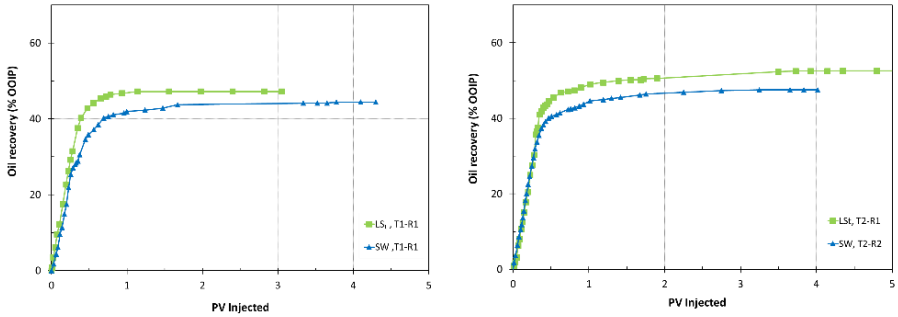


(a) (b)

Figure 39. Secondary oil recovery tests at 148 °C on cores T1 and T2. (a) Secondary Oil recovery profile of core T1 after 1st and 2nd restoration. (b) Secondary Oil recovery profile of core T2 after 1st and 2nd restoration.

For core T1, ultimate oil recoveries with secondary SW and secondary LS brine were respectively 44 and 47% OOIP. For core T2, secondary SW injection yielded 48 %OOIP while $LS_t$ gave a recovery plateau of 53%OOIP. Independent of core restoration, $LS_t$ gave significantly higher ultimate recovery and delayed water breakthrough, confirming that $LS_t$ are significantly more efficient injection brine compared to SW, and the results confirm that better performance of LS brine is not an effect of core restoration or the brine flooding sequence.

Produced Water (PW) pH was monitored during the brine injections and are presented in figure 40. During secondary $LS_t$ brine injection, the PW pH increased and stabilized about 7, while the PW pH during secondary SW injection stabilized about pH 6. This could explain why $LS_t$ injection is more efficient than SW.

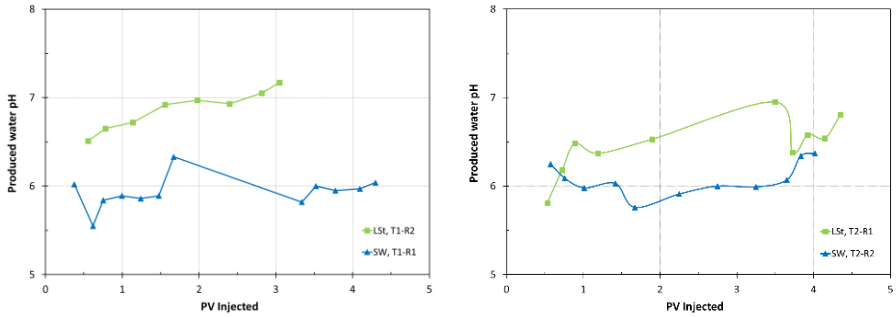


(a) (b)

Figure 40. Oil recovery tests at 148 °C on cores T1 and T2. (a) PW pH during secondary oil recovery tests on core T1 and (b) PW pH during secondary oil recovery tests on core T2.

High $FW_t$ salinity, presence of Anhydrite in the core material, and very high reservoir temperature are all parameters reported to reduce Smart Water EOR potentials. Still, the observed increased pH during $LS_t$ injection promotes potentials for wettability alteration towards more water wet conditions. A reasonable explanation could be the presence of feldspars, specially albite, which triggers a local pH at the pore surfaces needed for the wettability alteration, even at high reservoir temperatures (Piñerez Torrijos et al., 2017; Strand et al., 2014).

### *4.3.3 LS EOR potential after SW flooding*

Offshore oil reservoirs are typically water flooded by the easiest available brine which is SW. Thus, if LS brines should be implemented in a mature field, it has to be as a tertiary injection after SW.

Laboratory studies involving outcrop sandstone cores have indicated that tertiary LS EOR effects are reduced after the cores have been exposed to SW (Piñerez Torrijos et al., 2016a; Winoto et al., 2012).

In this section, the EOR potential of $LS_t$ brine after SW injection have been investigated on high temperature reservoir systems, cores T1 and T2 from reservoir T at 148 °C.

As presented in the previous section, core T1-R1 and core T2-R2 was initially flooded with SW. In both cases when the recovery plateau with SW was reached, the injection brine was switched to $LS_t$. The Oil recovery results are presented together with the Produced Water PH in figure 41 and figure 42.

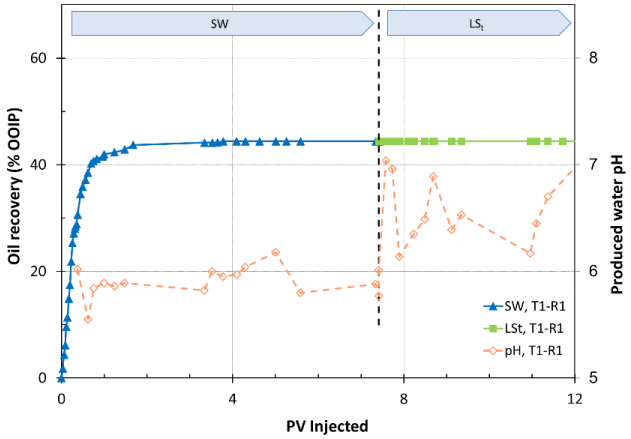


Figure 41. Oil recovery and PW pH on cores T1-R1 at 148° C. The core was successively flooded with SW–$LS_T$ with an injection rate of 4 PV/D.

No tertiary LS EOR effect was observed in any of the cores. A slight increase in PW pH is observed during $LS_t$ injection but it is not enough to promote significant changes in the Oil recoveries.

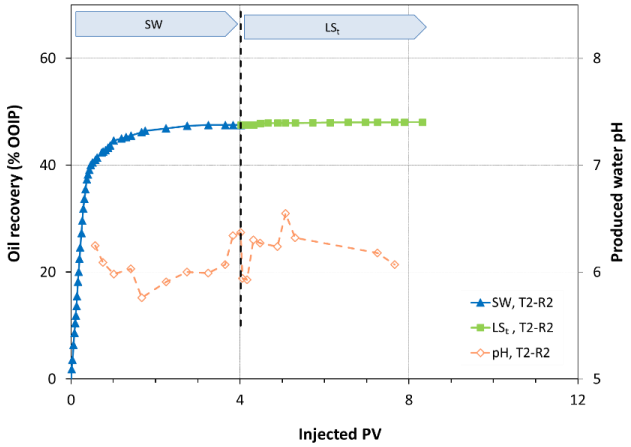


Figure 42. Oil recovery and PW pH on cores T2-R2 at 148° C. The core was successively flooded with SW–$LS_T$ with an injection rate of 4 PV/D.

The ion chromatography analyses of PW samples during SW and $LS_t$ injection can give supportive information about chemical interactions taking place during the recovery process. The content of $Ca^{2+}$, $Mg^{2+}$ and $SO_4^{2-}$ in the PW from core T1-R1 is shown in figure 43.

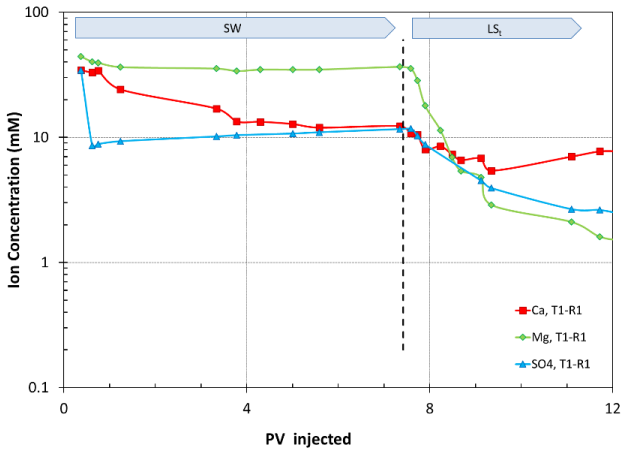


Figure 43. Chemical analysis of PW samples during the oil recovery test for core T1-R1 at 148 °C. The core was successively flooded with SW – $LS_t$ at a rate of 4 PV/D.

Significant differences in the concentration of $SO_4^{2-}$ in the bulk SW, table 8, and PW samples during SW flooding ar observed, 24 and 10 mM respectively. The results indicate precipitation of sulphate salts, most likely Anhydrite ($CaSO_4$), as the concentration of $Ca^{2+}$ also declined to 10 mM which is less than that in SW. When the injection brine was switched to $LS_t$, all ion concentrations declined as expected, but the stabilized concentration of $SO_4^{2-}$ and $Ca^{2+}$, 2 and 8 mM respectively are higher compared to $LS_t$ concentrations of 0.8 mM $SO_4^{2-}$ and 0.3 mM $Ca^{2+}$. The results indicate that the precipitated $CaSO_4$ during SW injection is redissolved during $LS_t$ injection. This will move the wettability alteration reaction in unfavorable direction. The high concentration of $Ca^{2+}$ could be also referred to the dissolution of other minerals such as dolomites $CaMg(CO_3)_2$, $Ca(Mg,Fe)(CO_3)_2$, calcite ($CaCO_3$), and calcium hydroxide $Ca(OH)_2$.

The QEMSCAN analysis of the cores confirms presence of 8.5% dolomite which is a considerable amount. In addition, reduced concentration of $Mg^{2+}$ during LS flooding can be explained by $Mg(OH)_2$ precipitation, which will take place at high temperatures and alkaline conditions.

Three important series of chemical reactions that could take place in reservoir sandstone systems have been summed up and need to be accounted for during water injection processes:

- Cation exchanges at mineral surfaces by $H^+$, Eq. A:

$$Ca^{2+}\cdots Clay \;+\; H_2O \;\rightleftarrows\; H^{+}\cdots Clay + Ca^{2+} + \; OH^{-}$$

$$Mg^{2+}\cdots Clay \;+\; H_2O \;\rightleftarrows\; H^{+}\cdots Clay + Ca^{2+} + \; OH^{-} \qquad \text{(A)}$$

$$NaAlSi_3O_8 + \; H_2O \;\rightleftarrows\; HAlSi_3O_8 + \; Na^{+} + OH^{-}$$

- Mineral dissolution reactions, Eq. B:

$$CaMg(CO_3)_2\;(s) \rightleftarrows\; Ca^{2+}(aq) + \; Mg^{+}(aq) + \; 2\,CO_3^{2-}\;(aq) \qquad \text{(B)}$$

$$CaSO_4\;(s) \;\rightleftarrows\; Ca^{2+}(aq) + \; SO_4^{2-}\;(aq)$$

- Precipitation at increased pH (increased $OH^-$ concentrations), Eq.C:

$$Ca^{2+}(aq) + 2OH^{-} \;\rightleftarrows\; Ca(OH)_2\;(s) \qquad \text{(C)}$$

$$Mg^{2+}(aq) + 2OH^{-} \;\rightleftarrows\; Mg(OH)_2\;(s)$$

In offshore Smart water EOR projects, Three different brines, FW, SW, and potential Smart Water presents. Different ions, in contact with reservoir minerals, will affect the wettability alteration process. In Addition at reservoir high temperature, the reactivity of ions and solubility of precipitated and minerals will be affected by the temperature, which has to be taken into account while investigating the potential for any individual reservoir.

### *4.3.4 Modified SW as smart water?*

Formation Waters in the sandstone reservoirs contain abundance concentrations of light divalent cations, i.e $Ca^{2+}$ and $Mg^{2+}$ and also less

concentration of heavy cations such as $Ba^{2+}$ and $Sr^{2+}$ (Crabtree et al., 1999). The reactivity of the divalent cations increases with increasing temperature, and in offshore reservoirs, at a temperature above 100 °C, SW with a high concentration of $SO_4^{2-}$ may cause reservoir souring and precipitation of $SO_4^{2-}$ -bearing minerals like anhydrite ($CaSO_4$), barite ($BaSO_4$) and celestine ($SrSO_4$). Barium scale will precipitate even at very low concentrations and need to be controlled (Olajire, 2015). By considering these issues, chemical modification of the seawater is often recommended. This was authenticated in the early 1990's during the development of the South Brae oilfield in the North Sea (Davis and McElhiney, 2002; Hardy et al., 1992).

In addition of scale problems, switching the injection brine to a LS brine may re-dissolve precipitates such as $CaSO_4$ and increase the concentration of $Ca^{2+}$ ions in the LS brine which could be unfavorable for observing wettability alteration. In high salinity reservoirs, secondary SW injection could reduce the potential of tertiary LS flooding. Then it is questioned if "modified seawater" (mSW) with reduced sulfate concentration for scale prevention can behave as a Smart Water? And if there is a LS brine EOR potential after mSW flooding?

To answer these questions, a new set of the oil recovery experiments have been performed on another high temperature North Sea sandstone reservoir, reservoir M, are tested for secondary mSW flooding and secondary and tertiary LS flooding with EOR purpose.

Twin core from reservoir M, M3 and M5, are sampled at the same depth and with similar physical properties as porosity, specific surface area, and permeability. XRD and QEMSCAN analysis of samples from the cores indicated clay content of 14-20%, and Feldspar contents of 3-4 wt%, high enough to contribute with ion exchange reactions and increased pH during the Smart Water flooding (Piñerez Torrijos et al., 2017; Reinholdtsen et al., 2011). Reservoir temperature is above 130 °C, and $FW_M$ has medium salinity of 63 000 ppm with a typical $Ca^{2+}/Mg^{2+}$ - ratio for sandstone reservoirs. The modified seawater (mSW) is a treated seawater (SW) with very low $SO_4^{2-}$ and reduced concentration of $Ca^{2+}$ and $Mg^{2+}$. Lastly, the low salinity ($LS_M$) brine is 20 times diluted mSW brine. The stabilized reservoir crude oil M used in these experiments had AN of 0.16 mg KOH/g and a BN of 0.76 mg KOH/g, POC concentrations high enough to give mixed wetting.

Four viscous flooding oil recovery tests were performed on core M5 to compare LS EOR potential of the core using $LS_M$ brine with mSW, SW and FW of the reservoir ($FW_M$) at reservoir temperature ($T_{res}$ > 130 °C). The Oil recovery results are presented figure 44.

After the first restoration, core M5-R1 was flooded with $LS_m$ with a rate of 4 PV/D. Ultimate oil recovery was of 58.3 %OOIP, which has achieved after 1.3 PV injected.

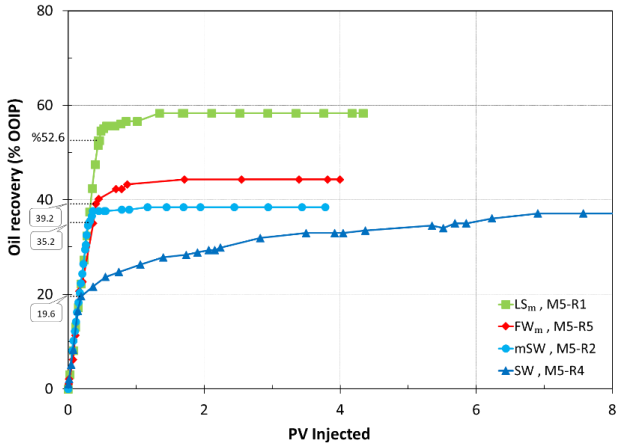


Figure 44. Oil recovery tests at $T_{res}$ > 130 °C on core C5, with $LS_m$, mSW, SW, or $FW_m$ at a rate of 4 PV/D.

The pH of PW increased from 5.5 to slightly above pH 7 during the $LS_m$ flooding, Figure 45.

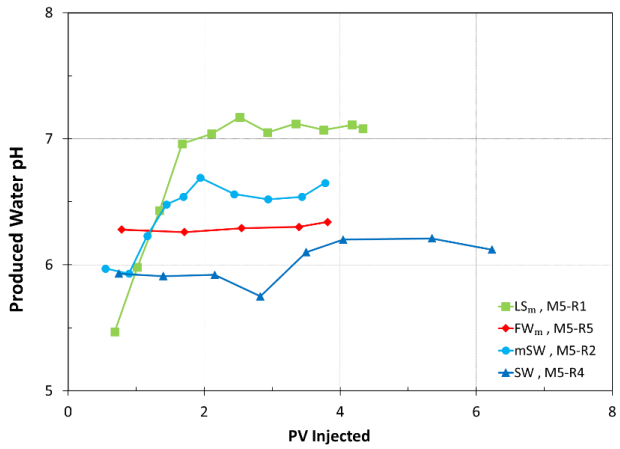


Figure 45. PW pH profiles during different oil recovery tests at $T_{res}$ > 130 °C on core C5. with $LS_m$, mSW, SW, or $FW_m$ at a rate of 4 PV/D

Ion chromatography analyses of PW are presented in figure 46. Significant amounts of $SO_4^{2-}$, 5 mM, are observed in the first samples and steadily declining to 2 mM after 4 PV of $LS_m$ injection, possibly

linked to the dissolution of anhydrite minerals. The concentration of $Ca^{2+}$ and $Mg^{2+}$ decreased to concentrations similar to the original LS brine concentrations after 3 PV $LS_m$ injection.

After second and forth restoration the core has been flooded respectively with mSW and SW in secondary mode and the tests are termed M5-R2 and M5-R4 respectively. Ultimate oil recovery plateaus of 39 %OOIP was reached for both mSW and SW. mSW reached to the plateau after 1 PV injected, while SW achieved the plateau after 7 PV.

To have the baseline without any chemical influence from the injection brine, a last recovery experiments was performed using $FW_M$ as the injection brine, core M5-R5. This test is termed M5-R5.

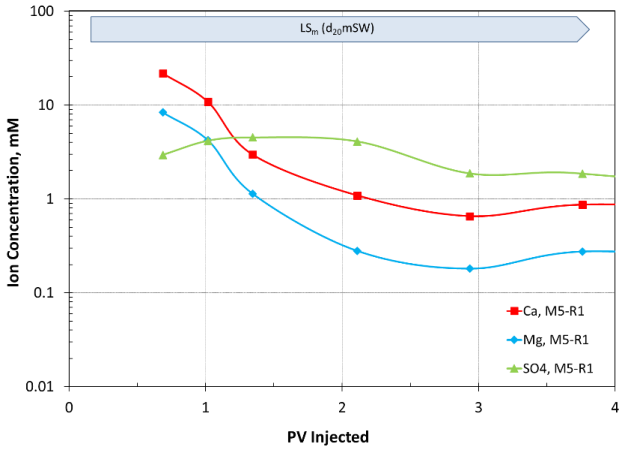


Figure 46. Chemical analyses of PW samples during the oil recovery test M5-R1. Ion concentrations are in mM. and they are reported as a function of PV injected.

The oil recovery experiments confirm the highest recovery was achieved during $LS_m$ injection, Figure 44, which also gave the highest PW pH. SW

injection gave the slowest and lowest oil recovery, and the results are supported by the lowest PW pH. Both SW and mSW gave lower ultimate oil recovery compared to baseline recovery during $FW_m$ injection. Clearly, also for this reservoir system, the LS brine behaved as the smartest water with the highest EOR potential.

The combination of high clay content, moderate FW salinity and low initial pH observed in all the experiments indicates favorable conditions for adsorption of POC at mineral surfaces, (Burgos et al., 2002; Fogden, 2012; Strand et al., 2016), creating reduced water wetness even at reservoir temperatures above 130 °C (Aghaeifar et al., 2015; Gamage and Thyne, 2011). Initially reduced water wetness is an absolute need for being able to observe Smart water EOR effects by wettability alteration.

#### 4.3.4.1 **Tertiary LS EOR after mSW injection**

After the secondary injection of modified SW, core M5-R2, a tertiary $LS_M$ injection was performed to evaluate the LS EOR potential in a reservoir pre-flooded by mSW. The full oil recovery profile and PW pH are presented in figure 47.

Ultimate oil recovery during mSW injection reached 38 %OOIP. When the injection brine was switched to $LS_m$, 6 %OOIP extra oil was recovered. The increased recovery was accompanied by an increase in PW pH from 6.5 to 7.7.

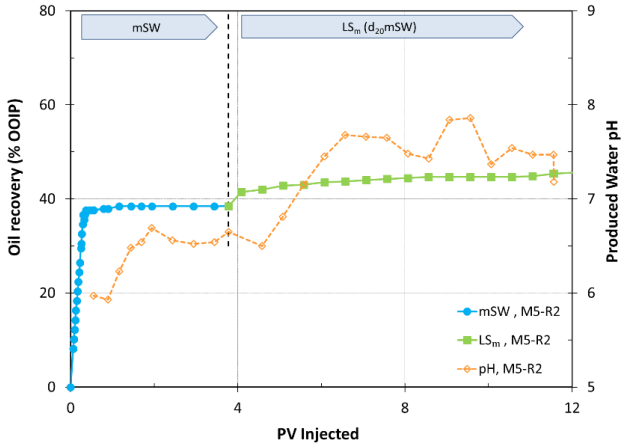


Figure 47. Oil recovery test M5-R2 at $T_{res}$ (> 130 °C). The core was successively flooded with mSW – $LS_m$ at a rate of 4 PV/D.

Comparing the ultimate tertiary $LS_M$ oil recovery of 45 %OOIP, figure 47, with the ultimate secondary LS recovery of 58 %OOIP, figure 44, shows that the LS EOR potential is significantly reduced when it is injected into a core pre-flooded with mSW. mSW contains low amount of $Mg^{2+}$ and $SO_4^{2-}$ ions, so the reason of reduced EOR potential cannot be referred to precipitation and dissolution of $Mg(OH)_2$ and anhydrite during mSW and $LS_m$ flooding; The main reduction in EOR potential in tertiary mode could be the increased in water saturation, $S_w$ when LS brine is ready to be injected. When wettability alteration is taking place during LS injection in secondary mode, the oil saturation is much larger which makes it easier for POC to desorb into. The POC are not water-soluble and need an oil phase to escape into during the wettability alteration process.

Successful tertiary LS EOR effect and getting the highest recovery in secondary mode using $LS_m$, both confirms the $LS_m$ brine can improve

microscopic sweep efficiency. It has to be noticed that improvement in the displacement efficiency cannot be related to the improved mobility ratio, as the viscosity of the $LS_m$ brine is slightly less than mSW brine viscosity, measured to 0.94 and 0.99 cP respectively at 20 °C. This also can be investigated by evaluating the monitored pressure drop across the core during the Oil recovery tests at reservoir temperature. Figure 48 shows how the pressure drop changes during the oil recovery test on core M5-R2 during secondary mSW injection followed by tertiary $LS_m$ injection.

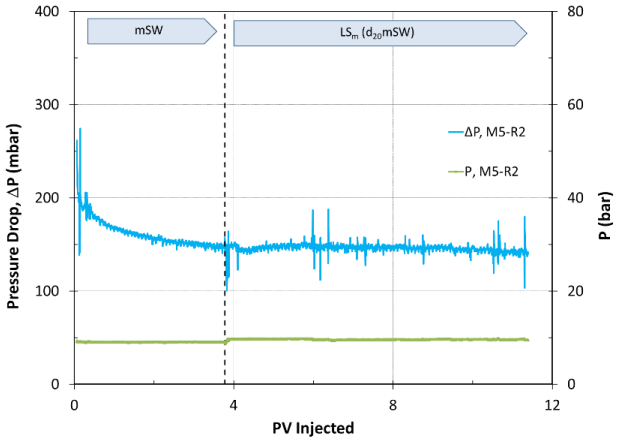


Figure 48. Inlet pressure (P) and pressure drop (ΔP) during the oil recovery test at $T_{res}$ on core M5-R2. The core was succesively flooded with mSW – $LS_m$ at a rate of 4 PV/D

We observe a steadily decrease in ΔP during mSW injection and stabilizing after 3 PV injected. When the injection brine is changed to $LS_M$, no significant changes in ΔP is observed confirming that changes in viscous forces could not explain the LS EOR effect of 6 %OOIP extra

oil. The fluctuations in ΔP observed during oil production are mainly due to two-phase flow of oil and brine across the back-pressure valve.

In figure 49, the pressure drop during secondary $LS_M$ injection in core M5-R1 is presented. With no larger differences in absolute pressure values and the same trend of gradually decrease in ΔP as the water saturation decreases, the observations are not supporting the idea of swelling of clays, fines migration, and diverted flow inside the core during LS brine flooding.

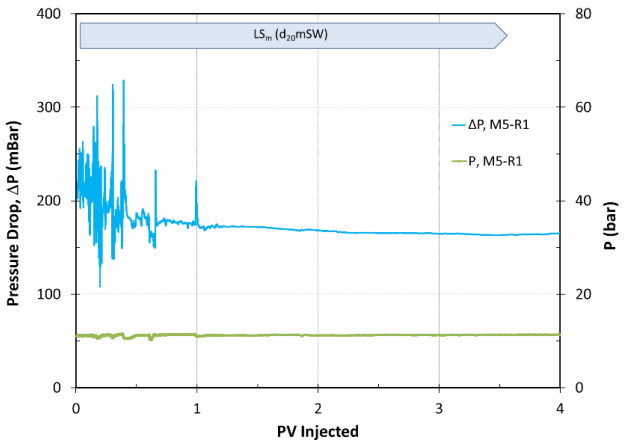


Figure 49. Inlet pressure (P) and pressure drop (ΔP) during oil recovery test on core M5-R1 by secondary $LS_m$ injection.

The ΔP observations support that the observed LS EOR effect is a result of wettability alteration. This will be discussed more in detail in section 4.4.

### 4.3.4.2 **Investigation of mSW EOR effects in a twin-core**

Oil recovery tests have been performed on a second core from reservoir M, core M3, to compare the $LS_m$ EOR potential both in secondary and tertiary mode with the results from core M5.

In test M3-R2 the core was flooded with $LS_m$ brine. The oil recovery profile and PW pH are presented in figure 50.

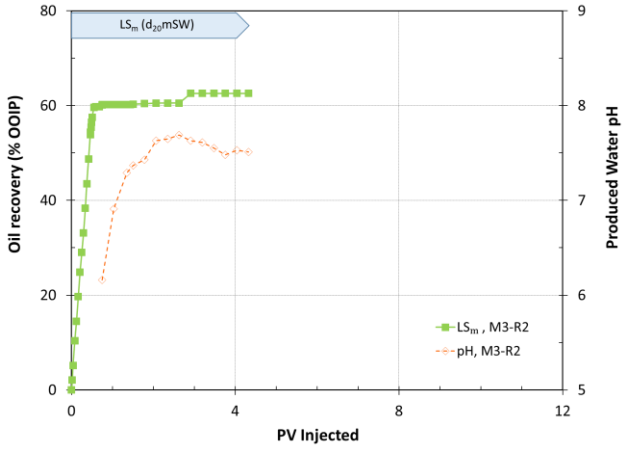


Figure 50. Oil recovery tests at $T_{res}$ > 130 °C on core M-R2. The core was flooded with $LS_M$ brine in secondary at rate of 4 PV/D.

In the second test, M3-R3, the flooding sequence was secondary mSW injection followed by $LS_m$. The oil recovery profile and PW pH are presented in figure 51.

The ultimate oil recovery by secondary $LS_m$ injection 63 %OOIP accompanied by 1.5 pH unite increase. Secondary mSW injection reached a plateau of 52 %OOIP and only 0.4 pH unit in increase. The tertiary LS EOR potential is also investigated in test C5-R3. During $LS_M$ injection, a slow increase in the recovery was observed, reaching a new

recovery plateau of 60 %OOIP after 4 PV injected. The PW pH one pH unit increased during the $LS_m$ injection.

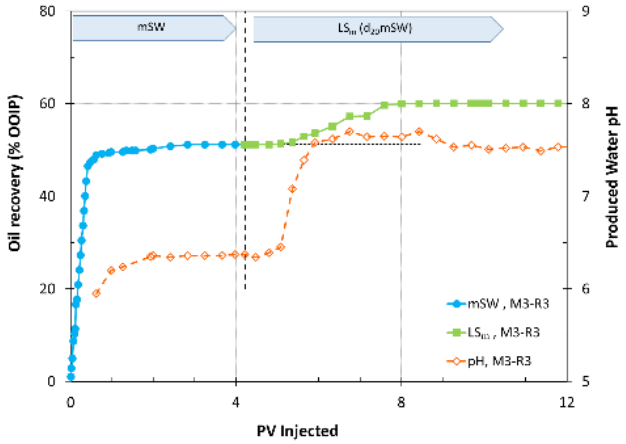


(b)

Figure 51. Oil recovery tests at $T_{res}$ > 130 °C on core M3-R3. The core was successively flooded with mSW – $LS_m$ at rate of 4 PV/D..

The most interesting point to notice is the significant difference in water breakthrough time during secondary mSW, figure 51, and secondary $LS_m$ injection, figure 50. The water breakthrough during mSW injection was observed after 46 %OOIP, while the $LS_m$ gave a significant delayed water breakthrough at 58 %OOIP.

The results from core C3 are in line with results concluded from core C5, and both are confirming that $LS_m$ brine is the Smartest brine compare to SW and mSW. When the $LS_m$ is introduced in the secondary mode it is proved to be very efficient, reaching the ultimate oil recovery just after 1PV injected.

According to the tests performed on the core material from reservoir M, T and P, tertiary LS EOR are dramatically reduced both in speed and ultimate recovery but is more promising when it is injected after mSW instead of normal SW.

## 4.4 Significance of Capillary Forces

In the previous part it is discussed that ion exchange at mineral surfaces promotes an alkaline environment needed for desorption of POC. This process leads to wettability alteration towards more water-wet conditions which results in increased capillary forces. (Austad et al., 2010; Piñerez Torrijos et al., 2016b). The wettability alteration is a result of CoBR-interactions at mineral pore surfaces. The process is time-dependent, and low flow rates could be needed to observe the LS EOR effect. Radial well geometries and reservoir heterogeneities result in low flow rates and low pressure drop in the main part of the reservoirs. The oil displacement could then be more dependent on capillary forces compared to the viscous forces.

In our experiments a low flow rate has been chosen, 4 PV/D, which will allow the chemical reactions to take place, so capillary forces could contribute to the recovery process. 4 PV/D corresponds approximately to the industry standard of 1ft/D (foot/Day).

The efficiency of LS brine injection has been tested by a large number of forced imbibition (viscous flooding) tests presented in the previous section. In this chapter, we will prove the idea of EOR by favorable

wettability changes and an increase in the capillary forces using LS brine. A series of spontaneous imbibition tests at $T_{res}$ have been performed on core M3 using any of the individual brines, $FW_m$, mSW and $LS_m$, to study the potential of different brines on generating positive capillary forces. Both secondary and tertiary SI tests have been performed on restored core M3.

After the fourth restoration of core M3, M3-R4, the core was placed in the SI setup, and $FW_m$ was used as imbibing brine. The result is presented in figure 52. The ultimate oil recovery of 42 %OOIP was reached after 5 days. No chemical-induced wettability alteration is expected to take place because the core is already equilibrated with the $FW_M$ during core restoration. The imbibition by itself confirms the presence of positive capillary forces in the core.

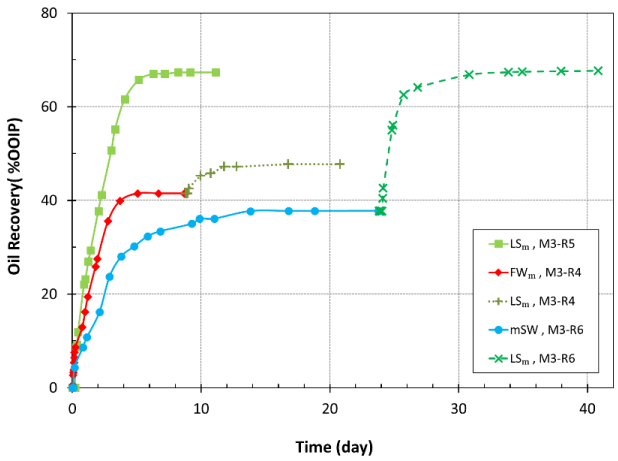


Figure 52. Oil recovery test at $T_{res}$ by spontaneous imbibition (SI) on core M3-R6 using mSW-LS brines, and in comparison, with spontaneous imbibition of LS in M3-R5 and FW-LS in core M3-R4.

After eight days, the imbibing brine was changed to $LS_m$, and 6 %OOIP extra oil is gradually recovered during the next five days, confirming wettability alteration and increased positive capillary forces during $LS_m$ imbibition, figure 52.

After the fifth restoration, M3-R5, the core is exposed to the $LS_m$ in the secondary mode. As expected, the LS brine significantly increased the capillary forces compared to FW, due to wettability alteration, and a oil recovery plateau of 67 %OOIP was reached after six days. Comparing the recoveries in the same time frame confirms an increased rate of imbibition with $LS_m$, which is a crucial parameter for optimized recovery processes.

Comparing the ultimate oil recoveries during SI and viscous flooding with $LS_M$ brine in secondary mode on core M3, SI with $LS_M$ gave the highest recovery of 67 %OOIP compared to 63%OOIP during viscous flooding. This confirms the key role of capillary forces during oil production from heterogeneous porous networks. Wettability alteration processes and capillary forces is normally ignored in mathematical reservoir modeling.

The final imbibition experiment, called M3-R6, was performed by SI with mSW followed by $LS_m$ brine. The result is presented in the figure 52. The ultimate oil recovery by mSW is 38 %OOIP, which is almost comparable with $FW_m$, but the rate of imbibition is far slower. The result confirms the mSW is not smart water, and not able to induce increased capillary forces. But interestingly, when the imbibition brine is switched

to $LS_M$, a huge amount of extra oil was recovered reaching 68%OOIP after six days.

The results of all three spontaneous imbibition tests and two viscous flooding (Forced immbibtion, FI) tests performed on core M3 are summarized in table 12.

Table 12. Summary of the oil recovery tests by SI and VF performed on core M3.

| Test no. | Test type | Brines | Secondary oil recovery plateau (%OOIP) | Tertiary LS oil recovery plateau (% OOIP) | LS EOR effect (%OOIP) |
|---|---|---|---|---|---|
| M3-R2 | VF | $LS_m$ | 63 | – | – |
| M3-R3 | | mSW – $LS_m$ | 51 | 60 | 9 |
| M3-R4 | SI | $FW_m$ – $LS_m$ | 42 | 48 | 6 |
| M3-R5 | | $LS_m$ | 67 | – | – |
| M3-R6 | | mSW – $LS_m$ | 38 | 68 | 30 |

The results from secondary and tertiary $LS_m$ spontaneous imbibition, emphasizes the importance of positive capillary forces generated by wettability alteration in the viscous flooding (FI) tests. Performing brine injection at low rates are essential for observing the capillary effects. This is in line with the observations by Johannesen and Graue (2007) in their series of water flooding experiments in chalk, confirming that both SI and FI recovery curves reached almost the same plateau (similar residual oil saturations) when the flooding rate was at the lowest. This is in line with what hypothesized earlier that in the main part of the reservoir, where the pressure drop is the least, the spontaneous imbibition

due to positive capillary forces are the main driving forces during smart water flooding process.

The recovery data presented in table 12, confirms that The $LS_M$ promoted the most water wet system, and also behaved the smartest brine for EOR purposes. The $LS_m$ brine gave the best sweep efficiency and showed the latest water breakthrough point during the FI test, figure 50. SI tests confirmed that the highest recovery is achieved in the most water wet system which is inconsistency with what Jadhunandan and Morrow (1995) stated that the highest oil recovery will be achieved in the neutral to slightly water-wet conditions.

Contrarily to the $LS_m$ brine, mSW could not contribute to increased capillary forces by wettability alteration compare to the base brine which is $FW_m$.

The oil recovery process during FW injection into heterogeneous porous systems can be explained by viscous displacement of oil from larger high permeable pores, and some contribution of capillary forces, figure 53b. When the flooding brine is switched to a Smart Water, the chemical wettability alteration will increase capillary forces and the oil recovery is increased by improving both the microscopic and macroscopic sweep efficiencies, figure 53c.

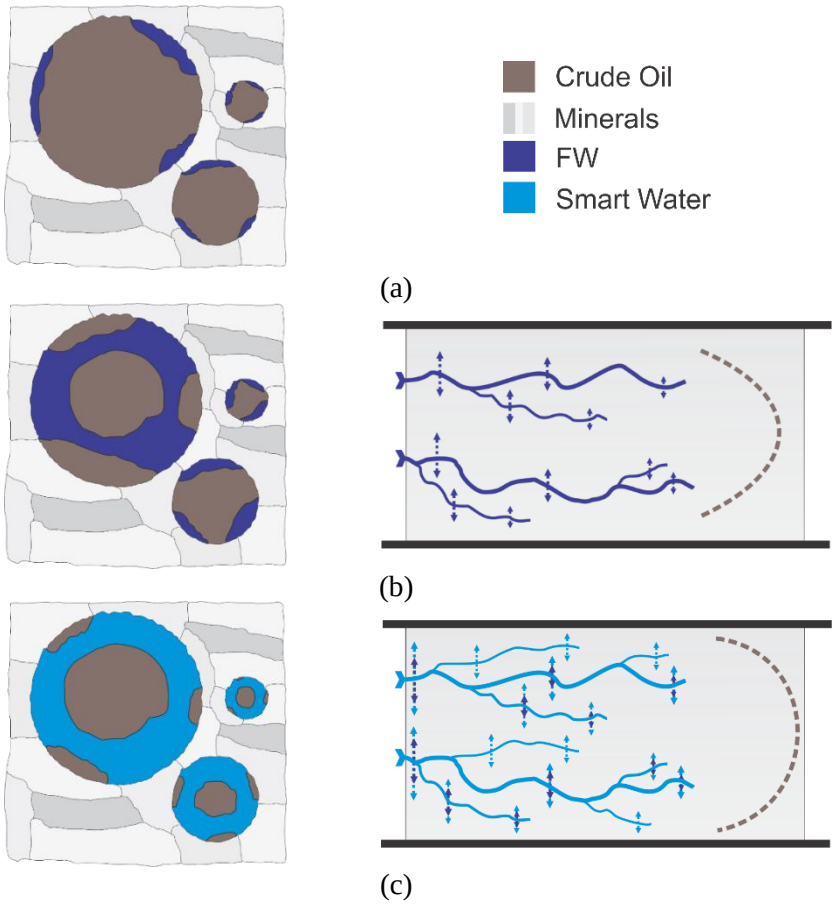


Figure 53. Oil distribution and displacement efficiency in a heterogeneous porous network with large, medium and small pores during FW and Smart Water injection.
**(a)** Initial oil saturation in heterogeneous pore systems. **(b)** Residual oil saturation after FW injection at fractional slightly water-wet conditions where the oil displacement is controlled by viscous and capillary forces, and **(c)** Residual oil saturation after wettability alteration with Smart Water where the oil displacement is controlled by viscous and stronger capillary forces.

# 5 Concluding remarks

## 5.1 Conclusions

By performing some fundamental experiments and also some case studies the potential of LS brine, seawater, and modified seawater injection for EOR purposes in high temperature sandstone offshore reservoirs was evaluated.

The results obtained from several number of oil recovery tests using an excellent promising restoration method provides the following points:

- Low salinity brine always shows the best EOR performance, resulting in higher ultimate oil recovery and better sweep efficiency by giving a later water breakthrough. Most of the recoverable oil can be produced after one PV injected. The higher oil recovery also corresponds to the higher ΔpH of the produced water during the water flooding EOR. Secondary LS EOR potential has consistent behaviour for a variety of formation water salinities with a low to high salinity.
- Seawater is not smart water in secondary mode at high temperature reservoir. And due to the high concentration of $Ca^{2+}$ and $Mg^{2+}$ and also $SO_4^{2-}$ it reduces the potential for wettability alteration by lowering the ΔpH during tertiary low salinity brine injection for EOR.
- Modified seawater also did not perform as an efficient secondary EOR method, and was not able to sufficiently increase the

capillary forces leading to incremental recovery factor, but due to lower divalent ion concertation, it still provides a good initial condition for tertiary LS smart water flooding.

In addition, parametric studies of the initial wetting and wettability alteration process were accomplished in two sets of experiments: Firstly adsorption/desorption tests of $Ca^{2+}$ and $Mg^{2+}$ to/from sand pack surfaces containing pure quartz, mixture of quartz-kaolinite and mixture of quartz-illite at ambient and elevated temperature, and secondly by adsorption/desorption study of a basic POC model (Quinoline) towards quartz, kaolinite and illite surfaces. The experiments confirmed:

- Far less importance of quartz minerals compared to both kaolinite and illite on the adsorption of both active cations and also the basic POC model, compared to kaolinite and illite clay. This result clearly highlights the clay presence importance on initiating the mixed wettability, by adsorption on the rock surface
- The affinity of $Ca^{2+}$ towards kaolinite and illite was much stronger than $Mg^{2+}$**.**
- The affinity of both ions, $Ca^{2+}$ and $Mg^{2+}$, towards kaolinite, increased as the temperature increased, i.e. the desorption process took place in a more extended time, confirming that desorption from the clay surface is an exothermic process.
- Adsorption/desorption of quinoline on the kaolinite is absolutely pH dependent, same as the results obtained by illite. Moreover,

the maximum adsorption on the kaolinite clay was obtained at pH ~5.

- The adsorption of quinoline is also temperature dependent, and the potential to adsorb on the clay surface is reduced by increasing temperature to 130 °C.
- The quinoline adsorption is higher when using LS brine, and it is reduced by an increase in the salinity of the brine, i.e by increasing the salinity of initial brine in the rock the potential of POC adsorption will be reduced and the rock will get more water wet.
- The adsorption of quinoline onto illite clay is significantly higher compared to the kaolinite clay, while the adsorption process of quinoline is not totally reversible from the illite surface.

## *5.2 Future work*

- Based on the experiments performed and results and observations made in this research, the following suggestion can be considered for the future study plans:
- Investigation of the potential of modified seawater in other reservoir cores with different mineralogy, specially the cases which do not contain dissolvable minerals.
- Combined LS brine EOR effect with other methods to get an even higher increase in the capillary number, such as polymer flooding which can be a reasonable option for the reservoirs with high permeability and, $CO_2$ LS water alternative gas ($CO_2$ LS WAG)

to get benefit of both wettability alteration and also improving gas flooding performance by controlling the gas mobility.

- Performing a single oil recovery scenario in single or twin cores at the different injection flow rate, to investigate how SI during FI oil recovery test can be affected.
- More extensive parametric study to prove the upper and lower salinity and composition limit for formation water, to have the optimum initial wetting condition. This can help to predict the performance of LS EOR for specific reservoirs.

# 6 References


Abdelgawad, K.Z. and Mahmoud, M.A., 2015. In-Situ Generation of CO2 to Eliminate the Problem of Gravity Override in EOR of Carbonate Reservoirs. SPE-172516-MS. SPE Middle East Oil & Gas Show and Conference, Manama, Bahrain, 8-11 March. https://doi.org/10.2118/172516-MS.

Abrams, A., 1975. The Influence of Fluid Viscosity, Interfacial Tension, and Flow Velocity on Residual Oil Saturation Left by Waterflood. SPE-5050-PA, 15(05): 437-447. https://doi.org/10.2118/5050-PA.

Aghaeifar, Z., Strand, S., Austad, T., Puntervold, T., Aksulu, H., Navratil, K., Storås, S. and Håmsø, D., 2015. Influence of formation water salinity/composition on the low salinity EOR effect in high temperature sandstone reservoirs. Energy & Fuels, 29(8): 4747-4754. https://doi.org/10.1021/acs.energyfuels.5b01621.

Ahmed, T. and McKinney, P.D., 2005. Performance of Oil Reservoirs. In: T. Ahmed and P.D. McKinney (Editors), Advanced Reservoir Engineering. Gulf Professional Publishing, Burlington, pp. 291-325. https://doi.org/10.1016/B978-075067733-2/50006-X.

Aksulu, H., Håmsø, D., Strand, S., Puntervold, T. and Austad, T., 2012. Evaluation of low salinity EOR-effects in sandstone: Effects of temperature and pH gradient. Energy & Fuels 26(6): 3497-3503. https://doi.org/10.1021/ef300162n.

Allard, B., Karlsson, M., Tullborg, E.-L. and Larson, S.Å., 1983. Ion exchange capacities and surface areas of some major components and common fracture filling materials of igneous rocks, Göteborg, Sweden.

Althani, M.G., 2014. An Evaluation of Low Salinity Waterflooding in Carbonates Using Simulation and Economics. Master thesis Thesis, Colorado School of Mines, Golden, Colorado.

Austad, T., 2013. Chapter 13 - Water-Based EOR in Carbonates and Sandstones: New Chemical Understanding of the EOR Potential Using "Smart Water". In: J.J. Sheng (Editor), Enhanced Oil Recovery Field Case Studies. Gulf Professional Publishing, Boston, pp. 301-335. https://doi.org/10.1016/B978-0-12-386545-8.00013-0.

Austad, T., Rezaeidoust, A. and Puntervold, T., 2010. Chemical mechanism of low salinity water flooding in sandstone reservoirs. SPE-129767-MS.

SPE Improved Oil Recovery Symposium, Tulsa, Oklahoma, USA, 24-28 April. https://doi.org/10.2118/129767-MS.

Babadagli, T., 2019. Philosophy of EOR. SPE-196362-MS. SPE/IATMI Asia Pacific Oil & Gas Conference and Exhibition, Bali, Indonesia, 29-31 October. https://doi.org/10.2118/196362-MS.

Bjørlykke, K. and Jahren, J., 2010. Sandstones and Sandstone Reservoirs. In: K. Bjorlykke (Editor), Petroleum Geoscience: From Sedimentary Environments to Rock Physics. Springer Berlin Heidelberg, Berlin, Heidelberg, pp. 113-140. https://doi.org/10.1007/978-3-642-02332-3_4.

Buckley, J.S. and Morrow, N.R., 1990. Characterization of crude oil wetting behavior by adhesion tests. SPE-20263-MS. SPE/DOE Seventh Symposium on Enhanced Oil Recovery, Tulsa, Oklahoma, April 22-25. https://doi.org/10.2118/20263-MS.

Burgos, W.D., Pisutpaisal, N., Mazzarese, M.C. and Chorover, J., 2002. Adsorption of quinoline to kaolinite and montmorillonite. Environmental Engineering Science, 19(2): 59-68. https://doi.org/10.1089/10928750252953697.

Cissokho, M., Bertin, H., Boussour, S., Cordier, P. and Hamon, G., 2010. Low Salinity Oil Recovery On Clayey Sandstone: Experimental Study. Petrophysics, 51(05): 9.

Crabtree, M., Eslinger, D., Fletcher, P., Johnson, A. and King, G., 1999. Fighting scale—removal and prevention. Oilfield Review, 11(3): 30-45.

Davis, R.A. and McElhiney, J.E., 2002. The advancement of sulfate removal from seawater in offshore waterflood operations. NACE-02314. Corrosion, Denver, Colorado, 7-11 April.

Denekas, M.O., Mattax, C.C. and Davis, G.T., 1959. Effects of Crude Oil Components on Rock Wettability. SPE-1276-G. AIChE-SPE Joint Symposium, Kansas City, Missouri, US, 17-20 May.

Didier, M., Chaumont, A., Joubert, T., Bondino, I. and Hamon, G., 2015. Contradictory trends for smart water injection method: Role of pH and salinity from sand/oil/brine adhesion maps. SCA2015-005. The International Symposium of the Society of Core Analysts, St. John's Newfoundland and Labrador, Canada, 16-21 August.

Donaldson, E.C., Yen, T.F. and Chilingarian, G.V., 1989. Chapter 16 Environmental Factors Associated with Oil Recovery. In: E.C.

Donaldson, G.V. Chilingarian and T.F. Yen (Editors), Developments in Petroleum Science. Elsevier, pp. 495-510. https://doi.org/10.1016/S0376-7361(08)70468-0.

Ehrenberg, S.N., Nadeau, P.H. and Steen, O., 2009. Petroleum reservoir porosity versus depth: Influence of geological age. The American Association of Petroleum Geologists Bulletin, 93(10): 1281-1296. https://doi.org/10.1306/06120908163.

Fan, T. and Buckley, J., 2000. Base number titration of crude oil samples. Personal communication.

Fan, T. and Buckley, J., 2006. Acid number measurements revisited. SPE-99884-MS. SPE IOR Symposium, Tulsa, OK, USA, 22-26 April. https://doi.org/10.2118/99884-MS.

Fogden, A., 2012. Removal of crude oil from kaolinite by water flushing at varying salinity and pH. Colloids and Surfaces A: Physicochemical and Engineering Aspects, 402: 13-23. https://doi.org/10.1016/j.colsurfa.2012.03.005.

Fogden, A. and Lebedeva, E., 2011. Changes in Wettability State Due to Waterflooding. The International Symposium of the Society of Core Analysts, Austin, TX, USA, 18-21 September.

Fuaadi, I.M., Pearce, J.C. and Gael, B.T., 1991. Evaluation of Steam-Injection Designs for the Duri Steamflood Project. SPE-22995-MS. SPE Asia-Pacific Conference, Perth. Australia, 4-7 November. https://doi.org/10.2118/22995-MS.

Gamage, P. and Thyne, G., 2011. Systematic investigation of the effect of temperature during aging and low salinity flooding of Berea sandstone and Minn. 16th European Symposium on Improved Oil Recovery Cambridge, UK, 12 April. https://doi.org/10.3997/2214-4609.201404798.

Green, D.W. and Willhite, G.P., 1998. Enhanced Oil Recovery. SPE Textbook Series, 6. Society of Petroleum Engineers, Richardson, Texas.

Hanzlik, E.J. and Mims, D.S., 2003. Forty Years of Steam Injection in California - The Evolution of Heat Management. SPE-84848-MS. SPE International Improved Oil Recovery Conference in Asia Pacific, Kuala Lumpur, Malaysia, 20-21 October. https://doi.org/10.2118/84848-MS.

Hardy, J.A., Barthorpe, R.T., Plummer, M.A. and Rhudy, J.S., 1992. Control of scaling in the South Brae field. OTC-7058-MS. Offshore

Technology Conference, Houston, Texas, 4-7 May. https://doi.org/10.4043/7058-MS.

Jadhunandan, P.P. and Morrow, N.R., 1995. Effect of wettability on waterflood recovery for crude-oil/brine/rock systems. SPE Reservoir Engineering, 10(01): 40-46. https://doi.org/10.2118/22597-PA.

Johannesen, E.B. and Graue, A., 2007. Systematic Investigation of Waterflood Reducing Residual Oil Saturations by Increasing Differential Pressures at Various Wettabilities. SPE-108593-MS. Offshore Europe, Aberdeen, Scotland, U.K., 4-7 September. https://doi.org/10.2118/108593-MS.

Jones, G., 1997. The Physical and Chemical Properties of Quinoline. In: G. Jones (Editor), Chemistry of Heterocyclic Compounds. John Wiley & Sons, Ltd, pp. 1-92. https://doi.org/10.1002/9780470187029.ch1.

Lager, A., Webb, K. and Seccombe, J., 2011. Low Salinity Waterflood, Endicott, Alaska: Geochemical Study & Field Evidence of Multicomponent Ion Exchange, 16th European Symposium on Improved Oil Recovery. European Association of Geoscientists & Engineers, Cambridge, UK.

Lager, A., Webb, K.J. and Black, C.J.J., 2007. Impact of brine chemistry on oil recovery. 14th European Symposium on Improved Oil Recovery Cairo, Egypt, 22–24 April

Lager, A., Webb, K.J., Black, C.J.J., Singleton, M. and Sorbie, K.S., 2008. Low Salinity Oil Recovery - An Experimental Investigation1. Petrophysics, 49(01).

Lake, L.W., 1989. Enhanced oil recovery. Prentice Hall, Englewood Cliffs, N.J.

Layti, F., 2017. Profitability of Enhanced Oil Recovery. Economic Potential of LoSal EOR at the Clair Ridge Field, UK. Master thesis Thesis, University of Stavanger, Norway, 54 pp.

Ligthelm, D.J., Gronsveld, J., Hofman, J.P., Brussee, N.J., Marcelis, F. and van der Linde, H.A., 2009. Novel waterflooding strategy by manipulation of injection brine composition. SPE-119835-MS. EUROPEC/EAGE annual conference and exhibition, Amsterdam, The Netherlands, 8-11 June. https://doi.org/10.2118/119835-MS.

Loahardjo, N., Xie, X. and Morrow, N., 2008. Oil recovery by cyclic waterflooding of mixed-wet sandstone and limestone. 10th International symposium on reservoir wettability, Abu Dhabi, UAE, 27-28 October.

Mair, C., 2010. Clair Ridge LoSal EOR Case Study : Laboratory measurement to Front End Engineering Design. IEA EOR Workshop & Symposium, Aberdeen, 18-20 October.

Moore, T.F. and Slobod, R.L., 1955. Displacement of Oil by Water-Effect of Wettability, Rate, and Viscosity on Recovery. Fall Meeting of the Petroleum Branch of AIME, New Orleans, Louisiana, 1955/1/1/. https://doi.org/10.2118/502-G.

Morrow, N.R., 1990. Wettability and its effect on oil recovery. Journal of Petroleum Technology, 42(12): 1476-84. https://doi.org/10.2118/21621-PA.

Morrow, N.R., Tang, G.-Q., Valat, M. and Xie, X., 1998. Prospects of improved oil recovery related to wettability and brine composition. Journal of Petroleum Science and Engineering, 20(3-4): 267-276. https://doi.org/10.1016/S0920-4105(98)00030-8.

Nasralla, R.A., Bataweel, M.A. and Nasr-El-Din, H.A., 2011. Investigation of wettability alteration by low salinity water. SPE-146322-MS. Offshore Europe, Aberdeen, UK, 6-8 September. https://doi.org/10.2118/146322-MS.

NPD, 2017. Resource Report 2017: Enhanced oil recovery (EOR) methods, Norway.

NPD, 2019. Resource report 2019 - discoveries and fields, Norway.

Olajire, A.A., 2015. A review of oilfield scale management technology for oil and gas production. Journal of Petroleum Science and Engineering, 135: 723-737. https://doi.org/10.1016/j.petrol.2015.09.011.

Park, S.-J. and Seo, M.-K., 2011. Chapter 6 - Element and Processing. In: S.-J. Park and M.-K. Seo (Editors), Interface Science and Technology. Elsevier, pp. 431-499. https://doi.org/10.1016/B978-0-12-375049-5.00006-2.

Piñerez Torrijos, I.D., Austad, T., Strand, S., Puntervold, T., Wrobel, S. and Hamon, G., 2016a. Linking low salinity EOR effects in sandstone to pH, mineral properties and water composition. SPE-179625-MS. SPE Improved Oil Recovery Conference, Tulsa, Oklahoma, USA, 11-13 April. https://doi.org/10.2118/179625-MS.

Piñerez Torrijos, I.D., Puntervold, T., Strand, S., Austad, T., Abdullah, H.I. and Olsen, K., 2016b. Experimental study of the response time of the low-salinity enhanced oil recovery effect during secondary and tertiary low-

salinity waterflooding. Energy & Fuels, 30(6): 4733-4739. https://doi.org/10.1021/acs.energyfuels.6b00641.

Piñerez Torrijos, I.D., Puntervold, T., Strand, S., Austad, T., Tran, V.V. and Olsen, K., 2017. Impact of temperature on the low salinity EOR effect for sandstone cores containing reactive plagioclase. Journal of Petroleum Science and Engineering, 156: 102-109. https://doi.org/10.1016/j.petrol.2017.05.014.

Reddick, C.E., Buikema, T.A. and Williams, D., 2012. Managing Risk in the Deployment of New Technology: Getting LoSal into the Business. SPE Improved Oil Recovery Symposium, Tulsa, Oklahoma, USA, 14-18 April. https://doi.org/10.2118/153933-MS.

Reinholdtsen, A.J., RezaeiDoust, A., Strand, S. and Austad, T., 2011. Why such a small low salinity EOR - potential from the Snorre formation? 16th European Symposium on Improved Oil Recovery, Cambridge, UK, 12-14 April. https://doi.org/10.3997/2214-4609.201404796

Rezaeidoust, A., Puntervold, T. and Austad, T., 2010. A discussion of the low-salinity EOR potential for a North Sea sandstone field. SPE-134459-MS. SPE Annual Technical Conference and Exhibition, Florence, Italy, 19-22 September. https://doi.org/10.2118/134459-MS.

RezaeiDoust, A., Puntervold, T. and Austad, T., 2011. Chemical Verification of the EOR Mechanism by Using Low Saline/Smart Water in Sandstone. Energy & Fuels, 25(5): 2151-2162. https://doi.org/10.1021/ef200215y.

Robbana, E., Buikema, T.A., Mair, C., Williams, D., Mercer, D.J., Webb, K.J., Hewson, A. and Reddick, C.E., 2012. Low Salinity Enhanced Oil Recovery - Laboratory to Day One Field Implementation - LoSal EOR into the Clair Ridge Project. SPE-161750-MS. Abu Dhabi International Petroleum Conference and Exhibition, Abu Dhabi, UAE, 11-14 November. https://doi.org/10.2118/161750-MS.

Seccombe, J.C., Lager, A., Webb, K.J., Jerauld, G. and Fueg, E., 2008. Improving Wateflood Recovery: LoSalTM EOR Field Evaluation. SPE Symposium on Improved Oil Recovery, Tulsa, Oklahoma, USA, 20-23 April. https://doi.org/10.2118/113480-MS.

Smalley, P.C., Muggeridge, A.H., Dalland, M., Helvig, O.S., Høgnesen, E.J., Hetland, M. and Østhus, A., 2018. Screening for EOR and Estimating Potential Incremental Oil Recovery on the Norwegian Continental Shelf. SPE-190230-MS. SPE Improved Oil Recovery Conference,

Tulsa, Oklahoma, USA, 14-18 April. https://doi.org/10.2118/190230-MS.

Springer, N., Korsbech, U. and Aage, H.K., 2003. Resistivity index measurement without the porous plate: A desaturation technique based on evaporation produces uniform water saturation profiles and more reliable results for tight North Sea chalk. International Symposium of the Society of Core Analysts Pau, France, 21-24 September.

Strand, S., Austad, T., Puntervold, T., Aksulu, H., Haaland, B. and RezaeiDoust, A., 2014. The impact of plagioclase on the low salinity EOR-effect in sandstone. Energy & Fuels, 28(4): 2378-2383. https://doi.org/10.1021/ef4024383.

Strand, S., Puntervold, T. and Austad, T., 2016. Water based EOR from clastic oil reservoirs by wettability alteration: A review of chemical aspects. Journal of Petroleum Science and Engineering, 146: 1079-1091. https://doi.org/10.1016/j.petrol.2016.08.012.

Taber, J.J., 1981. Research on Enhanced Oil Recovery: Past, Present and Future. In: D.O. Shah (Editor), Surface Phenomena in Enhanced Oil Recovery. Springer US, Boston, MA, pp. 13-52. https://doi.org/10.1007/978-1-4757-0337-5_2.

Taber, J.J., Martin, F.D. and Seright, R.S., 1997. EOR Screening Criteria Revisited - Part 1: Introduction to Screening Criteria and Enhanced Recovery Field Projects. SPE Reservoir Engineering, 12(03): 189-198. https://doi.org/10.2118/35385-PA.

Tang, G.-Q. and Morrow, N.R., 1999. Influence of brine composition and fines migration on crude oil/brine/rock interactions and oil recovery. Journal of Petroleum Science and Engineering, 24(2-4): 99-111. https://doi.org/10.1016/S0920-4105(99)00034-0.

Tang, G.Q.Q. and Morrow, N.R., 1997. Salinity, Temperature, Oil Composition, and Oil Recovery by Waterflooding. SPE Reservoir Engineering, 12(04): 269-276. https://doi.org/10.2118/36680-PA.

Thomas, S., 2008. Enhanced Oil Recovery - An Overview. Oil & Gas Science and Technology - Rev. IFP, 63(1): 9-19. https://doi.org/10.2516/ogst:2007060.

Winoto, W., Loahardjo, N., Xie, S.X., Yin, P. and Morrow, N.R., 2012. Secondary and tertiary recovery of crude oil from outcrop and reservoir rocks by low salinity waterflooding. SPE-154209-MS. SPE Improved

Oil Recovery Symposium, Tulsa, Oklahoma, USA, 14-18 April. https://doi.org/10.2118/154209-MS.

Wolcott, J.M., Groves, F.R., Jr., Trujillo, D.E. and Lee, H.G., 1993. Investigation Of Crude-Oil/Mineral Interactions: Factors Influencing Wettability Alteration. SPE-21042-PA, 1(01): 117-126. https://doi.org/10.2118/21042-PA.

Zavitsas, A.A., 2005. Aqueous Solutions of Calcium Ions: Hydration Numbers and the Effect of Temperature. The Journal of Physical Chemistry B, 109(43): 20636-20640. https://doi.org/10.1021/jp053909i.

# Paper I

"**Smart Water injection strategies for optimized EOR in a high temperature offshore oil reservoir**", Z. Aghaeifar, S. Strand, T. Puntervold, T. Austad. Journal of Petroleum Science and Engineering, June 2018, 165, pp 743-751. https://doi.org/10.1016/j.petrol.2018.02.021

Journal of Petroleum Science and Engineering 165 (2018) 743–751

Contents lists available at ScienceDirect

Journal of Petroleum Science and Engineering

journal homepage: www.elsevier.com/locate/petrol

# Smart Water injection strategies for optimized EOR in a high temperature offshore oil reservoir

Zahra Aghaeifar *, Skule Strand, Tina Puntervold, Tor Austad, Farasdaq Muchibbus Sajjad

*University of Stavanger, 4036 Stavanger, Norway*

A B S T R A C T

Smart Water injection is an EOR technique that is both environmentally friendly and easily implementable to a fractional cost compared to other water-based EOR methods. EOR by Smart Water is a wettability alteration process towards more water-wet conditions, which induces increased positive capillary forces and increased microscopic sweep efficiency.

The objective of this work was to evaluate the injection strategy for Smart Water in an offshore high temperature sandstone reservoir, and compare the efficiency of seawater-based injection brines with low salinity brines, which can behave as Smart Water in sandstone reservoirs. Oil recovery experiments have been performed at reservoir conditions using preserved reservoir cores and reservoir fluids.

Secondary low salinity injection gave an average of 33.5 %OOIP extra oil produced, compared to modified seawater injection. The tertiary low salinity EOR effect after modified seawater flooding gave an average of 11.8 %OOIP extra oil. Significant changes in produced water pH from initially acidic to alkaline conditions during low salinity injection were observed, favoring wettability alteration towards more water-wet conditions.

The results confirmed that low salinity brine behaved as a Smart Water, contributing with significant extra oil recovery in a high temperature sandstone reservoir. Introducing Smart Water from day one in a reservoir, i.e. in secondary recovery mode, is significantly more efficient, regarding both response time and ultimate oil recovery, than tertiary mode Smart Water injection.

## 1. Introduction

Waterflooding is extensively practiced in sandstone oil reservoirs to provide pressure support and to improve the oil displacement efficiency, and is typically introduced after a primary pressure depletion period. The water source used in the waterflooding process is typically the easiest available at the lowest possible cost. Considering Crude Oil/Brine/Rock (COBR) interactions, the injection water chemistry has been shown to have an impact on oil recovery. The first experimental investigation on the effect of waterflood salinity was performed by Bernard (1967). Years later, in early 1990's, the effect of injection water composition was broadly examined by Morrow and co-workers (Jadhunandan, 1990; Jadhunandan and Morrow, 1995). The results confirmed that the oil recovery increased when the salinity of the injection brine decreased. Recent research has confirmed that not only the salinity, but also the ion composition in the injection brine is important for optimizing the EOR effect (Austad et al., 2010; Piñerez Torrijos et al., 2016a; Piñerez Torrijos et al., 2016c; RezaeiDoust et al., 2011). It was experimentally verified that injecting a 25 000 ppm NaCl brine can give the same ultimate oil recovery as that observed by injecting a 1000 ppm NaCl brine (Piñerez Torrijos et al., 2016c). Therefore the term "Smart Water" is used for a brine that is able to alter rock wettability for increased oil recovery. The composition of the Smart Water brine is not fixed, but may vary for the individual reservoir rocks.

Seawater (SW) is the natural injection fluid in offshore oil reservoirs. The typical formation water (FW) has high salinity and high divalent cation concentrations (Crabtree et al., 1999). SW contains high amounts of sulfate ($SO_4^{2-}$), which may cause precipitation upon contact with divalent cations, and therefore chemical modification of the seawater is often recommended, especially for high reservoir temperatures ($T_{res}$). This was authenticated in the early 1990's during the development of the South Brae oilfield in the North Sea (Davis and McElhiney, 2002; Hardy et al., 1992). SW was modified to prevent reservoir souring and precipitation of anhydrite ($CaSO_4$), barite ($BaSO_4$), celestine ($SrSO_4$) or other $SO_4^{2-}$ -bearing minerals, by decreasing the divalent ion concentrations of $Ca^{2+}$, $Mg^{2+}$, and especially $SO_4^{2-}$. The salinity of the modified SW was still in the range of 30 000 ppm, and the Smart Water EOR potential of using such a brine for injection purposes could be limited. Therefore, it is of great scientific interest to verify if SW or modified SW (mSW) can behave as Smart Water. Furthermore, by diluting the SW or the modified SW 20 times, the usually recommended salinity of 1500 ppm to observe Smart Water EOR effects was reached, containing an ionic composition, which

* Corresponding author.
*E-mail address:* z.aghaeifar@gmail.com (Z. Aghaeifar).

https://doi.org/10.1016/j.petrol.2018.02.021
Received 25 July 2017; Received in revised form 9 February 2018; Accepted 10 February 2018
Available online 14 February 2018

is achievable at offshore installations.

The pore surface minerals, FW composition, and specific crude oil components affect the reservoir pH, and they are also the main parameters controlling the initial wettability in sandstone reservoirs (Buckley and Morrow, 1990; Didier et al., 2015; Fogden, 2012; Strand et al., 2016). Reservoir temperature and the competition between all species that could interact with negative charged sites at the mineral surfaces will influence the established wettability equilibrium in a reservoir, as seen in Fig. 1.

The minerals constitute the wetting surfaces, and the properties of the mineral surfaces are controlled by the mineral distribution within the pore space, available surface area, surface charge, cation exchange capacity (CEC), and the ionic composition and salinity of FW (Mamonov et al., 2017). The sour gasses $CO_2$ and $H_2S$ in crude oil partition into the brine phase, and can also affect the reservoir pH. The clay minerals contribute with a large portion of the pore surface, and with permanent negative charges, they can interact with protonated polar organic components at acidic conditions, creating a fractional wetting. With increasing pH, the degree of protonation of the polar organic components decreases, and at alkaline conditions the polar organic components will not adsorb to the negatively charged clay mineral surface (Austad et al., 2010; Burgos et al., 2002; Håmsø, 2011; Madsen and Lind, 1998).

The Smart Water EOR effect is described as a wettability alteration process towards more water-wet conditions (Austad et al., 2010; Lager et al., 2008; Morrow and Buckley, 2011; Nasralla et al., 2011). According to the suggested chemical Smart Water EOR model, cation desorption and proton ($H^+$) adsorption at mineral surfaces induces a local pH increase, needed for the wettability alteration, as the high salinity FW is displaced by the Smart Water. This model is illustrated by the following chemical equations using $Ca^{2+}$ as the active cation (Austad, 2013; Austad et al., 2010; RezaeiDoust et al., 2011).

$$\text{Slow reaction: Clay-}Ca^{2+} + H_2O \leftrightarrow \text{Clay-}H^+ + Ca^{2+} + OH^- + \text{HEAT} \quad (1)$$

$$\text{Fast reaction: Clay- } R_3NH^+ + OH^- \leftrightarrow \text{Clay} + R_3N: + H_2O \quad (2)$$

$$\text{Fast reaction: Clay-RCOOH} + OH^- \leftrightarrow \text{Clay} + RCOO^- + H_2O \quad (3)$$

It should be noticed that desorption of $Ca^{2+}$ ions from clay minerals,

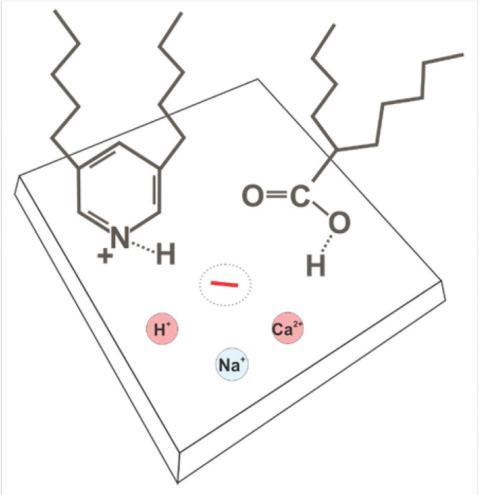


**Fig. 1.** The competition between active species towards negatively charged sites on the sandstone mineral surfaces will dictate the initial wettability (Strand et al., 2016).

Eq. (1), is an exothermic process, generating heat. The induced pH gradient when switching from FW to LS brine will be smaller with increased $T_{res}$ (Aghaeifar et al., 2015a; Aksulu et al., 2012). An exothermic contribution to the low salinity EOR effect in sandstone reservoirs was previously also suggested by Gamage and Thyne (2011). A combination of high $T_{res}$ and high FW salinity reduces the adsorption of organic material onto the clay minerals, and as a consequence the mineral pore surfaces could become too water-wet for observing significant Smart Water EOR effects (Aghaeifar et al., 2015a).

Offshore oil reservoirs at temperatures above 100 °C and with high FW salinity may contain anhydrite ($CaSO_4$) minerals. SW injection can also cause anhydrite precipitation. Dissolution of $CaSO_4$ during LS injection will increase the concentration of $Ca^{2+}$ in the brine, and according to Le Chatelier's principle, move Eq. (1) to the left, resulting in a reduced pH gradient. As a result, reduced tertiary LS EOR effects after secondary flooding with SW could be expected for high temperature reservoirs.

In this work the Smart Water EOR potential for an undeveloped sandstone oil reservoir at a temperature above 130 °C, has been evaluated. The objective was to compare the oil recovery results by secondary LS brine injection and by tertiary LS brine injection after modified (reduced sulfate to minimize scale potential) seawater flooding.

## 2. Experimental

### 2.1. Material

#### 2.1.1. Reservoir cores

Four preserved reservoir cores were used, C#1, C#3, C#4 and C#5. All cores were sampled from the same reservoir zone, only centimeters apart. Mineralogical data from neighboring cores were provided by the field operator, and are presented in Table 1. It should be noted that during core cleaning, anhydrite ($CaSO_4$) was detected in the effluent samples, however anhydrite minerals were not reported in the given XRD data. Physical core properties are listed in Table 2.

#### 2.1.2. Brines

Different synthetic brines based on given ionic compositions were prepared in the laboratory. The reservoir formation water (FW) has medium salinity of 63 000 ppm, with a typical FW ionic composition and $Ca^{2+}/Mg^{2+}$ -ratio for sandstone reservoirs. The modified seawater (mSW) is a treated seawater (SW) with reduced concentration of $SO_4^{2-}$, $Ca^{2+}$ and $Mg^{2+}$, for reduced scale potential. The low salinity (LS) brine is a 20 times diluted mSW brine. The brine properties are presented in Table 3.

#### 2.1.3. Oil

A stabilized reservoir crude oil (stock tank oil) was used in the oil recovery experiments. The crude oil was centrifuged and filtered through a 5.0 μm Millipore filter to remove any solid particles or water phase. The acid number (AN) and base number (BN) were determined by potentiometric titration with an accuracy of ±0.02 mg KOH/g. The methods used were developed by Fan and Buckley, and are modified versions of ASTM D664 and ASTM D2896 (Fan and Buckley, 2000, 2006). The asphaltene content was measured based on a modified version of the ASTM D6560, proposed by J. Buckley. The crude oil viscosity was measured at 20 and 60 °C using a MCR 302 rheometer delivered by Anton Paar. The crude oil properties are given in Table 4.

### 2.2. Core preparation and restoration

All cores used in the experiments went through the same core preparation procedure. The preserved cores were initially mildly cleaned at ambient temperature in a core holder. The core was first flooded with low aromatic kerosene to displace the crude oil phase. At clear effluents, the kerosene was displaced by heptane. At the end, the core was flooded with

**Table 1**
Mineralogical data from XRD analyses reported in wt%.

| Illite/ Smectite | Illite/ Mica | Kaolinite | Chlorite | Quartz | K-feldspar | Plagioclase | Dolomite | Total |
|---|---|---|---|---|---|---|---|---|
| 0–0.2 | 6.1–10.0 | 6.8–9.0 | 0.9–1.2 | 74.2–81.6 | 2.5–3.2 | 1.0–1.4 | 0.8–1 | 100 |

**Table 2**
Reservoir core properties.

| Core | Length, cm | Diameter, cm | Pore Volume, ml | Porosity, % | Permeability [a]$k_{wro}$, md | [b]BET, $m^2/g$ |
|---|---|---|---|---|---|---|
| C#1 | 7.26 | 3.84 | 11.77 | 14.0 | 6 | 0.67 |
| C#3 | 7.03 | 3.84 | 11.82 | 14.6 | 9 | 0.92 |
| C#4 | 7.00 | 3.84 | 11.10 | 13.7 | 5 | 1.40 |
| C#5 | 7.25 | 3.84 | 11.64 | 13.9 | 8 | 0.97 |

[a] $k_{wro}$: 1000 ppm NaCl permeability measured at heptane $S_{or}$. Measured during the first restoration.
[b] BET: Specific surface area using TriStar II PLUS from Metromeritics®.

**Table 3**
Brine compositions, with ionic concentrations given in millimole/L (mM).

| Ions | FW mM | SW mM | mSW mM | LS mM |
|---|---|---|---|---|
| $Na^+$ | 929.8 | 450.1 | 477.2 | 23.9 |
| $K^+$ | 17.8 | 10.1 | 8.1 | 0.4 |
| $Ca^{2+}$ | 44.2 | 13.0 | 8.2 | 0.4 |
| $Mg^{2+}$ | 7.0 | 44.5 | 13.5 | 0.7 |
| $Ba^{2+}$ | 5.2 | 0.0 | 0.0 | 0.0 |
| $Sr^{2+}$ | 3.0 | 0.0 | 0.0 | 0.0 |
| $Cl^-$ | 1058.8 | 525.1 | 527.9 | 26.4 |
| $HCO_3^-$ | 7.7 | 2.0 | 0.3 | 0.02 |
| $SO_4^{2-}$ | 0.0 | 24.0 | 0.4 | 0.02 |
| pH | 6.8 | 7.7 | 7.0 | 6.4 |
| TDS, mg/kg | 63 000 | 33 390 | 30 725 | 1536 |
| Density, $g/cm^3$ | 1.042 | 1.023 | 1.020 | 0.999 |

**Table 4**
Chemical and physical properties of the stabilized reservoir crude oil.

| AN (mg KOH/g) | BN (mg KOH/g) | Asphaltene (wt%) | Density @ 20 °C ($g/cm^3$) | Viscosity @ 20 °C (mPas) | Viscosity @ 60 °C (mPas) |
|---|---|---|---|---|---|
| 0.16 | 0.76 | 1.1 | 0.847 | 7.0 | 2.9 |

4 pore volumes (PV) of 1000 ppm NaCl brine to remove initial brine and any easily dissolvable salts. Effluent brine samples were collected for chemical analyses. Finally, the core was dried at 60 °C to constant weight.

Initial FW saturation of $S_{wi} = 15\%$ was established using the desiccator technique (Springer et al., 2003), and the core was equilibrated in a closed container for 3 days to establish an even ionic distribution throughout the core. Afterwards the core was mounted in a core holder, briefly evacuated down to the water vapor pressure, and then saturated by crude oil followed by 2 PV crude oil flooding in both directions to secure an even oil distribution. Finally, the core was placed on marble balls inside a steel aging cell surrounded by crude oil and aged for 2 weeks at $T_{res}$ (>130 °C).

After completion of the subsequent oil recovery test, the core was removed from the Hassler core holder and restored according to the same procedure as described above. By using this method to establish the initial water and oil saturations, the uncertainties of the initial saturation generation in each restoration are reduced.

### 2.3. Oil recovery tests

The restored core was placed into a temperature controlled Hassler core holder. The oil recovery experiment was performed with a confining pressure of 20 bar and a back pressure of 10 bar at constant $T_{res}$ (above 130 °C). The core was successively flooded with different injection brines at $T_{res}$ and using a constant flooding rate of 4 pore volumes per day (PV/D), corresponding to approximately 1 ft/day. At the end of each experiment, the flooding rate was increased four times to 16 PV/D to investigate any possible end-effects. The schematic illustration of the setup is shown in Fig. 2.

The accuracy of the injection rate was ±5%. Cumulative oil production with an accuracy of ±0.1 ml was monitored versus PV injected. Produced water (PW) samples, each containing 2–3 ml, were regularly collected and pH, density, and ionic composition were analyzed. Process parameters such as temperature, inlet pressure and pressure drop (ΔP) over the core were also monitored. A PT100 element with an accuracy of ±0.03 °C was used to ensure stable oven temperature of ±0.2 °C. Pressures were monitored using Rosemount 3051 pressure gauges with an accuracy of ±0.075% of full scale.

### 2.4. Surface reactivity/pH-screening test

A mildly cleaned, 100% FW saturated core was mounted in the Hassler core holder and flooded with FW – mSW – LS – FW – LS – FW at a rate of 4PV/D at $T_{res}$ (>130 °C). Effluent samples, each containing 2–3 ml, were collected, and pH and density of the produced water were monitored.

### 2.5. Analyses

#### 2.5.1. Ion analysis

Chemical analysis of effluent brine samples was performed using a Dionex ICS5000 + ion chromatograph (IC). The effluent samples were diluted 1000 times with deionized water and filtered through a 0.02 μm pore size paper filter prior to analyses. Ion concentrations were calculated based on the external standard method.

#### 2.5.2. Fluid density

Fluid densities were measured using a density meter DMA-4500 from Anton Paar.

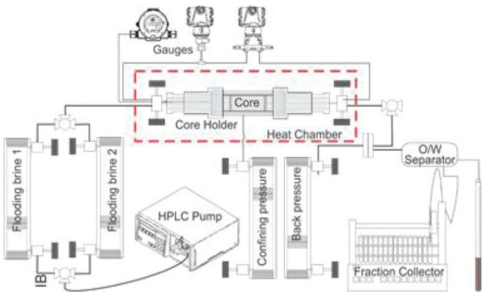


**Fig. 2.** Experimental setup for the oil recovery tests.

#### 2.5.3. Viscosity

A Physica MCR 302 rotational rheometer from Anton Paar was used for viscosity measurements. The measurements were performed with a cone and plate geometry at constant shear rates in the range of 10–100 $s^{-1}$, and at 20–60 °C.

#### 2.5.4. BET surface area

BET surface area measurements were carried out in a TriStar II PLUS instrument from Metromeritics®. The measurements were performed on rock samples taken from the same block as the core material used in this study, and the measurement accuracy was 0.02 $m^2/g$.

#### 2.5.5. pH measurements

The pH was measured using the Seven Easy™ pH meter delivered by Mettler Toledo, with a Semi-micro pH electrode optimized for small sample volumes. The measurements were performed at ambient temperature with a repeatability of ±0.02 pH units.

## 3. Results and discussion

The Smart Water EOR potential for a high temperature (>130 °C), medium FW salinity offshore sandstone oil reservoir has been evaluated. The Smart Water EOR effect is the result of a wettability alteration process towards more water-wet conditions, which induces increased positive capillary forces and improved microscopic sweep efficiency. A series of oil recovery experiments has been performed using preserved reservoir cores sampled close to each other in the same well. Core data are given in Table 1. The average core porosity was 14%, and the water permeability at residual heptane saturation measured during the core cleaning, was in the range of 5–9 mD. Due to the low permeability, even small wettability modifications toward more water-wet condition can significantly enhance capillary forces and improve the microscopic sweep efficiency during Smart Water injection.

The mineralogical data of the two cores are also expected to be comparable, as is indicated by the XRD data given in Table 2. A total clay content of 14–20 wt%, with equal amounts of kaolinite and illite/mica, which are characterized as non-swelling clays, are good initial conditions for observing LS EOR effects (RezaeiDoust et al., 2011; Robbana et al., 2012). The content of feldspar minerals is low, about 3–4 wt%, and therefore these minerals are not expected to contribute significantly to CEC and increased pH during the Smart Water flooding (Piñerez Torrijos et al., 2017; Reinholdtsen et al., 2011).

The presence of polar organic components in the crude oil is needed to create a mixed reservoir wetting. Positively charged polar organic components are anchor molecules attaching to negatively charged sites at the mineral surfaces (Burgos et al., 2002; Madsen and Lind, 1998; RezaeiDoust et al., 2011). As expected for a high temperature oil reservoir, the AN = 0.16 mgKOH/g is low due to decarboxylation during geological time. The BN of 0.76 mg KOH/g is moderate, but still high enough to partly wet mineral surfaces at acidic reservoir pH. The combination of high clay content and moderate FW salinity are promising for creating initial mixed wetting even at reservoir temperatures above 130 °C (Aghaeifar et al., 2015a; Gamage and Thyne, 2011).

In this experimental work, the efficiency of using LS brine as a Smart Water has been evaluated. Secondary injections of LS brine and modified SW (mSW), which is a possible injection brine for a high temperature offshore reservoir (>130 °C) have been compared. The efficiency of using the LS brine in tertiary mode after mSW injection has also been evaluated.

A mildly cleaned reservoir core was used in a surface reactivity test to evaluate the pore surface mineral – brine interactions at reservoir temperature. CEC at mineral surfaces will affect the pH development during FW, mSW and LS injection. The results give valuable information about the initial reservoir wettability and the potential of observing Smart Water EOR effect during mSW and LS injection.

Seven oil recovery experiments were performed using three initially preserved reservoir cores. All cores went through the same core restoration procedure prior to testing for minimizing experimental variation between each experiment. Each core was used in more than one oil recovery experiment, and to reduce experimental uncertainties, the brine flooding sequences varied for the individual cores.

### 3.1. Investigation of surface reactivity

The preserved and mildly cleaned reservoir core C#4 was successively flooded with FW – mSW – LS – FW – LS – FW brines at a constant rate, 4 PV/D, at $T_{res}$ (>130 °C). At each stage, the flooding continued until the pH and density of eluted brine stabilized as shown in Fig. 3.

During the first FW flooding, the effluent pH stabilized at 7.2. Then the injection brine was changed to mSW, and a decrease in the effluent density was observed, but the pH stabilized at 7.3, confirming that the mSW did not influence the pH that had stabilized during the FW flooding. Next, when LS brine was injected, a decrease in density was observed and when it was low enough after about 2 PV injected, a rapid increase in pH was observed. The pH stabilized above pH 8 with an ultimate ΔpH = 1.0. Switching back to FW, the salinity increased again and pH decreased to values below 7. The highest ultimate pH increase was observed when the LS brine was injected directly after FW, with an ultimate ΔpH = 1.8. Thus, simply based on pH increment values, the possibility of wettability alteration is larger with LS brine than with mSW brine.

The effluent concentrations of $Ca^{2+}$, $Mg^{2+}$ and $SO_4^{2-}$ were determined, and the results are shown in Fig. 4.

The most significant observation from the chemical analysis was that during the first FW flooding, the first effluent samples had $SO_4^{2-}$ concentrations close to 10 mM, indicating that the cores may contain small amounts of dissolvable anhydrite, $CaSO_4$. It must be noted that no sulfate was initially present in FW. During mSW flooding, the $SO_4^{2-}$ concentration decreased to 1.5 mM, which is more than 3 times the $SO_4^{2-}$ concentration initially present in mSW. During the flooding with LS brine containing 0.02 mM $SO_4^{2-}$, a concentration of 1 mM $SO_4^{2-}$ was observed in the effluent. After 12 PV injected, the anhydrite dissolution was dramatically reduced and effluent $SO_4^{2-}$ concentrations were reduced to the expected low values during both FW and LS brine injection.

Anhydrite dissolution was confirmed by increased concentration of $SO_4^{2-}$, but it also contributed to increased $Ca^{2+}$ concentrations. An increase in $Ca^{2+}$ concentration during LS injection will move Eq. (1) to the left, and consequently decrease the pH gradient. Thus, the presence of dissolvable $CaSO_4$ might reduce wettability alteration and thus decrease the LS EOR potential.

The $Ca^{2+}$ and $Mg^{2+}$ concentrations in the LS brine were 0.4 and 0.7 mM, respectively. Effluent concentrations during LS injections confirm $Ca^{2+}$ concentrations close to 0.4 mM, but the Mg concentration

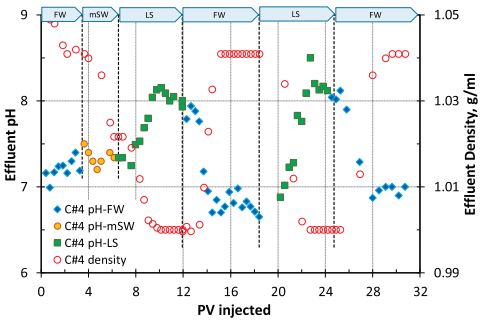


**Fig. 3.** Surface reactivity test performed on mildly cleaned core C#4 at $T_{res}$ (>130 °C). The flooding sequence was FW – mSW – LS – FW – LS – FW at a rate of 4 PV/D. pH and density of the effluent samples are presented vs. PV injected.

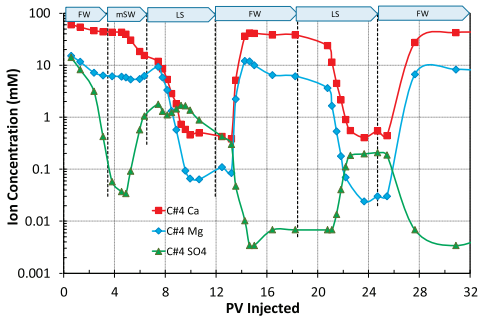


**Fig. 4.** Chemical analysis of effluent samples during the pH screening test on core C#4 at $T_{res}$ (>130 °C). The flooding sequence was FW – mSW – LS – FW – LS – FW at a rate of 4 PV/D. The concentration in mM of $Ca^{2+}$, $Mg^{2+}$, and $SO_4^{2-}$ ions are reported as a function of PV injected.

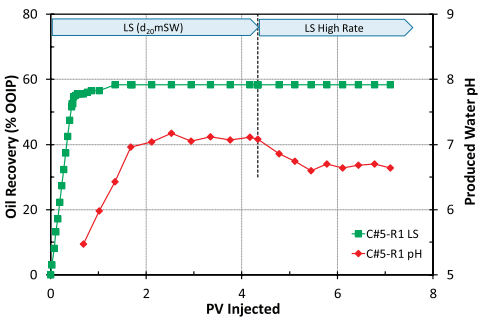


**Fig. 5.** The first oil recovery test on core C#5 at $T_{res}$ (>130 °C), termed C#5-R1. The core was restored with $S_{wi} = 0.15$, and saturated and aged in reservoir crude oil. The core was successively flooded with LS at 4 PV/D and LS at high rate (16 PV/D). The oil recovery (%OOIP) and pH of PW samples are plotted against PV injected.

dropped to values as low as 0.03 mM. This can be explained by $Mg(OH)_2$ precipitation, which increases with increasing $OH^-$ concentration (at high pH) and increasing temperature, as shown by Austad et al. (2010). The results also indicate that the observed pH increase in the effluent samples during the LS injection could have been even higher without the buffering effect of $Mg^{2+}$-ions. Additionally, the pH close to the mineral surface, where the wettability alteration takes place, could have been even higher without $Mg^{2+}$-ions present. If $OH^-$ is consumed by $Mg^{2+}$ ions, the reaction equations Eqs. (2) and (3) move toward left, and a lower amount of polar organic components is released from the clay mineral surface, and the wettability alteration is reduced.

### 3.2. Secondary low salinity injection

In order to study the potential of secondary LS EOR effects and to compare the recovery potential against secondary mSW injection, seven oil recovery tests were performed using 3 reservoir cores, C#1, C#3, and C#5, which were received in a preserved state. Prior to each core restoration, the cores were mildly cleaned. All cores were restored with $S_{wi} = 15\%$, and saturated, flooded and aged with the same amount of crude oil.

At least two oil recovery tests were performed on each core. It has been observed in laboratory studies that multiple core restorations can give some variations in initial core properties, which can lead to higher oil recoveries in the following restorations (Loahardjo et al., 2008). To compensate for these uncertainties, the brine injection sequence was not the same for all cores. After the 1st restoration of core C#5 and C#3, LS brine was injected in secondary mode, and after the 2nd core restoration the flooding sequence was mSW – LS. Core C#1 was flooded with mSW – LS after the 1st restoration, while LS brine was injected in secondary mode after the 2nd restoration.

After the 1st restoration on core C#5, the core was flooded with LS brine at a rate of 4 PV/D, and the test was termed C#5-R1. Water breakthrough took place at 0.5 PV injected, and the oil recovery plateau of 58.3 %OOIP was reached after 1.3 PV injected, Fig. 5. After 4 PV injected, the injection rate was increased to 16 PV/D, denoted LS high rate (LSHR), but no increased production was observed.

The first PW during LS injection had a pH of 5.5, showing the initial pH of the restored and equilibrated core, Fig. 5. In the next effluent samples, the pH steadily increased and stabilized slightly above 7. During the LSHR injection, the PW pH slightly reduced and stabilized close to 6.7. It should be noticed that the pH of 5.5 in the first PW sample was much lower than the pH observed during the pH screening test on core C#4 during FW flooding, Fig. 3. A low initial water saturation and presence of crude oil acidic and basic components affect the initial pH established during core restoration. The low initial pH observed is positive for adsorption of polar organic components onto mineral surfaces (Burgos et al., 2002; Fogden, 2012; Strand et al., 2016), and for creating initial mixed wet conditions.

The ΔP was monitored during the LS water injection. The initial ΔP was 260 mbar (average value), and with increasing water saturation ($S_w$) the ΔP gradually decreased and stabilized at 170 mbar, Fig. 6a. During the oil production, large fluctuations in ΔP was observed, which could be an indication of mobilization of oil droplets within the pore space, or an effect of two phase flow in the back pressure regulator. After 1 PV injected the fluctuation ceased, corresponding to the ultimate oil recovery plateau during LS injection.

The chemical analysis of PW ion concentrations, given in Fig. 6b, confirmed significant amounts of $SO_4^{2-}$ in the first samples, possibly linked to dissolution of anhydrite minerals. The concentration of $Ca^{2+}$ and $Mg^{2+}$ decreased to concentrations similar to the original LS brine concentrations.

### 3.3. Secondary modified seawater injection

After the first oil recovery test with secondary LS injection, C#5-R1, the core was mildly cleaned and a second core restoration was performed. A new oil recovery test was performed, but in this case mSW was used as injection brine, followed by LS injection in tertiary mode. The results from the second test, C#5-R2, are shown in Fig. 7.

Injection of mSW gave an oil recovery plateau of 38.4 %OOIP, which is much lower than the 58.3 %OOIP produced during the secondary LS injection, C#5-R1 in Fig. 5. The low efficiency by using mSW as injection brine is also reflected in the limited pH increase, which stabilized at 6.6. mSW contains higher concentrations of divalent cations compared to the LS brine, especially $Ca^{2+}$, which is a key ion in the Smart Water EOR process in sandstones. Based on Eq. (1), the concentration of $Ca^{2+}$ ions in the injection brine will affect desorption of initially adsorbed $Ca^{2+}$ ions. A high salinity brine with high $Ca^{2+}$ concentration will reduce the ability to exchange the $Ca^{2+}$ or other cations like $Na^+$ with $H^+$, which is necessary for creating an alkaline environment close to the rock surface.

The initial ΔP during mSW injection was 250 mbar, and it rapidly decreased and stabilized close to 140 mbar, Fig. 8a. Upon switching to LS brine, no change in pressure drop was observed. The extra oil produced by LS brine injection could not be explained by increased viscous forces. By quadrupling the injection rate, an increase in pressure drop was observed, but no extra oil was produced. Based on these observations, end-effects should be negligible.

During secondary mSW flooding the $SO_4^{2-}$-concentration in PW was much higher than the initial $SO_4^{2-}$-concentration in mSW (0.4 mM), as shown in Fig. 8b. With also a somewhat higher $Ca^{2+}$-concentration, this

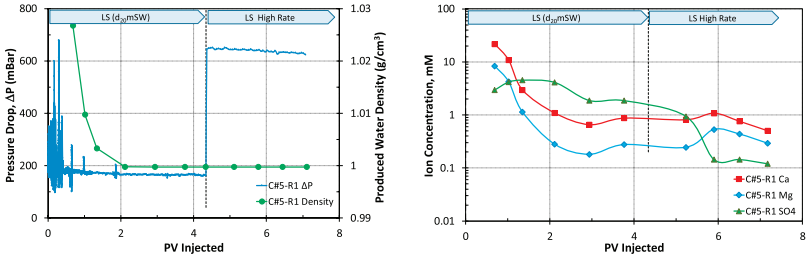


**Fig. 6.** Observations during the oil recovery test C#5-R1 at $T_{res}$ (>130 °C). **(a)** Pressure drop (ΔP) in mbar, and PW density in g/cm$^3$. **(b)** Chemical analyses of PW samples containing $Ca^{2+}$, $Mg^{2+}$ and $SO_4^{2-}$ ion concentrations in mM. All data are reported as a function of PV injected.

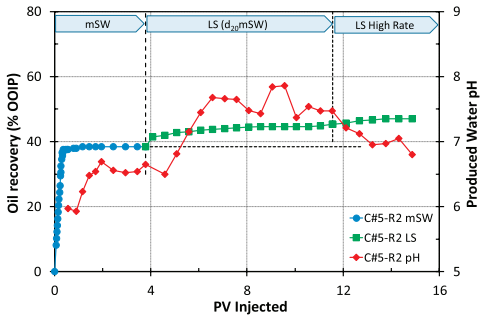


**Fig. 7.** Oil recovery test C#5-R2 at $T_{res}$ (>130 °C). The core was restored with $S_{wi} = 0.15$, and saturated and aged in reservoir crude oil. The core was successively flooded with mSW – LS at a rate of 4 PV/D. At the end, the injection rate was increased to 16 PV/D, LSHR. The oil recovery (%OOIP) and PW pH are plotted against PV injected.

indicates anhydrite dissolution.

### 3.4. LS EOR potential after modified seawater injection

Most offshore oil reservoirs have already been seawater flooded, so it is important to verify the tertiary LS EOR potential.

When the oil recovery plateau with mSW was reached in C#5-R2, the injection fluid was switched to LS brine, Fig. 7. The pH increased from 6.5 to 7.7 accompanied by an increased recovery from 38.4 to 44.6 %OOIP after 7 PV LS injected. A large pH increase was not enough to generate a large tertiary LS EOR effect up to the recovery level observed in secondary LS injection in Fig. 5. The ability for polar components to desorb from the mineral surface seemed to be reduced with increased water saturation, $S_w$. The polar crude oil components dictating the wettability are large organic molecules that are more or less insoluble in the water phase. At high $S_w$, the distance to the oil phase increases and less polar organic components desorb from the mineral surfaces. Increasing the injection rate to 16PV/D had very low effect on the recovery, and only 2 %OOIP extra oil was observed after several PV injected.

Only minor changes in ΔP was observed when the injection brine was changed to LS, but increased pressure fluctuations were observed, which could be an indication of redistribution of oil droplets within the pore space, Fig. 8a. This oil is not easily recoverable as observed by very little extra oil produced by increasing the injection rate 4 times, Fig. 7.

Comparing the ultimate tertiary LS oil recovery of 44.6 %OOIP, Fig. 7, with the ultimate secondary LS recovery of 58.3 %OOIP, Fig. 5, confirms a huge difference in the recovery potential. The reason for the difference in recovery is believed to be due to the water saturation, $S_w$. When wettability alteration is taking place during LS injection in secondary mode, the oil saturation is much larger than that during tertiary LS injection. Thus, it is easier and preferable for the desorbed large polar organic crude oil components to solubilize into a large oil phase, than solubilizing in the water phase and diffusing into the oil phase. When the amount of released organic components from the rock surface increases, the surface becomes more water-wet and capillary forces and consequently the microscopic sweep efficiency increases.

The results emphasize that for new field developments, optimized Smart Water EOR brines should be an important part of the development plan and their injection could significantly improve the field economics, both in the required amount of brine and in the ultimate oil recovery potential. The experimental laboratory results also show that optimized brines should be injected from day one.

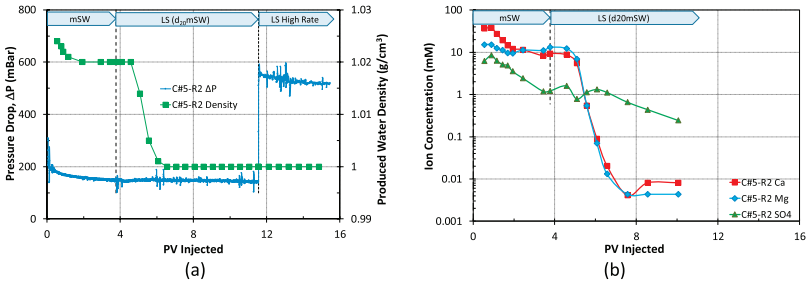


**Fig. 8.** Observations during the oil recovery test C#5-R2 at $T_{res}$ (>130 °C). **(a)** ΔP in mBar, and PW density in g/cm$^3$ during mSW - LS injection. **(b)** Chemical analyses of PW samples with $Ca^{2+}$, $Mg^{2+}$ and $SO_4^{2-}$ ion concentrations in mM. All data are reported as a function of PV injected.

### 3.5. EOR effects in multiple core experiments

In order to validate the low oil recovery observed in secondary mSW injection compared to secondary LS injection on core C#5, the experiment was repeated in a third restoration, test C#5-R3. The oil recovery results are presented in Fig. 9.

The test C#5-R3 successfully reproduced the initial wetting conditions and confirmed the previous results observed in C#5-R2 in Fig. 7. The mSW injection gave an ultimate oil recovery of 38.4 %OOIP, and the recovery increased to 43.7 %OOIP during tertiary LS injection. High rate LS injection gave no extra oil. The results confirmed that with optimized core handling and core restoration procedures in the laboratory, comparable oil recovery experiments can be performed using the same reservoir core.

Comparable Smart Water oil recovery experiments were also performed on core C#3. In test C#3-R2 the core was flooded with LS brine, and in test C#3-R3 the core was flooded with mSW followed by LS brine. The results are presented in Fig. 10.

The first oil recovery experiment on core C#3 failed, therefore the tests are termed C#3-R2 and C#3-R3. Large differences in the secondary ultimate oil recovery were also observed for this core. Secondary LS injection gave an ultimate recovery of 62.1 %OOIP as observed in Fig. 10a, while secondary mSW injection gave an ultimate oil recovery of 51.2 %OOIP, Fig. 10b. The first PW sample had an initial pH close to 6 in both tests. The pH increased 1.4 units with LS brine injection, while mSW injection only gave a pH increase of 0.3 pH units, confirming the link between pH increase and Smart Water EOR effects, which has been reported previously (Piñerez Torrijos et al., 2016a; Piñerez Torrijos et al., 2016b). Tertiary LS injection gave 8.9 %OOIP extra oil, which was supported by a high pH increase. However, the first extra oil was not observed until 1.5 PV injected, and the ultimate oil recovery plateau was not reached before a total of 4 PV of LS brine had been injected, which could be economically unfavourable.

When the oil recovery tests on C#1 were performed, the flooding sequence was deliberately changed, to prevent possible restoration effects on oil recovery as was reported by Loahardjo et al. (2008), and is explained above. After the first restoration, test C#1-R1, the flooding sequence was mSW – LS, while in test C#1-R2 LS brine was injected in secondary mode. The results are shown in Fig. 11.

The oil recovery with mSW injection reached a recovery plateau of 49.2 %OOIP which was obtained before 1 PV injected, Fig. 11a. From the oil recovery profile, the core appeared quite water-wet, also confirmed by no extra tertiary oil recovery when switching to the LS brine. Even a high flooding rate of 16 PV/D did not increase the recovery. The first PW had a pH of 6.2, which slightly increased to 6.7 during the mSW flooding. By switching from mSW to LS brine, the pH increased to 7.5. The increase in pH without extra oil production is an indication that the core most likely is quite water-wet.

In the test C#1-R2, the LS brine was injected in secondary mode, Fig. 11b. An ultimate oil recovery plateau of 53.1 %OOIP was reached after 2 PV injected. No extra oil was observed after increasing the flooding rate to 16 PV/D. The pH of the first PW sample was 5.8, and the pH increased and stabilized at 7.2. Even though core C#1 seemed to behave quite water-wet, 3.9 %OOIP extra oil was produced with LS compared to mSW in secondary mode. The extra oil was well synchronized with the increased pH observed during the LS flooding.

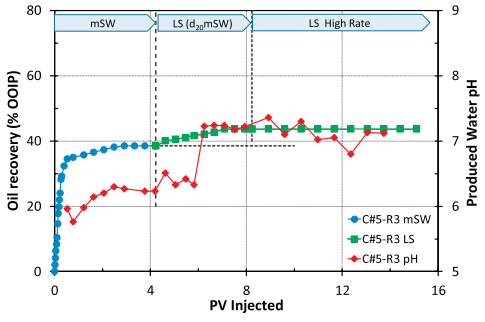


**Fig. 9.** Oil recovery test C#5-R3 at $T_{res}$ (>130 °C). The core was restored with $S_{wi} = 0.15$, and saturated and aged in reservoir crude oil. The core was successively flooded with mSW – LS at a rate of 4 PV/D. At the end, the injection rate was increased to 16 PV/D. The oil recovery (%OOIP) and pH of produced water are plotted against PV injected.

### 3.6. Comparing injection strategy possibilities

The core samples were collected from the same well at the same depth, within 15 cm distance. According to the XRD mineralogy data, the formation has high clay content but low content of feldspars/plagioclase. Therefore, it is reasonable to assume that the observed pH increase during LS injection is related to the CEC (exchange of protons for inorganic ions) at the clay surface, as described by Eq. (1) (Piñerez Torrijos et al., 2017), and that the contribution from feldspars, which have a lower CEC, is negligible (Allard et al., 1983). The clay minerals contribute with most of active mineral pore surfaces in sandstones, due to their large surface area (Allard et al., 1983), and they are therefore key factors for the observed Smart Water EOR effects (Aghaeifar et al., 2015b).

All oil recovery results are summarized in Table 5. Secondary LS injection was always more efficient and gave significantly higher

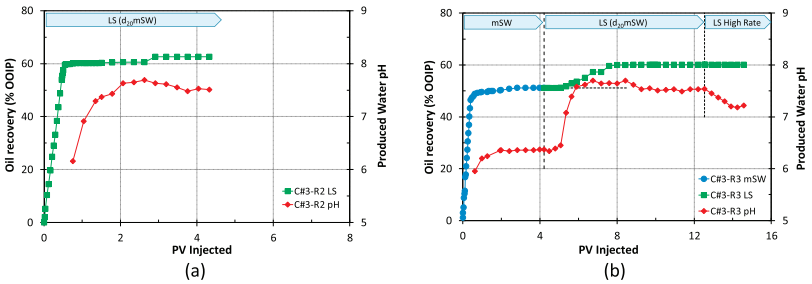


**Fig. 10.** Oil recovery tests on core C#3 at $T_{res}$ (>130 °C). After mild cleaning, the core was restored with $S_{wi} = 0.15$, and saturated and aged in reservoir crude oil. **(a)** In test C#3-R2 the core was flooded with LS brine in secondary mode. **(b)** In test C#3-R3 the core was successively flooded with mSW – LS brine. The flooding rate was 4 PV/D.

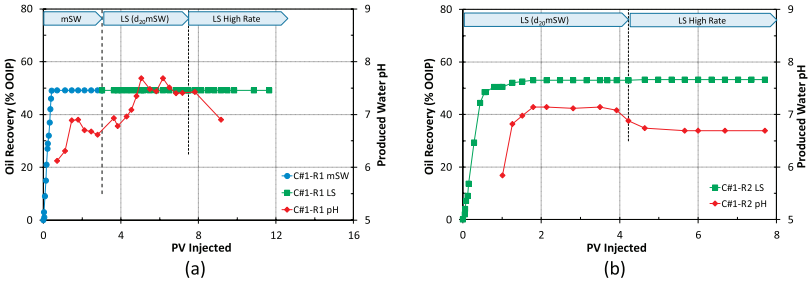


**Fig. 11.** Oil recovery tests from core C#1 at $T_{res}$ (>130 °C). The core was restored with $S_{wi} = 0.15$, and saturated and aged in reservoir crude oil before core flooding at a constant rate of 4 PV/D. **(a)** The core was successively flooded with mSW - LS brine, test C#1-R1. **(b)** The core was flooded with LS brine in secondary mode, C#1-R2.

**Table 5**
Results from the forced displacement tests on all tested cores.

| Core | Test | Brine flooding sequence | Secondary oil recovery (%OOIP) | Tertiary LS oil recovery (%OOIP) | Tertiary oil produced (%OOIP) | Improved secondary LS effect (%) | Tertiary LS effect (%) | Total number of PV injected |
|---|---|---|---|---|---|---|---|---|
| C#5 | C#5-R1 | LS | 58.3 | – | – | | | ~7 |
| | C#5-R2 | mSW-LS | 38.4 | 44.6 | 6.2 | 51.8[a] | 16.1[b] | ~15 |
| | C#5-R3 | mSW-LS | 38.4 | 43.7 | 5.3 | 51.8 | 13.8 | ~15 |
| C#3 | C#3-R2 | LS | 62.6 | – | – | 22.3 | 17.4 | ~4 |
| | C#3-R3 | mSW-LS | 51.2 | 60.1 | 8.9 | | | ~15 |
| C#1 | C#1-R1 | mSW-LS | 49.2 | 49.2 | 0 | 7.9 | 0.0 | ~12 |
| | C#1-R2 | LS | 53.1 | – | – | | | ~8 |

[a] Improved secondary LS effect (%) = ((Secondary LS oil recovery (%OOIP) – Secondary mSW oil recovery (%OOIP))/Secondary mSW oil recovery (%OOIP))*100 = ((58.3–38.4)/38.4)*100 = 51.8.
[b] Tertiary LS effect (%) = ((Tertiary oil produced (%OOIP) - Secondary mSW oil recovery (%OOIP))/Secondary mSW oil recovery (%OOIP))*100 = ((44.6–38.4)/38.4)*100 = 16.1.

recoveries than injection of mSW in secondary mode.

The incremental oil produced with secondary LS injection over secondary mSW injection varied from 7.9 to 51.8%, with an average of 33.5%. Most of this extra oil was produced after only 1PV of LS brine injected. Together with the observed EOR during LS injection, a significant change in pH was observed, supporting wettability alteration induced by the LS brine injection according to the proposed chemical mechanism, illustrated by Eqs. (1)-(3). Spontaneous imbibition into smaller non-swept pores takes place, producing the extra oil from these pores, improving the microscopic sweep efficiency and delaying the breakthrough of the injection brine. This work only includes viscous flooding experiments. No quantitative data of wettability indices were obtained before and after water flooding, to verify changes in wettability. A series of spontaneous imbibition experiments could have provided such numbers, but was not performed in this study due to the limited access of preserved reservoir cores. Wettability alteration with LS brine have previously been confirmed in spontaneous imbibition experiments, although on a different COBR-system (Piñerez Torrijos et al., 2017). Nevertheless, the viscous flooding experiments confirm that Smart Water injection in secondary mode could be an extremely efficient EOR method.

Introducing the Smart Water in tertiary mode after mSW flooding, gave a tertiary EOR effect of 0.0–17.4%, with an average of 11.8%, extra oil produced with LS injection after mSW injection. Tertiary LS oil production was a much slower process, and 3–4 PV with LS brine was needed to reach the recovery plateau. A large pH increase is not enough to guarantee a large tertiary LS EOR effect. The ability for polar components to desorb from the mineral surface seems to be reduced with increased $S_w$. The polar crude oil components dictating the surface wettability are large organic molecules, which are not soluble in the water phase. At high $S_w$, the distance to the oil phase increases and less polar organic components desorb.

## 4. Conclusions

The Smart Water EOR potential for an undeveloped high temperature (>130 °C), medium FW salinity, offshore sandstone oil reservoir was evaluated. Modified seawater (mSW), treated for reduced scaling potential, is a typical injection water for this type of reservoir. The Smart Water EOR potential was evaluated using a low salinity (LS) brine made by diluting mSW 20 times. Secondary LS EOR potential and tertiary LS EOR potential after mSW flooding were evaluated by comparing a series of oil recovery tests performed on reservoir cores sampled close to each other. The results are shortly summarized below:

- A surface reactivity test performed on a mildly cleaned reservoir core confirmed significant pH gradients (ΔpH) when FW was displaced by LS brine, and when mSW was displaced by LS brine. Only minor pH changes were observed when FW was displaced by mSW brine. The results confirm that the pore surface minerals contribute with CEC during LS injection, inducing a pH increase needed for observing wettability alteration and EOR.
- Secondary oil recovery tests at $T_{res}$ showed a significant increase in oil recovery using LS brine compared to mSW. The extra produced oil varied from 7.9 to 51.8%, with an average of 33.5% for the 3 tested cores.
- Tertiary LS injection after mSW injection gave LS EOR effects from 0 to 17.4%, with an average of 11.8% extra oil for the 3 tested cores.
- A significant increase in PW pH from initially acidic, favoring fractional wetting to slightly more alkaline, favoring more water-wet conditions, were observed in all oil recovery experiments during LS injection.
- When LS brine as Smart Water was introduced to the core in secondary mode, it proved to be very efficient, and most of the extra oil

was produced after 1PV injected. In contrast, during tertiary LS injection, up to 4PV brine was needed to reach the recovery plateau.

## Acknowledgements

The authors are grateful to the oil company for supplying the reservoir material, and for financial support of research activities in the Smart Water EOR group at the University of Stavanger. Bachelor student Gadiah Albraji for participating in some of the laboratory work.

## References

Aghaeifar, Z., Strand, S., Austad, T., Puntervold, T., Aksulu, H., Navratil, K., Storås, S., Håmsø, D., 2015a. Influence of formation water salinity/composition on the low salinity EOR effect in high temperature sandstone reservoirs. Energy Fuel. 29 (8), 4747–4754. https://doi.org/10.1021/acs.energyfuels.5b01621.

Aghaeifar, Z., Strand, S., Puntervold, T., Austad, T., Aarnes, S., Aarnes, C., 2015b. Adsorption/desorption of $Ca^{2+}$ and $Mg^{2+}$ to/from kaolinite clay in relation to the low salinity EOR effect. In: IOR 2015–18th European Symposium on Improved Oil Recovery, Dresden, Germany, 14-16 April. https://doi.org/10.3997/2214-4609.201412132.

Aksulu, H., Håmsø, D., Strand, S., Puntervold, T., Austad, T., 2012. Evaluation of low salinity EOR-effects in sandstone: effects of temperature and pH gradient. Energy Fuel. 26 (6), 3497–3503. https://doi.org/10.1021/ef300162n.

Allard, B., Karlsson, M., Tullborg, E.-L., Larson, S., 1983. Ion Exchange Capacities and Surface Areas of Some Major Components and Common Fracture Filling Materials of Igneous Rocks. SKB/KBS Technical Report TR 83–64, Göteborg, Sweden.

Austad, T., 2013. Water based EOR in carbonates and sandstones: new chemical understanding of the EOR potential using "Smart Water". In: Sheng, J.J. (Ed.), Enhanced Oil Recovery Field Case Studies. Elsevier, Oxford, UK, pp. 301–335.

Austad, T., Rezaeidoust, A., Puntervold, T., 2010. Chemical mechanism of low salinity water flooding in sandstone reservoirs. In: SPE-129767-MS. SPE Improved Oil Recovery Symposium, Tulsa, Oklahoma, USA, 24–28 April. https://doi.org/10.2118/129767-MS.

Bernard, G.G., 1967. Effect of floodwater salinity on recovery of oil from cores containing clays. In: SPE-1725-MS. Annual California Regional Meeting, Los Angeles, California, USA, 26–27 October. https://doi.org/10.2118/1725-MS.

Buckley, J.S., Morrow, N.R., 1990. Characterization of crude oil wetting behavior by adhesion tests. SPE-20263-MS. In: SPE/DOE Seventh Symposium on Enhanced Oil Recovery, Tulsa, Oklahoma, April 22–25. https://doi.org/10.2118/20263-MS.

Burgos, W.D., Pisutpaisal, N., Mazzarese, M.C., Chorover, J., 2002. Adsorption of quinoline to kaolinite and montmorillonite. Environ. Eng. Sci. 19 (2), 59–68. https://doi.org/10.1089/10928750252953697.

Crabtree, M., Eslinger, D., Fletcher, P., Johnson, A., King, G., 1999. Fighting scale—removal and prevention. Oilfield Rev. 11 (3), 30–45.

Davis, R.A., McElhiney, J.E., 2002. The Advancement of Sulfate Removal from Seawater in Offshore Waterflood Operations. NACE-02314. CORROSION, Denver, Colorado, 7–11 April.

Didier, M., Chaumont, A., Joubert, T., Bondino, I., Hamon, G., 2015. Contradictory trends for smart water injection method: Role of pH and salinity from sand/oil/brine adhesion maps. SCA2015–005. In: The International Symposium of the Society of Core Analysts, St. John's Newfoundland and Labrador, Canada, 16-21 August.

Fan, T., Buckley, J., 2000. Base Number Titration of Crude Oil Samples. Personal Communication.

Fan, T., Buckley, J., 2006. Acid number measurements revisited. In: SPE-99884-MS. SPE IOR Symposium, Tulsa, OK, USA, 22–26 April. https://doi.org/10.2118/99884-MS.

Fogden, A., 2012. Removal of crude oil from kaolinite by water flushing at varying salinity and pH. Colloid. Surface. Physicochem. Eng. Aspect. 402, 13–23. https://doi.org/10.1016/j.colsurfa.2012.03.005.

Gamage, P., Thyne, G., 2011. Systematic investigation of the effect of temperature during aging and low salinity flooding of Berea sandstone and Minn. In: 16th European Symposium on Improved Oil Recovery Cambridge, UK, 12 April. https://doi.org/10.3997/2214-4609.201404798.

Håmsø, D., 2011. Adsorption of Quinoline onto Illite at High Temperature in Relation to Low Salinity Water Flooding in Sandstone Reservoirs. Master Thesis. University of Stavanger, Norway.

Hardy, J.A., Barthorpe, R.T., Plummer, M.A., Rhudy, J.S., 1992. Control of scaling in the South Brae field. In: OTC-7058-MS. Offshore Technology Conference, Houston, Texas, 4–7 May. https://doi.org/10.4043/7058-MS.

Jadhunandan, P.P., 1990. Effects of Brine Composition, Crude Oil and Aging Conditions on Wettability and Oil Recovery. PhD Thesis. New Mexico institute of mining and technology, Socorro, New Mexico.

Jadhunandan, P.P., Morrow, N.R., 1995. Effect of wettability on waterflood recovery for crude-oil/brine/rock systems. SPE-22597-PA. SPE Reservoir Eng. 10 (01), 40–46. https://doi.org/10.2118/22597-PA.

Lager, A., Webb, K.J., Black, C.J.J., Singleton, M., Sorbie, K.S., 2008. Low salinity oil recovery - an experimental Investigation1. Petrophysics 49 (01).

Loahardjo, N., Xie, X., Morrow, N., 2008. Oil recovery by cyclic waterflooding of mixed-wet sandstone and limestone. In: 10th International Symposium on Reservoir Wettability, Abu Dhabi, UAE, 27–28 October.

Madsen, L., Lind, I., 1998. Adsorption of carboxylic acids on Reservoir minerals from organic and aqueous phase. SPE-37292-PA. SPE Reservoir Eval. Eng. 1 (01), 47–51. https://doi.org/10.2118/37292-PA.

Mamonov, A., Puntervold, T., Strand, S., 2017. EOR by smart water flooding in sandstone reservoirs - effect of sandstone mineralogy on initial wetting and oil recovery. In: SPE-187839-MS. SPE Russian Petroleum Technology Conference, Moscow, Russia, 16–18 October. https://doi.org/10.2118/187839-MS.

Morrow, N., Buckley, J., 2011. Improved oil recovery by low-salinity waterflooding. J. Petrol. Technol. 63 (05), 106–112. https://doi.org/10.2118/129421-JPT.

Nasralla, R.A., Bataweel, M.A., Nasr-El-Din, H.A., 2011. Investigation of wettability alteration by low salinity water. In: SPE-146322-MS. Offshore Europe, Aberdeen, UK, 6–8 September. https://doi.org/10.2118/146322-MS.

Piñerez Torrijos, I.D., Austad, T., Strand, S., Puntervold, T., Wrobel, S., Hamon, G., 2016a. Linking low salinity EOR effects in sandstone to pH, mineral properties and water composition. In: SPE-179625-MS. SPE Improved Oil Recovery Conference, Tulsa, Oklahoma, USA, 11–13 April. https://doi.org/10.2118/179625-MS.

Piñerez Torrijos, I.D., Puntervold, T., Strand, S., Austad, T., Abdullah, H.I., Olsen, K., 2016b. Experimental study of the response time of the low-salinity enhanced oil recovery effect during secondary and tertiary low-salinity waterflooding. Energy Fuel. 30 (6), 4733–4739. https://doi.org/10.1021/acs.energyfuels.6b00641.

Piñerez Torrijos, I.D., Puntervold, T., Strand, S., Austad, T., Tran, V.V., Olsen, K., 2017. Impact of temperature on the low salinity EOR effect for sandstone cores containing reactive plagioclase. J. Petrol. Sci. Eng. 156, 102–109. https://doi.org/10.1016/j.petrol.2017.05.014.

Piñerez Torrijos, I.D., Puntervold, T., Strand, S., Rezaeidoust, A., 2016c. Optimizing the low salinity water for EOR effects in sandstone reservoirs - composition vs salinity. In: 78th EAGE Conference and Exhibition, Vienna, Austria, 30 May- 2 June. https://doi.org/10.3997/2214-4609.201600763.

Reinholdtsen, A.J., RezaeiDoust, A., Strand, S., Austad, T., 2011. Why such a small low salinity EOR - potential from the Snorre formation?. In: 16th European Symposium on Improved Oil Recovery, Cambridge, UK, 12–14 April https://doi.org/10.3997/2214-4609.201404796.

RezaeiDoust, A., Puntervold, T., Austad, T., 2011. Chemical verification of the EOR mechanism by using low saline/smart water in sandstone. Energy Fuel. 25 (5), 2151–2162. https://doi.org/10.1021/ef200215y.

Robbana, E., Buikema, T.A., Mair, C., Williams, D., Mercer, D.J., Webb, K.J., Hewson, A., Reddick, C.E., 2012. Low salinity enhanced oil recovery - laboratory to day one field implementation - LoSal EOR into the clair ridge project. SPE-161750-MS. In: Abu Dhabi International Petroleum Conference and Exhibition, Abu Dhabi, UAE, 11–14 November. https://doi.org/10.2118/161750-MS.

Springer, N., Korsbech, U., Aage, H.K., 2003. Resistivity index measurement without the porous plate: a desaturation technique based on evaporation produces uniform water saturation profiles and more reliable results for tight North Sea chalk. In: International Symposium of the Society of Core Analysts Pau, France, 21–24 September.

Strand, S., Puntervold, T., Austad, T., 2016. Water based EOR from clastic oil reservoirs by wettability alteration: a review of chemical aspects. J. Petrol. Sci. Eng. 146, 1079–1091. https://doi.org/10.1016/j.petrol.2016.08.012.

**The remaining papers of this thesis are unfortunately not available in Brage due to copyright.**



# Paper II

"**Significance of Capillary Forces during Low-Rate Waterflooding**", Z. Aghaeifar, S. Strand, T. Austad, T. Puntervold. Energy Fuels, 2019, 33 (5), pp 4747–4754. https://doi.org/10.1021/acs.energyfuels.9b00023

# Paper III

"**Seawater as a Smart Water in Sandstone reservoirs?**", Iván D. Piñerez Torrijos, Zahra Aghaeifar, Tina Puntervold and Skule Strand. Manuscript submitted to SPE Reservoir Evaluation & Engineering journal, 2019

# Paper IV

"**Low Salinity EOR Effects After Seawater Flooding In A High Temperature And High Salinity Offshore Sandstone Reservoir**", Z. Aghaeifar, T. Puntervold, S. Strand, T. Austad, B. Maghsoudi and J. C. Ferreira, SPE-191334-MS, SPE Norwegian One Day Seminar, Bergen, Norway, 2018. https://doi.org/10.2118/191334-MS

# Paper V

"**Influence of Formation Water Salinity/Composition on the Low-Salinity Enhanced Oil Recovery Effect in High-Temperature Sandstone Reservoirs**", Z. Aghaeifar, S. Strand, T. Austad, T. Puntervold, H. Aksulu, K. Navratil, S. Storås, and D. Håmsø. Energy Fuels, 2015, 29 (8), pp 4747–4754. https://doi.org/10.1021/acs.energyfuels.5b01621

# Paper VI

"**The role of kaolinite clay minerals in EOR by low salinity water injection**", T. Puntervold; A. Mamonov, Z. Aghaeifar, G. O. Frafjord, G. M. Moldestad, S. Strand, T. Austad. Energy Fuels, 2018, 32 (7), pp 7374–7382. https://doi.org/10.1021/acs.energyfuels.8b007

# Paper VII

"**Adsorption/desorption of $Ca^{2+}$ and $Mg^{2+}$ to/from Kaolinite Clay in Relation to the Low Salinity EOR Effect**", Z. Aghaeifar, S. Strand, T. Puntervold, T. Austad, S. Aarnes and Ch. Aarnes. 18th European Symposium on Improved Oil Recovery, At Dresden, Germany, April 2015. https://doi.org/10.3997/2214-4609.20